



universität
wien

MASTERARBEIT / MASTER'S THESIS

Titel der Masterarbeit / Title of the Master's Thesis

Characterizing Wnt proteins and cytoskeletal
effectors during MuSK signaling

verfasst von / submitted by

Sandra Parzer, BSc

angestrebter akademischer Grad / in partial fulfilment of the requirements for the
degree of

Master of Science (MSc)

Wien, 2016 / Vienna 2016

Studienkennzahl lt. Studienblatt /
degree programme code as it appears on
the student record sheet:

A 066 834

Studienrichtung lt. Studienblatt /
degree programme as it appears on
the student record sheet:

Masterstudium Molekulare Biologie
UG2002

Betreut von / Supervisor:

Dr. Ruth Herbst, Priv.- Doz.

Table of contents

1	Abbreviations	7
2	Zusammenfassung.....	10
3	Abstract	12
4	Introduction	14
4.1	Neuromuscular Junction	14
4.1.1	Overview	14
4.1.2	NMJ-Formation	15
4.1.3	NMJ: Diseases	17
4.2	Muscle specific kinase	19
4.3	Lrp4.....	22
4.4	Docking protein-7	24
4.5	Agrin & Cytoskeletal rearrangements	25
4.6	Focal Adhesion & Focal Adhesion Kinase	27
4.7	Acetylcholine Receptor	29
4.8	Myogenic differentiation	30
4.9	Tet-On-System.....	32
4.10	Wnt proteins	33
4.10.1	Wnt in Prepatterning, NMJ formation and AChR clustering	36
4.11	Aim of the study	38
5	Materials and Methods.....	40
5.1	Chemicals and Reagents.....	40
5.1.1	List of chemicals and reagents used in molecular and biochemistry methods	40
5.1.2	List of supplied lab-utensils	42
5.2	Antibodies and Toxins	43
5.2.1	Primary Antibodies and Toxins	43
5.2.2	Secondary Antibodies and Others.....	43
5.3	Solutions and Buffers	44
5.3.1	Commonly used Solutions and Buffers for biochemical and molecular biology methods	44
5.3.2	Media components for cell culture methods	47
5.4	Plasmids and Primers	47
5.4.1	Plasmid List.....	47

5.4.2	List of Primers	48
5.5	Cell Culture Methods.....	49
5.5.1	Freezing Cells	49
5.5.2	Thawing Cells stored at -80°C	49
5.5.3	Splitting cells.....	49
5.5.4	Proliferation of mouse C2C12 muscle cells.....	50
5.5.5	Differentiation of muscle cells	50
5.5.6	Doxycycline start	50
5.5.7	Transient calcium phosphate transfection.....	50
5.5.8	Transient Turbofect transfection	51
5.5.9	Stable transfection of CHO cells with Wnt4, 9a and 11	51
5.5.10	Stable Transfection Method with retroviral infection.....	51
5.5.11	Clonal selection of C2 cells	52
5.5.12	Agrin stimulation.....	52
5.6	Molecular biology DNA methods	53
5.6.1	DNA linearization, purification and further precipitation...	53
5.6.2	Generation of competent bacteria	53
5.6.3	Transformation efficiency of competent bacteria	54
5.6.4	Digestion/ Klenow fill-in and Dephosphorylation.....	54
5.6.5	Electrophoretic separation of digested DNA and elution...	55
5.6.6	DNA Ligation	55
5.6.7	Transformation of competent bacteria with DNA	56
5.6.8	Plasmid Mini/Midi/Maxi preparations.....	56
5.6.9	DNA Sequencing	56
5.6.10	Oligo annealing, PCR and sub-cloning of shRNAs for RNAi	57
5.6.11	Subcloning in Wnt Isolation Experiments.....	58
5.7	Protein biochemistry methods	59
5.7.1	Preparation of protein extract from heterologous cells	59
5.7.2	Preparation of cell lysates from C2C12 mouse muscle cells	59
5.7.3	Co-Immunoprecipitation of Wnt protein via MuSK in HEK cells	60
5.7.4	SDS-Page Gel electrophoresis of proteins.....	60
5.7.5	Western blotting	61

5.7.6	Stripping and reprobing	61
5.7.7	Silver staining of proteins in polyacrylamide gels	61
5.7.8	Wnt protein purification with Ni-NTA Resin beads	62
5.7.9	Antibody and shRNA specificity tests in HEK and C2C12 cells	63
5.8	Immunocytochemistry methods.....	63
5.8.1	AChR cluster Assay	63
5.8.2	Clathrin-BGT staining	65
5.8.3	Tubulin staining	65
5.8.4	Colocalization stainings of Cos-7 cells with Wnt, MuSK and Lrp4	65
6	Results.....	68
6.1	RNAi-mediated downregulation of proteins in mouse C2 muscle cells	68
6.1.1	EB3 downregulation in mapre.423 and 1355 expressing C2 cell lines transiently transfected with EB3-GFP.....	68
6.1.2	Downregulation of endogenous Lrp4 in Lrp4.1058 expressing C2 cell lines	69
6.1.3	RNAi-mediated depletion of transfected Dynamin-2 in C2-Tet cells	71
6.1.4	RNAi-mediated downregulation of endogenous Dynamin in stably Dnm2.838 expressing C2 cells using different doxycycline treatments.....	72
6.1.5	RNAi-mediated depletion of FAK in C2 cells	73
6.2	Assaying AChR cluster formation in C2 cells expressing shRNAs against Lrp4 and FAK	75
6.2.1	The effect of RNAi-mediated Lrp4 depletion on AChR clustering	75
6.2.2	Downregulation of FAK and its effect on AChR clustering.....	76
6.3	Studying Wnt during MuSK signaling	77
6.3.1	His-Wnt protein purification with Ni-NTA Resin beads	78
6.3.2	Examining Wnt - MuSK interaction using co-immunoprecipitation	80
6.3.3	Wnt, MuSK, Lrp4 colocalization in Cos-7 cells	82
7	Discussion and Outlook	86
7.1	Downregulation of candidate proteins in C2 cells	86
7.1.1	Downregulation of Lrp4.....	88
7.2	Isolation of Wnt proteins and their interaction with MuSK	89

Table of Contents

7.2.1	Purification of Wnt11 protein	89
7.2.2	Determination of the interaction between Wnt4 and MuSK by co-immunoprecipitation	90
7.2.3	Co-localization studies of Wnt protein, MuSK and Lrp4 using immunostaining and confocal microscopy	91
8	Appendix	94
8.1	Reference List	94
8.2	List of Figures	100
8.3	Statutory Declaration	101
8.4	Curriculum Vitae	102
8.5	Lebenslauf	103

1 Abbreviations

α	Alpha
A	Alanine
ACh	Acetylcholine
AChE	Acetylcholinesterase
AChR	Acetylcholine receptor
AChRs	Acetylcholine receptors
AChR β	AChR subunit β
A-loop	Activation loop
APC	Adenomatous polyposis coli
APS	Ammoniumperoxidisulfate
ATP	Adenosine triphosphate
β	Beta
BGT	Bungarotoxin
bp	Base pair
BSA	Bovine serum albumin
$^{\circ}\text{C}$	Degree centigrade
C2C12 cells	mouse myoblast cell line
Ca^{2+}	Calcium
CaCl_2	Calcium chloride
CaN	Calcineurin
CHO cells	Chinese hamster ovary cells
CK1	Casein kinase 1
cm	Centimeter
CMS	Congenital myasthenic syndromes
CNS	Central nervous system
CRD	Cysteine rich domain
Crk	CT 10 regulator of kinase
DVL	Dishevelled
δ	Delta
D	Aspartic acid
DAAM	Dishevelled-associated activator of morphogenesis
DABCO	1,4-diazabicyclo [2.2.2] octane
ddH ₂ O	Distilled water
DMEM	Dulbecco 's modified eagle 's medium
DMSO	Dimethylsulfoxide
DNA	Deoxyribonucleic acid
Dok-7	Docking protein-7
DTT	Dithiothreitol
ϵ	Epsilon
E	Embryonic day
ECL	Enhanced chemiluminescence
E.Coli	Escherichia coli
EDTA	Ethylene-diamine-tetraacetic acid
EGTA	Ethylene glycol bis (2-aminoethyl)-tetraacetic acid
EtOH	Ethanol
FBS	Fetal bovine serum

Fig	Figure
FzR	Frizzled receptor
Y	Gamma
g	Gram
GSK3	Glycogen synthase kinase 3
h	Hour
HA	Hemagglutinin
HBBS	Hank's buffered salt solution
HCl	Hydrochloric acid
HEK 293 T	Human embryonic kidney 293 T cells
HRP	Horse reddish peroxidase
HS	Horse serum
IB	Immunoblot
Ig	Immunoglobulin-like domains
IgG	Immunoglobulin G
IHC	Immunohistochemistry
IP	Immunoprecipitation
JIR	Jackson Immuno-Research
JNK	c-Jun n-terminal kinase
K ⁺	Potassium
KCl	Potassium chloride
kDa	Kilo Dalton
KH ₂ PO ₄	Potassium dihydrogen phosphate
Lrp4	Low density lipoprotein related protein 4
LRP5/6	low-density lipoprotein receptor-related protein 5/6
Lys	Lysine
M	Molar
mAB	Monoclonal antibody
mM	Milli molar
μl	Micro liter
μg	Micro gram
μm	Micro meter
MG	Myasthenia gravis
MeOH	Methanol
MgCl ₂	Magnesium chloride
mg	Milligram
min	Minute(s)
ml	Milliliter
mRNA	Messenger RNA
MuSK	Muscle-specific kinase
Na ⁺	Sodium
NaCl	Sodium chloride
NaF	Sodium fluoride
Na ₂ HPO ₄ .2H ₂ O	Sodium hydrogen phosphate dihydrate
NaH ₂ PO ₄ .2H ₂ O	Sodium dihydrogen phosphate dihydrate
NaN ₃	Sodium azide
NaOH	Sodium hydroxide
NFAT	Nuclear factor of activated T cells
ng	Nanogram

nm	Nanometer
NMJ	Neuromuscular junction
NP-40	Nonidet P-40 or octylphenoxypolyethoxyethanol
o/n	Over night
Ori	Origin of replication
%	Percentage
P	Postnatal day
PAGE	Polyacrylamide gel electrophoresis
PBS	Phosphate buffered saline
PBS-T	Phosphate buffered saline-triton
PFA	Paraformaldehyde
PH	Pleckstrin-homology
PKC	Protein kinase C
PLC	Phospholipase C
PMSF	Phenylmethanesulfonylfluorid
PNS	Peripheral nervous system
PTB	Phosphotyrosine binding domain
PVDF	Polyvinylidene difluoride
pY	Phosphotyrosine
Rapsyn	Receptor associated protein of the synapse
RNA	Ribonucleic acid
ROCK	Rho-associated protein kinase
Rpm	Revolutions per minute
RT	Room temperature
rtTA	reverse Transactivator
S	Serine
SDS	Sodium dodecyl sulfate
Sec	second(s)
TAE	Tris acetate EDTA
TBS-T	Tris buffered saline-tween
TEA	Triethylamine
TEMED	Tetramethylethylene diamine
TKD	Tyrosine kinase domain
TM	Transmembrane spanning region
TRE	Tetracycline-responsive element
Tris	Tris (hydroxymethyl) aminomethane
Tyr	Tyrosine
UT	Untreated/ Untransfected
V	Volt
WT	Wildtype
Y	Tyrosine

2 Zusammenfassung

Die neuromuskuläre Synapse ist die spezialisierte Verbindung zwischen einer Muskelfaser und einem Motorneuron. Diese Synapse reguliert jegliche Art der Bewegung, inklusive der Atmung, innerhalb eines Organismus. Ein wichtiger Faktor für die erfolgreiche Synapsenbildung ist die Aktivierung der muskelspezifischen Rezeptor-Tyrosinkinase (MuSK) und die daraus folgenden Signalkaskaden bis zum Clustering von Acetylcholinrezeptoren (AChR). Die korrekte Synapsenbildung während der Embryonalentwicklung und frühen postnatalen Entwicklung ist lebensnotwendig für einen Organismus. Die postsynaptische Seite charakterisiert sich durch hochkonzentrierte AChR in „Pretzelform“, welche der präsynaptischen, aktiven Zone mit akkumulierten Acetylcholinvesikeln an der Nervenendigung gegenüber steht. Der muskelinnervierende Motornerv initiiert die Freisetzung von Agrin, einem Proteoglycan, welches zur Aktivierung von MuSK und Lrp4 führt. Die Bildung und Stabilisierung der neuromuskulären Synapse erfordert das genaue Zusammenspiel aller beteiligten molekularen Faktoren. In den letzten Jahren wurde erkannt, dass MuSK auch durch Wnt Proteine aktiviert werden kann und dass Wnt Proteine eine Rolle beim Nerv-unabhängigen Clustering von AChR spielen. Wnt Proteine erkennen und binden die cysteinreiche Domäne von MuSK, welche deren nativen Rezeptor Frizzled ähnelt, führen zu MuSK Phosphorylierung und AChR Anhäufung. Die Rolle von Wnt Proteinen und weiteren synapsenbildenden Hilfsproteinen während der AChR Clusterbildung soll in dieser Masterarbeit untersucht werden.

Der erste Teil dieser Arbeit beschäftigt sich mit Proteinen, die das Zytoskelett remodellieren und somit zum Proteintransport und zum Aufbau der AChR Cluster beitragen. Dynamin-2, FAK, Lrp4 und EB3 wurden mit Hilfe von RNAi herunterreguliert und dessen Auswirkung auf AChR Clusterbildung untersucht. Ziel war es, Muskelzelllinien zu etablieren, welche ein Tet-ON Expressionssystem stabil exprimieren. Somit kann die shRNA Expression mit Doxycyclinzugabe präzise

gesteuert werden. In vier Proteinen konnte eine erfolgreiche Herunterregulierung in den jeweiligen Zelllinien erzielt werden. Dynamin2, EB3 und FAK wiesen eine signifikante Knockdownrate von ca. 50% auf, Lrp4 eine Runterregulierung von etwa 40%. Allerdings zeigte nur Lrp4 knockdown eine Reduktion von AChR Clustern, bei FAK knockdown war die AChR Clusterbildung nicht beeinflusst.

Der Zweite Teil konzentrierte sich auf die Agrin-unabhängige MuSK Aktivierung durch Wnts. Wnt Proteine wurden in heterologen Zellen (CHO, Chinese Hamster Ovary cells) exprimiert und aus dem Überstand aufgereinigt. Der Fokus wurde auf die Erstellung von Wnt 4, 9a und 11 stabil exprimierenden CHO Zelllinien und die Optimierung der Proteinisolierung gelegt. Außerdem wurde die spezifische Bindung der Wnt Proteine an MuSK und deren Lokalisation in der Zelle untersucht. Wnt Proteine konnten erfolgreich angereichert werden, jedoch in zu geringer Konzentration um sie für weiterführende Versuche an C2C12 Zellen verwenden zu können. Weiters konnte die spezifische Bindung von Wnt4 an MuSK durch Ko-Immunopräzipitation gezeigt werden und Ko-lokalisierung der drei interagierenden Proteine Wnt, MuSK und Lrp4 an der Zelloberfläche nachgewiesen werden.

3 Abstract

The neuromuscular junction is the connection between muscle and the innervating motoneuron. Its highly specialized structure is important for muscle movement, including breathing and thus the non- or malfunction leads to severe diseases or even death. The innervating motoneuron approaches the muscle guided by the prepatterned AChR cluster region, stabilizes the clusters and leads to their 'Pretzel'-shaped form. The presynaptic motoneuron accumulates vesicles carrying the neurotransmitter acetylcholine at the active zone, opposite of the muscle's postsynaptic density region, where AChRs become concentrated. The motoneuron releases agrin, a proteoglycan, which diffuses through the synaptic cleft, binds to Lrp4 and leads to homodimerization of MuSK and its activation. Subsequent signaling events lead to phosphorylation of AChR- β subunit and the stabilization of AChR cluster and NMJ maturation. More recently, Wnt proteins have been implicated in MuSK activation and nerve-independent AChR clustering, termed pre patterning. In this thesis the role of Wnt proteins and specific cytoskeletal effectors was studied.

The focus of the first project in this thesis was set on the creation of a model system for doxycycline-induced downregulation of MuSK target proteins involved in MuSK activation, internalization, AChR clustering and cytoskeletal rearrangements. Therefore, the method of RNAi or RNA-induced silencing was applied for controlled downregulation of Dynamin-2, Lrp4, EB3 and FAK. The aim was to test target protein downregulation, differentiation of myotubes and the effect on AChR clustering in doxycycline-treated and untreated C2 myotubes. Results indicated successful downregulation of endogenous Dynamin-2, FAK and EB3 by more than 50%. Lrp4 showed a downregulation rate of approximately 40%. A reduced number of AChR clusters in response to agrin suggested that Lrp4 downregulation was successful, whereas FAK downregulation appeared to have no influence on AChR clustering.

The second part of the thesis addressed the agrin-independent MuSK activation by Wnt proteins. The goal was to establish a heterologous cell line (CHO cell line) to stably express soluble Wnt 4, 9a and 11 for further purification of recombinant Wnt. Numerous subcloning strategies, different transfection methods, differently tagged Wnt proteins and purifying optimizations were assayed. Expression and purification of Wnt proteins were achieved but obtained Wnt concentrations were too low for further experiments. In additional experiments I was able to demonstrate specific binding of Wnt4 to MuSK using co-immunoprecipitation. Finally, I examined the interaction of Wnt, MuSK and Lrp4 using co-localization studies of the three proteins on the cell surface of Cos- 7 cells.

4 Introduction

4.1 Neuromuscular Junction

4.1.1 Overview

The neuromuscular junction (NMJ), has been intensively studied because of its role as a model for all synapses in the nervous system. Its unmatched accessibility, the rather large size and its relative simplicity makes it much easier to explore processes from synaptogenesis, maintenance of synapses, to pathology of neuronal and muscular diseases (Shi et al., 2012). The mammalian skeletal neuromuscular junction is the connection between motoneuron and skeletal muscle fiber and is controlling our muscle movements and ability to breathe. Therefore, it is important for simple survival and its non-function leads to severe diseases and also death (see section 4.1.3). Its highly specific and differentiated pre- and postsynaptic structure is important to ensure proper signal transduction upon nerve innervation (Burden, 2011). In general it consists out of a presynaptic site, a synaptic cleft with a width of approx. 20nm and a postsynaptic apparatus.

The motor nerve terminal of an established synapse releases the neurotransmitter acetylcholine (ACh), which binds to nicotinic acetylcholine receptors (nAChRs) in the muscle fiber membrane on the postsynaptic side. This binding opens the ligand-gated channel, depolarizes the muscle membrane (e.g.: Na⁺ ions enter, K⁺ leave) and the subsequent excitatory postsynaptic potential leads to muscle contraction. To ensure that acetylcholine elicits a sufficient depolarization with further downstream signaling for synapse formation and their maintenance, the pre- and post-synaptic apparatus is strictly organized. The post synaptic side receives a signal from the presynaptic nerve terminal which initiates changes in size, shape and molecular architecture as it matures (J. R. Sanes & Lichtman, 2001). An important factor to trigger the action potential mechanism is the density of AChR-clusters. They must be concentrated in the muscle membrane at a

density greater than 10000 AChRs/ μm^2 . AChR clustering and synapse-specific gene transcription is initiated when the motor nerve approaches and innervates the muscle fiber. In addition, presynaptic mechanisms and differentiation steps like the organization of active zones, neurotransmitter release sites and reorganization upon direct muscle-derived retrograde signals are important to stabilize the motor nerve terminals (Yumoto, Kim, & Burden, 2012). Figure 1 illustrates the development of a synapse from day P0 to adult with its pre- and postsynaptic specializations and important basal lamina proteins.

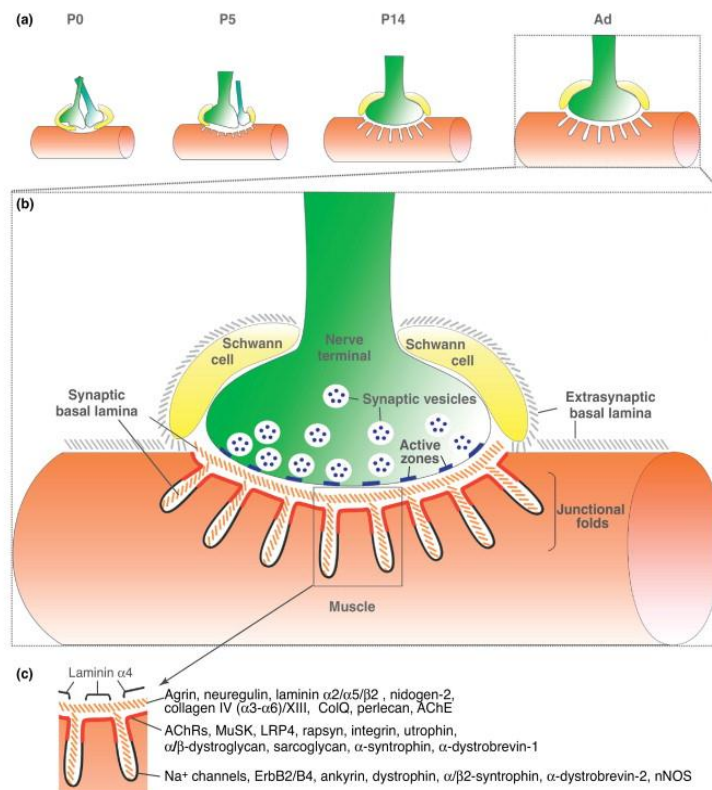


Figure 1: Development of the synapse; its invagination process and basal lamina proteins (a) Formation of synaptic contact and junctional folds during postnatal maturation of NMJ from postnatal day (P) to adult (Ad) **(b)** An adult vertebrate NMJ. **(c)** Molecules expressed at junctional folds, as well as at the synaptic basal lamina. Such molecules include glycoproteins (e.g., laminins), receptors (e.g., MuSK and ErbB receptors), and scaffolding proteins (e.g., dystrophin, syntrophins, and utrophin). Reviewed in (Shi, Fu, & Ip, 2012).

4.1.2 NMJ-Formation

The NMJ is a peripheral, cholinergic synapse. NMJ formation requires a precise interaction between muscle fiber and motor neurons. Agrin, a heparan sulfate basal lamina glycoprotein (Figure 2), plays an initial role in this formation. It is secreted by motor axons, deposited in the basal lamina of the synaptic cleft and binds the first β -propeller domain of Lrp4 (low-density lipoprotein receptor-related protein 4).

Conformational change in this bound Lrp4 facilitates the activation of another key player, the muscle specific kinase MuSK (Figure 2) (Hubbard & Gnanasambandan, 2013). MuSK is a receptor tyrosine kinase (RTK), which plays a central role in NMJ formation and stabilization. MuSK undergoes heterodimerization with Lrp4, autophosphorylation on Tyr553 residue in the juxtamembrane region and binds to docking protein-7 (Dok-7), an adaptor protein, which helps MuSK to activate its catalytic kinase domain (Bergamin, Hallock, Burden, & Hubbard, 2010). This MuSK activation results in a rapsyn-dependent pathway including the anchoring and clustering of AChRs leading to organized and stabilized plaque to pretzel postsynaptic specializations at the site of nerve-muscle contact (Bolliger et al., 2010). Autophosphorylation of Tyr553 in the juxtamembrane region is a critical step. MuSK Y553F mutant does not undergo activation and phosphorylation (Bergamin et al., 2010; Herbst & Burden, 2000). Focusing on the general postsynaptic structure, there are two different stages of NMJ formation and stabilization. The initial stage, called 'prepatternning' is characterized by the formation and stabilization of primitive postsynaptic specialization of

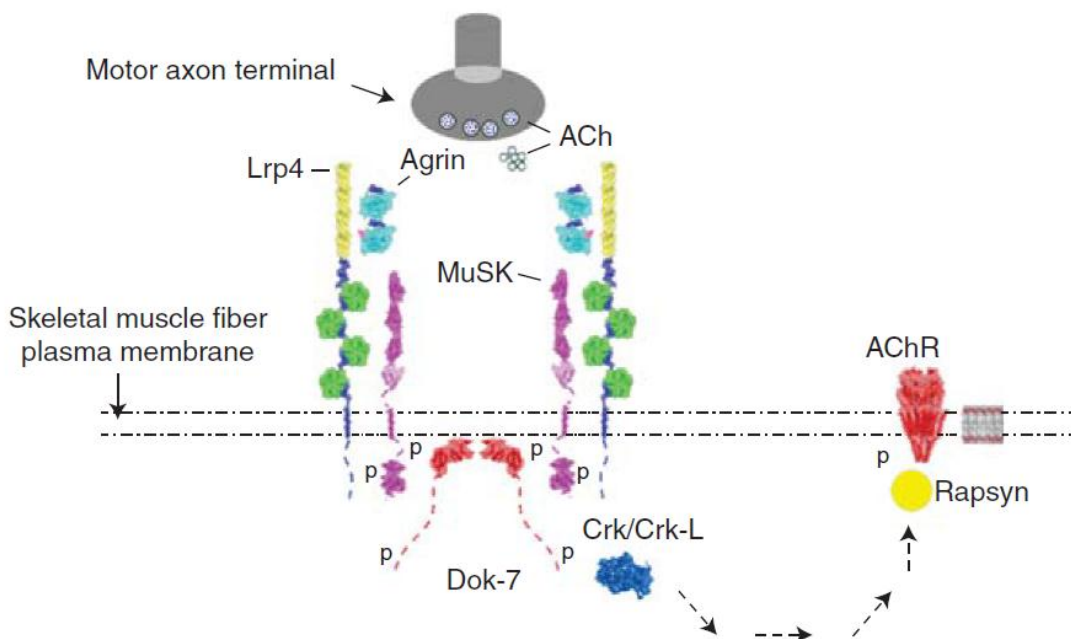


Figure 2: **Motor axons release Agrin and ACh.** Agrin binds to Lrp4, which stimulates association between Lrp4 and MuSK and MuSK phosphorylation. Once phosphorylated in the juxtamembrane region, MuSK recruits Dok-7, which forms a dimer and stabilizes dimerization of MuSK. Tyrosine phosphorylation of Dok-7 stimulates recruitment of Crk/Crk-L, which activates a poorly understood signaling pathway that leads to the anchoring of Rapsyn and AChRs at sites where MuSK is activated. Reviewed in (Burden et al., 2013)

clustered AChRs. After agrin-mediated differentiation of the postsynaptic apparatus and maturation of the presynaptic side, the plaque-like early NMJ transforms to the typical pretzel-like structure characteristic for the mature endplate. During this remodeling phase the postsynaptic membrane changes from flat and homogeneous to an invaginated area with complex molecular compartments (Figures 1, 3). Interestingly, a removal of postsynaptic components appears, forming pretzel-like structures. These transform into plaques with large and multiple perforations and then into complex pretzel-shaped mature NMJ (Figure 3a, 3c).

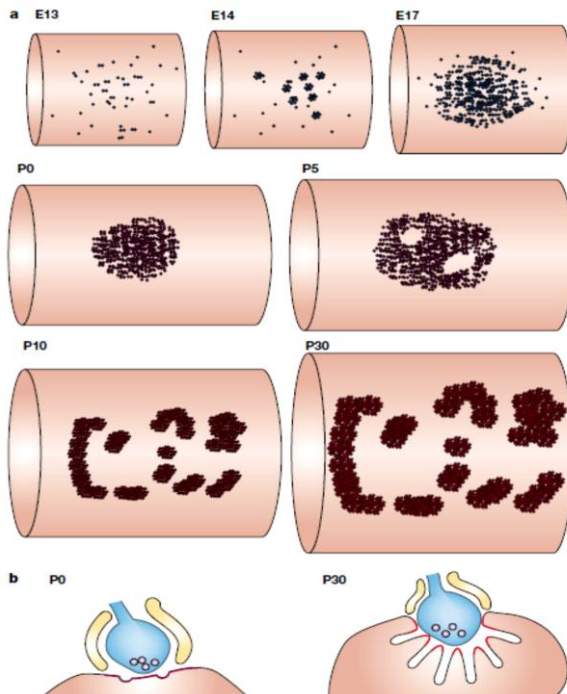
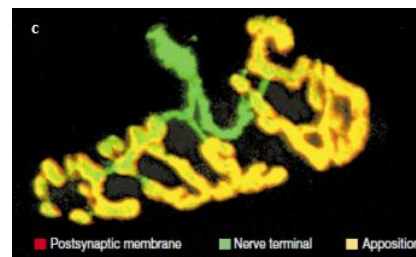


Figure 3: Postsynaptic maturation. (a) At E13 and E14 the microclusters of AChRs are visible, which aggregate and form an oval-shaped plaque at E17. After birth the plaque starts to lose AChRs, which results in the pretzel-like shape of AChR distribution. **(b)** The part of the postsynaptic membrane, which is opposite the nerve terminal starts to form postjunctional folds after birth through invagination. AChRs are concentrated at the crests of the folds and voltage-gated Na⁺ channels are located at the troughs. **(c)** Image of a neuromuscular junction with its typical pretzel-like AChR distribution. The innervating nerve terminals of branching motor axons (green) perfectly align with the AChR-rich postsynaptic membrane (Maselli et al.); (image modified from Sanes and Lichtmann, 2001)



4.1.3 NMJ: Diseases

The tightly regulated interplay of agrin, Lrp4, MuSK, Dok7, together with many proteins more is very important for a fully functional pre- and postsynaptic signaling complex that coordinates NMJ formation and maintenance (Figure 2). Impaired function of already only one of these components can lead to severe diseases or even prenatal death (Burden et al., 2013). Affected function, caused by either auto-antibodies

(myasthenia gravis, MG) or mutations (congenital myasthenia gravis, CMS), can lead to denervation of the muscle and muscle weakness (Figure 4). Muscle weakness, which worsens after activity, is the hallmark feature of MG. About 80% of MG cases are caused by autoantibodies against the α -subunit of AChRs (for AChR structure see section 4.7; Figures 8 and 9). These antibodies are directed to the main immunogenic region (MIR), which can block AChR function, increase AChR turnover, and stimulate complement-mediated damage. Only about 15% of the MG patients show antibodies against MuSK. This anti-MuSK MG is a severe form, which requires even respiratory assistance in some cases. The monovalent anti-MuSK antibodies are largely IgG4, which inhibit the binding of LRP4 to MuSK and reduce agrin-induced AChR clustering. In contrast, IgG1-3 antibodies are not inhibiting LRP4-MuSK binding but inhibit agrin-induced clustering and are also contributing to the reduced AChR density and neuromuscular dysfunction in myasthenia patients with MuSK antibodies (Konecny, Cossins, Waters, Beeson, & Vincent, 2013).

Congenital myasthenia	
Agrin MuSK Dok-7 Rapsyn	Mutations impair postsynaptic differentiation, compromising synaptic transmission and leading to muscle weakness and fatigue.
AChR AChE ChAT Nav1.4	Mutations impair synaptic transmission, leading to muscle weakness and fatigue.
Myasthenia gravis	
Autoantibodies to AChRs	Inhibit binding of ACh, stimulate accelerated degradation of AChRs and cause structural disorganization of the synapse.
Autoantibodies to MuSK or Lrp4	Autoantibodies to MuSK are IgG4, suggesting that they interfere with MuSK function, rather than recruiting complement.

Figure 4: **Neuromuscular diseases**: congenital myasthenia and autoimmune myasthenia gravis; reviewed in .(Burden, Yumoto, & Zhang, 2013)

Acetylcholinesterase (AChE) inhibitors, in this case, are the most common treatment of myasthenia gravis. They prevent the breakdown and re-uptake of ACh at the synaptic cleft and prolong signaling (Hubbard & Gnanasambandan, 2013). In turn, these AChE inhibitors should be used with caution in patients with MuSK auto-antibodies due to hypersensitivity reactions and in CMS patients with MuSK or Dok7 mutations because of a bad response to this treatment. MuSK restoration would be a possible alternative therapy.

Patients with amyotrophic lateral sclerosis (ALS) exhibit similar symptoms like patients with MG or CMS: denervation and muscle weakness. Although MuSK is not directly linked to ALS pathogenesis, its ectopic expression can restore retrograde muscle to nerve signaling, muscle innervation and can even lead to a delay of the onset of denervation (Perez-Garcia & Burden, 2012).

4.2 Muscle specific kinase

Muscle specific kinase (MuSK) is a RTK that plays a crucial role in NMJ formation and maintenance (Figure 5). It is a 120 kDa single-pass transmembrane glycoprotein (in mammals glycosylated). MuSK is expressed in skeletal muscle cells and once activated, contributes to three pathways: (1) clustering and anchoring of AChRs and muscle proteins responsible for synaptic transmission, (2) enhancing the transcription and translation of synaptic proteins in the muscle 'synaptic nuclei', and promotion of retrograde signals stimulating presynaptic differentiation (Burden et al., 2013). MuSK can act in two important phases of synapse formation: (1) prepatterning of the muscle in the prospective synaptic region before innervation, and (2) responding to neuronal agrin to form and stabilize synapses. Without innervation, AChRs and synaptic proteins are expressed and clustered in the central, prospective synaptic region of the muscle. They are nerve-independent but dependent on MuSK and Lrp4. This mechanism is called muscle

prepatterning and has a role in directing where motor axons grow and form synapses (Burden et al., 2013).

Kim and Burden (2008) showed that MuSK is prepatterned in the muscle and becomes confined to the prospective synaptic region. How this MuSK expression at these specific sites is regulated is not well understood. Some suggestions on what prepatterning is dependent on are: (1) early expression of Lrp4 and MuSK in myotubes and activation of MuSK by Lrp4, (2) positive-feedback regulation, which enhances MuSK and Lrp4 expression in muscle nuclei close to MuSK activated sites which form clusters of Lrp4 and MuSK and (3) the pattern of the growing muscle itself which is due to fusion of myoblasts (Kim & Burden, 2008). Additionally, further muscle-derived ligands may activate MuSK and stimulate prepatterning. Wnt proteins (see section 4.10) bind frizzled-MuSK cysteine-rich domain (fz-MuSK-CRD) in an agrin-independent manner and can participate in this mechanism.

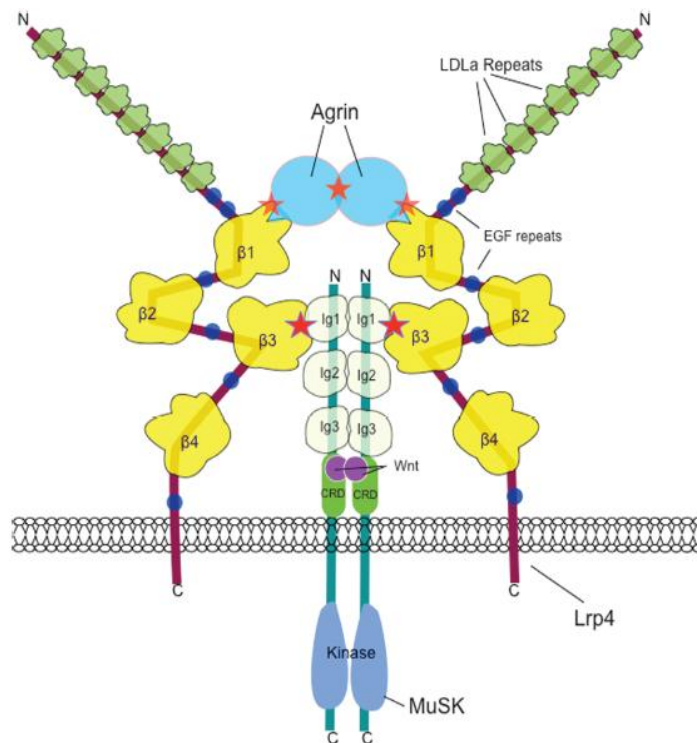


Figure 5: Agrin-Lrp4-MuSK complex. Two agrin-Lrp4 binary complexes associate with each other with a noncrystallographic two-fold symmetry (Zong and Jin, 2012; Zong et al., 2012). MuSK dimerization is important for MuSK activation (Stiegler et al., 2006). Agrin interacts with Lrp4 at the first $\beta 1$ propeller domain (Zong et al., 2012). Lrp4 and MuSK interact through the third $\beta 3$ propeller of Lrp4 and the Ig1 domain of MuSK. Wnts may interact with the CRD domain of MuSK. Red stars indicate the sites of interaction. Reviewed in (Barik, Zhang, Sohal, Xiong, & Mei, 2014)

Motor axons release agrin and ACh. Agrin binds to Lrp4, which stimulates the association between Lrp4 and MuSK (Figure 5). This leads to MuSK phosphorylation. Once phosphorylated in the juxtamembrane

region, MuSK recruits adaptor protein Dok-7, which forms a dimer and further stabilizes the dimerization of MuSK (Figure 2). Phosphorylation of two tyrosine residues in the C-terminal domain of Dok-7 stimulates recruitment of the two adaptor proteins Crk/Crk-L, which activate a poorly understood signaling pathway that leads to the anchoring of Rapsyn and AChRs at sites where MuSK is activated (Burden et al., 2013).

Figure 6 shows the structural details of MuSK. The extracellular domain comprises three immunoglobulin-like domains (Ig1-3) and a cysteine-rich domain (fz-CDR). This CRD has a high structural similarity to the CRD of Frizzled proteins (Wnt receptor), mediating its interaction with several Wnt proteins including Wnt4, Wnt9a and Wnt11, which will be mentioned in more detail later in this thesis (Maselli et al., 2010). Wnt molecules have been shown to play a role in agrin-independent prepatterning but also regulate agrin-induced AChR clustering *in vitro*. However, the general role of Wnt-induced NMJ formation remains largely unknown. The cytoplasmic domain of MuSK contains the tyrosine kinase domain (TKD). MuSK autophosphorylation in *trans* occurs on Tyr553 in the cytoplasmic juxtamembrane domain and contributes to the action of MuSK activation (Till et al., 2002). Furthermore Tyr750, 754 and 755 in the activation loop of the kinase domain are autophosphorylated, which relieves autoinhibition in the kinase domain and leads to MuSK activation and further downstream signaling as already mentioned (Watty et al., 2000). MuSK is not only involved in NMJ formation in embryogenesis, but also in its maintenance in adults. Deletion of and mutations in MuSK CRD in mice, as well as auto-antibodies against Ig1, Ig2 and the CRD of MuSK can cause MG and other severe defects in muscle prepatterning, which contributes to the first step of NMJ formation (Barik, Lu, et al., 2014). Furthermore it has been shown that these synapses associate with a drastic defect in AChR clusters, severe NMJ dismantlement, show excessive outgrowth of motor axons bypassing the AChR clusters and the inability of MuSK interacting with adaptor proteins like Dok-7 (Maselli et al., 2010).

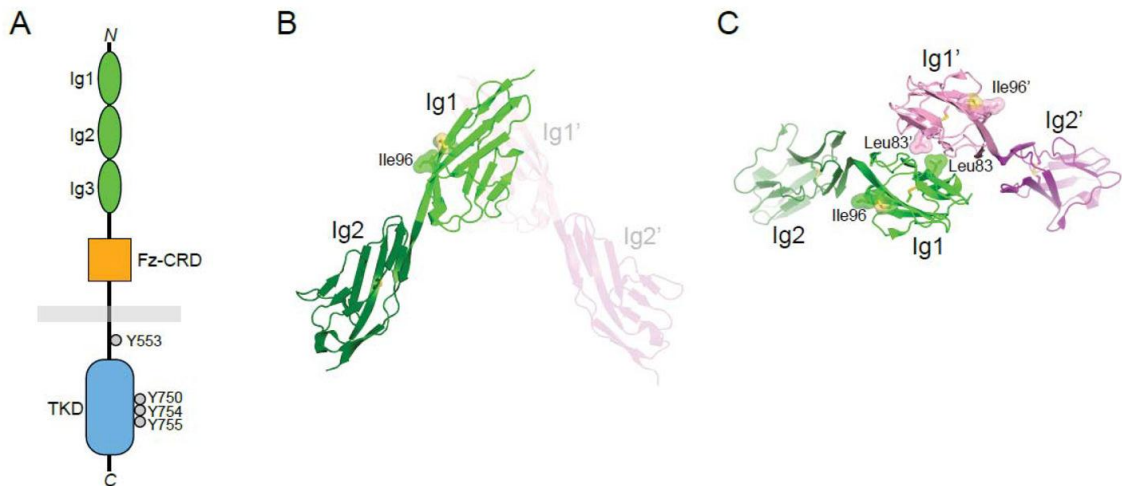


Figure 6: MuSK architecture and structure (A) Schematic diagram of MuSK. The extracellular region contains three immunoglobulin (Ig)-like domains and a Frizzled-like cysteine-rich domain (Fz-CRD). The cytoplasmic domain contains the catalytic tyrosine kinase domain (TKD). Autophosphorylation (in trans) occurs on Tyr553 in the juxtamembrane region and Tyr750/754/755 in the activation loop of the kinase domain. **(B)** Crystal structure of Ig1-2 (PDB ID: 2IEP), highlighting in Ig1 a solvent exposed disulfide bridge and adjacent Ile96. The second protomer in the crystallographic asymmetric unit is shown in light colors, and the domains are labeled with a prime ('). **(C)** Dimer of Ig1-2 mediated by Leu83 in Ig1. The view is approximately 90° from that in (B), from the top. Coloring and labeling as in (B). Reviewed in (Hubbard & Gnanasambandan, 2013)

4.3 Lrp4

Low-density lipoprotein related protein 4 (Lrp4) is an important *cis*-acting member of the low-density lipoprotein (LDL) receptor (LDLR) family. It serves as an Agrin receptor (in *trans*), is required for Agrin-induced MuSK activation (in *cis*), NMJ formation and AChR clustering in muscle cells (Weatherbee, Anderson, & Niswander, 2006). It plays an

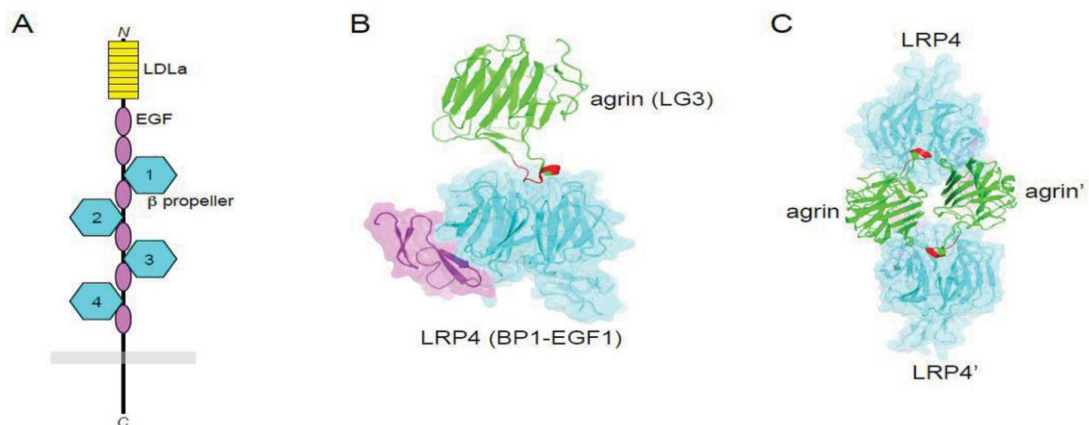


Figure 7: Structure of Lrp4 and its interaction with agrin (A) Structure of LRP4. The extracellular region consists of eight LDLa repeats, two EGF-like domains, four β propeller-EGF units and a short cytoplasmic region **(B)** Crystal structure of agrin (LG3 domain) bound to the first β propeller-EGF unit of LRP4. Coloring of LRP4 as in **(A)**. The $\alpha 8$ splicing insert of agrin is colored red. **(C)** 2:2 complex of agrin and LRP4 observed in the crystal structure. Same coloring as in **(B)**. The domains in the second 1:1 agrin:LRP4 complex are labeled with a prime ('). ; Reviewed in (Hubbard & Gnanasambandan, 2013)

important bidirectional role in pre- and postsynaptic differentiation (Bergamin et al., 2010; Glass et al., 1996). It is a direct muscle-derived retrograde signal and its effect in presynaptic differentiation is secondary to MuSK activation and postsynaptic differentiation (Yumoto et al., 2012).

Similar as mice lacking MuSK, agrin or Dok-7, *Lrp4*-mutant mice die at birth and do not form NMJs (D. C. Berwick & K. Harvey, 2013). Since MuSK is not directly activated by agrin the missing link between them is Lrp4. It is a 220 kDa single-transmembrane protein with a large extracellular domain containing multiple LDLR repeats, EGF-like and β -propeller-repeats (Gomez & Burden, 2011). Additionally, Lrp4 contains a transmembrane domain and a short C-terminal region with so far unidentifiable catalytic activities (Figure 7).

After binding of nerve-derived agrin to Lrp4 and following MuSK activation, stabilization and anchoring of key postsynaptic proteins, Lrp4 has a direct role in motor axon growth and differentiation. Furthermore, AChR cluster fragmentation, decreased junctional folds and diminished synaptic vesicles are observed in *Lrp4* inducible muscle-specific knock-out mice (imKO-mice). Doxycycline-dependent depletion of *Lrp4* in an adult mutant mouse strain leads to impaired synaptic transmission due to reduced amplitude and frequency of endplate potentials (Barik, Lu, et al., 2014). Lrp4 can activate MuSK in the absence of agrin and muscle prepatterning depends upon Lrp4 and MuSK but not on agrin. Increased MuSK expression is sufficient to rescue AChR clustering in *Lrp4*-mutant and *agrin*-mutant mice indicating that agrin and Lrp4 act to ensure sufficient MuSK activity (Burden et al., 2013; Samuel, Valdez, Tapia, Lichtman, & Sanes, 2012). MuSK overexpression can bypass the normal requirement for Lrp4 in postsynaptic differentiation. However, MuSK overexpression cannot rescue presynaptic differentiation or the neonathality of *Lrp4*-mutant mice. This shows that Lrp4 has an essential role in early presynaptic differentiation as to arrest motor axon growth and clustering of synaptic vesicles (Yumoto et al., 2012). As explained before, *Lrp4*-mutant myotubes are unresponsive to agrin. Experiments

show that introduction of only the extracellular part, even in the soluble form (without intracellular and transmembrane domains) can restore agrin-stimulated MuSK activation and AChR clustering (Gomez & Burden, 2011). Revealing the structural complexity of the agrin-Lrp4-MuSK complex (Figure 5), it was shown that for neural agrin binding, the LDLa repeats 6-8, the first β -propeller domain and the two intervening EGF-like domains in Lrp4 are sufficient. However, for Lrp4 binding to MuSK the LDLa repeats 4-8, β -propeller domain 1-3 and the two intervening EGF-like domains are necessary (Figure 7) (W. Zhang, Coldefy, Hubbard, & Burden, 2011).

4.4 Docking protein-7

Docking protein-7 (Dok-7) is a cytoplasmic adaptor protein, which has the unique function of being a substrate of MuSK as well as an activator of MuSK's kinase activity. In human, 504 members of adaptor proteins that include Dok 1-7 and insulin receptor substrates 1-4 can be found. They are all characterized by an N-terminal pleckstrin-homology (PH) and phosphotyrosine-binding (PTB) domains and C-terminal tyrosine-phosphorylation sites. CMS can be caused by recessive mutations in Dok-7. Revealing the structure, Bergamin and Hubbard (2010) show that Dok-7 PH and PTB forms a dimeric structural unit that dimerizes MuSK and facilitates its trans-autophosphorylation of tyrosines in the activation loop of MuSK. The important phosphorylation step of MuSK Tyr553 (pTyr553) leads to binding of the PTB domain of Dok-7 to this sequence motif and driving Dok-7, besides being a substrate of MuSK, into activating the MuSK catalytic kinase activity. The PH-domain facilitates this interaction by binding to phosphoinositides in the plasma membrane (Hubbard & Gnanasambandan, 2013). The Dok-7 PH-PTB-dimer is only formed when MuSK pTyr553 is present. This indicates that dimerization is dependent on the connection of the PTB domain with the MuSK juxtamembrane region. Phosphorylation of two tyrosine residues in the C-terminal domain of Dok-7 leads to recruitment of two adapter proteins Crk and Crk-L (Hallock et al., 2010). It is possible, that Crk/Crk-

L associated with phosphorylated Dok-7 forms complexes with Rac/Rho GEFs and thereby links MuSK activation, with a change in actin dynamics and redistribution of postsynaptic proteins including AChRs in myotubes (Figure 2).

4.5 Agrin & Cytoskeletal rearrangements

Agrin is a nerve-derived proteoglycan with a size of 200 kDa. It is an important organizer of postsynaptic differentiation, which becomes concentrated in the synaptic cleft as the NMJ develops. The alternatively spliced 'z-agrin' produced only by motor neurons binds to its postsynaptic receptor Lrp4, which additionally forms a tetramer with MuSK initiating the signaling cascade. Z-agrin binds Lrp4 to subsequently activate MuSK to stabilize aneurally formed clusters of AChR and induce formation of new clusters in the muscle membrane (Figure 7) (Matsumoto-Miyai et al., 2009)

Agrin normally binds to the N-terminal region of Lrp4 and stimulates the association between Lrp4 and MuSK. Especially the LDLa repeats 6-8 and the first β -propeller domain of the extracellular Lrp4 is important for binding to agrin (Figure 7). Loss of *agrin* by conditional deletion from adult mice motoneurons therefore results in depletion of AChR receptors, dispersal of basal lamina components, NMJ dystrophies and can even lead to nerve retraction (McMahon & Boucrot, 2011; Samuel et al., 2012). Additionally, the presynaptic deficits can also disrupt postsynaptic development due to disruption of the retrograde signaling from muscle back to nerve. Altered NMJs can be explained with altered distribution of synaptic cleft components like agrin and synaptic laminins. A key-step in the process of plaque-to-pretzel maturation of the postsynaptic membrane is the structural reorganization, which is said to be regulated by specific cleavage of agrin. The agrin-cleaving protease is called neurotrypsin and cuts agrin at two specific, highly conserved sites, which results in a 90 kDa fragment and the 22 kDa fragment, which is neurotrypsin dependent (Pato et al., 2008). One

product is the soluble NMJ-promoting C-terminal domain of agrin. Bolliger et al. (Bolliger et al., 2010) demonstrated the correlation between the efficiency of agrin cleavage and its effect on NMJ formation. They found that the plaque-to-pretzel maturation is dependent on agrin signaling. Excessive overexpression of neurotrypsin in motoneurons leads to high reorganization activity and rapid dispersal of synaptic specialization (Bolliger et al., 2010).

Another important agrin-triggered mechanism involved in AChR stabilization is actin cytoskeleton polymerization. Especially in muscle, so-called membrane rafts are involved in AChR clustering. These membrane raft components regulate the assembly and stabilization of synaptic proteins of the postsynaptic membrane at the NMJ. (Cartaud, Stetzkowski-Marden, Maoui, & Cartaud, 2011). Upon agrin signaling two proteins are transiently raft-associated: The actin-nucleation factors, N-WASP (neuronal Wiscott-Aldrich syndrome protein) and Arp2/3 (actin-related protein). Muscle membrane lipid rafts provide the appropriate microenvironment for AChR clusters. Studies by Pato et al. in 2008 and Stetzkowsky-Marden et al. in 2006 (Pato et al., 2008; Stetzkowski-Marden, Gaus, Recouvreur, Cartaud, & Cartaud, 2006) showed that agrin-induced clusters correspond to sarcolemma-domains, a specific state of lipid bilayer that is thought to characterize clustered rafts. Numerous studies have already shown the downstream partners of activated MuSK, which are involved in actin-remodeling as so-called actin nucleation proteins: Tyrosine kinase Abl, geranylgeranyltransferase, serine/threonine kinase Pak1, small GTPases of the Rho family, Rac and Cdc42 (cell division cycle 42), Src family kinases and Rho-GEF. Additionally at mature or developing NMJs, cytoplasmic actin and actin binding proteins such as vinculin, α -actinin, filamin, utrophin, APC (adenomatous polyposis coli protein) and cortactin are accumulating at AChRs. Agrin triggers the activation of Rac and Cdc42, which leads to AChR clustering. Cdc42 drives actin polymerization by N-WASP-activation, which subsequently switches on Arp2/3 complex. It is already reviewed (Viola & Gupta, 2007) that the

complex mechanism underlying the actin-based regulation of raft dynamics on ligand stimulation is a complex mechanism involving several actin-polymerization or nucleation factors and requires several degrees of actin regulation. The multiple step process involves Arp2/3 in the early phase and since it's no longer observed, in fully developed AChR clusters there must be a novel, unknown organizer upon cluster maturation.

4.6 Focal Adhesion & Focal Adhesion Kinase

Focal adhesions (FAs) represent the physical link between the extracellular matrix (ECM) and the intracellular actin cytoskeleton (Brinas, Vassilopoulos, Bonne, Guicheney, & Bitoun, 2013). It is an important platform supporting intracellular membrane traffic, endocytosis from the plasma membrane and several signaling pathways. FAs are the major site of cell attachment and composed of transmembrane receptors including integrins, structural proteins like vinculin, talin, α -actinin and signaling proteins such as focal adhesion kinase (FAK). In addition, assembly and disassembly of FAs are important mechanisms in cell adhesion, migration and endocytosis. During cell movement, FAs form at the leading edge of the cell to anchor cytoplasmic stress fibers and generating a contractile force (Chin et al., 2015). Disassembly of these FAs on the leading edge contributes to ECM detachment.

Three different proteins involved in FA assembly, endocytosis, intracellular membrane trafficking, vesicle formation and subsequent AChR cluster stabilization are important in this study: Focal adhesion kinase (FAK), Dynamin-2 (Dyn2) and EB3.

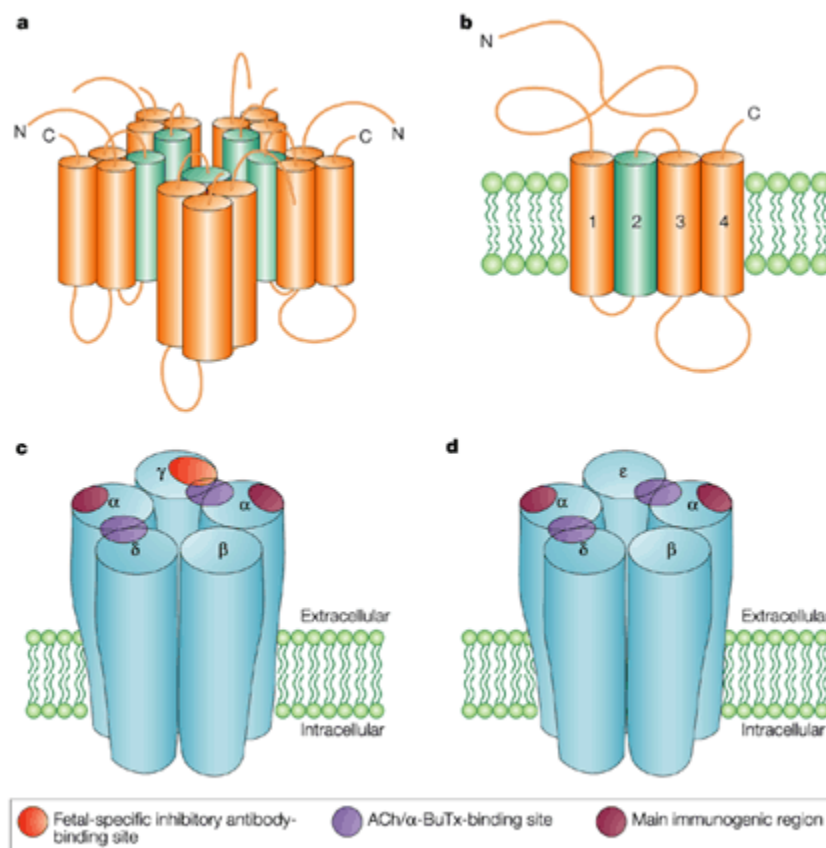
Dynamin-2 (Dyn-2) is an ubiquitously expressed large GTPase, involved in vesicle formation and release in clathrin-dependent and -independent endocytosis. Furthermore, Dyn-2 mutations are associated with human muscle diseases like centronuclear myopathy (CNM) and Charcot-Marie-Tooth (CMT) (Liu, Lukiyanchuk, & Schmid, 2011;

Sidiropoulos et al., 2012). Besides transportation of vesicles from endosomal system and the Golgi apparatus, Dyn-2 directly interacts with microtubule and actin cytoskeleton. Dyn-2 is a 98 kDa protein composed of an N-terminal catalytic GTPase domain, a middle domain involved in Dyn-2 self-assembly, a pleckstring homology domain (PH), which interacts with membrane phosphatidylinositol 4, 5-bisphosphate and therefore is involved in the targeting of Dynamin to the membrane. Additionally, a GTPase effector domain is regulating the GTPase activity and the C-terminal proline-rich domain (PRD) containing multiple Src homology 3 (SH3)-binding motifs participates in protein-protein interactions. Dyn-2 is phosphorylated at FAs by Src kinase and is recruited to FAs by a direct interaction with the 4.1/ezrin/radixin/moesin (FERM) domain of FAK. FAK itself functions as an adaptor mediating between Src and Dyn-2, facilitating Dyn-2 phosphorylation. FAK and Src are both non-receptor tyrosine kinases acting as the central key players of FA turnover (Y. Wang, Cao, Chen, & McNiven, 2011).

After invagination, Dyn-2 is accumulating at the neck of the forming pit and -together with actin filaments-responsible for the fission of the coated vesicle. Inhibition of Dyn-2 activity inhibits clathrin-mediated integrin internalization, FA disassembly and impairs cell migration as does depletion of clathrin. This is true for motor neural cells as well as Schwann cells, which show strongly impaired myelination (Burden, 2011). FAK is a known FA scaffolding, actin binding adaptor and cytoskeletal protein. The FAK SH2-domain (pTyr-379) binds and activates Src. Src in turn phosphorylates FAK on multiple tyrosine residues, recruiting additional FA proteins. The activated FAK binds Dyn-2 directly via its FERM-domain, facilitating Dyn-2 tyrosine phosphorylation and activation. Phospho-Dyn-2 (pDyn-2-Tyr231) regulates then clathrin-mediated endocytotic internalization of β 1-integrins and subsequent FA disassembly. This Src-FAK-Dyn-2 complex is activated when integrines bind ECM.

4.7 Acetylcholine Receptor

Muscle and neuronal nicotinic AChRs are pentameric receptors with subunits clustered around a central pore. They are located at the terminal expansions of postsynaptic junctional folds in a density of about 10000 AChRs/ μm^2 (Borges et al., 2008). These receptors are members of a superfamily of ligand-gated ion channels, which mediate fast synaptic transmission. Each receptor subunit consists out of an extracellular domain, four transmembrane domains (M1-M4) and a cytoplasmic region (Figures 8 and 9). The adult form comprises $(\alpha)_2$, β , δ and ϵ subunits, whereas the fetal form consists out of $(\alpha)_2$, β , δ and γ .



Nature Reviews | Immunology

Figure 8: (a) The acetylcholine receptor (AChR) is a pentameric membrane protein. (b) Each subunit consists out of an extracellular domain, four transmembrane regions and a cytoplasmic domain. The receptor consists of $(\alpha)_2$, beta, gamma and delta subunits in the fetal form (c), and $(\alpha)_2$, beta, delta and alt epsilon subunits in the adult form (d). A large proportion of the antibodies in the sera of myasthenia gravis patients bind to the main immunogenic regions that are on both of the α subunits (α_{64-76}). In addition, many patients' antibodies bind to the fetal-specific gamma subunit. In some cases, these antibodies inhibit the function of the AChR in vitro, and in pregnant mothers, they can cross the placenta, causing fetal muscle paralysis and severe, and often fatal, deformities. Alpha-BuTx, α -bungarotoxin. Reviewed in (Vincent, 2002)

The two dimeric ACh binding sites ($\alpha 1/\epsilon$ and $\alpha 1/\delta$) are formed by three or more peptide loops in the α -subunit with two peptide loops in its adjacent subunit, which are at the same time the α -Bungarotoxin (BGT) binding regions. The α -subunit forms the ACh binding site and contributes to the main immunogenic region (MIR, AA64-76 in the extracellular region) and the β -subunit regulates rapsyn-

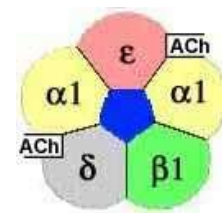


Figure 9: **Structure of the pentameric, adult muscle AChR** with two ACh binding sites at the α subunit (image extracted from <http://neuromuscular.wustl.edu/mother/acetylcholine.htm#achrnic>)

dependent, cytoskeletal rearrangements and AChR anchoring via phosphorylation of its Tyr390 residue (Borges & Ferns, 2001; Sabourin & Rudnicki, 2000). A large proportion of antibodies found in the sera of MG patients as well as the antagonistic neurotoxin α -Bungarotoxin bind to the MIR in the α -subunit, thereby blocking the action of ACh in the postsynaptic membrane and leading to muscle paralysis and respiratory failure.

4.8 Myogenic differentiation

Myogenic differentiation, skeletal muscle formation and formation of muscle fibers is regulated by many hormones, growth factors, signaling cascades and transcription factors. C2C12 cells for instance start differentiation to multinucleated myotubes upon withdrawal of serum or mitogens from myoblast cultures. The two most important transcription factor families involved in fate determination are MEF2 (myocyte enhancer-binding factor 2) and MRFs (myogenic regulatory factors). These intracellular signaling pathways include the extracellular signal-regulated kinase/MAPK, p38 MAPK and phosphatidylinositol 3-kinase (PI3K)/AKT pathways. The ERK/MAPK pathway elicits differentiation signals to promote or inhibit differentiation and fusion in the presence of mitogens (Li, Jiang, Ensign, Vogt, & Han, 2000). The p38 MAPK pathway is required for myogenic differentiation and also promotes skeletal muscle differentiation, at least in part via activation of myocyte enhancer binding factor 2 (MEF2). In addition, PI3K/AKT signaling

positively regulates myogenic differentiation when insulin-like growth factor (IGF) is stimulated

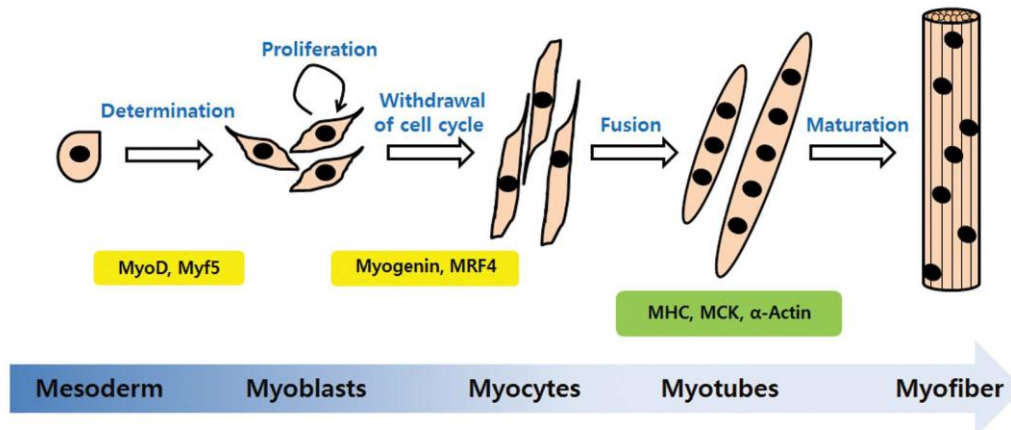


Figure 10: **The steps of myogenic differentiation.** Myoblasts originate from the mesoderm and are converted to skeletal muscle lineage myoblasts after MyoD and Myf5 expression. First, myoblasts enter the cell cycle and proliferate. Upon withdrawal of myoblast growth factor or mitogen, proliferating cells exit from the cell cycle and initiate differentiation. Myogenin and MRF4 are involved in initiation of differentiation. In this step, myoblasts changed to an elongated shape and are called myocytes. Myocytes fuse with neighboring cells into multinucleated myotubes. The multinucleated myotubes express the muscle specific proteins, MHC (myosin heavy chain), muscle creatine kinase (MCK) and α -actin. The mature form of myotubes is turned to myofiber. Reviewed in (Jang & Baik, 2013)

Myo-satellite cells are mitotically quiescent cells, which re-enter the cell cycle and start proliferation via activation by exercise, muscle injury or a pathological state (Chappie et al., 2011). Entering differentiation, cells irreversibly withdraw from the cell cycle, start fusion with myofibrils, differentiate into mononucleated myocytes and fuse then to multinucleated myotubes expressing myosin heavy chain (MHC), α -actin and muscle creatine kinase (MCK) (B. Zhang et al., 2008). The most important members of the MRF family are MyoD and Myf5, which initiate the myogenic program and convert non-muscle cells to the skeletal muscle lineage (Choi & Holtzer, 1990; Serna & Imbalzano, 2005). Le Grand et al.(2007) suggested, that Myf5 regulates the proliferation rate of myoblasts and MyoD is required for their differentiation (Figure 10).

JAKs (Table 1) are a family of non-receptor tyrosine kinases (JAK1-3 and TYK2 in mammals) with its downstream counterpart of the

STAT-family (STAT1, 2, 3, 4, 5A, 5B, 6) (Kisseleva, Bhattacharya, Braunstein, & Schindler, 2002). The Janus Kinase (JAK)/signal transducer and activator of transcription (STAT)-pathway is activated by binding of cytokines or growth factors to their receptors, activating /phosphorylating the receptor-associated JAKs on specific tyrosine residues, leading to phosphorylation of selected STATs. Activated STAT dimerize and translocate into the nucleus, functioning as a transcription factor and initiating target gene activation (Hankey, 2009).

This pathway not only regulates proliferation and differentiation of muscle cells, but also that of many cell types, including immune cells, hematopoietic stem cells, osteoblasts and neuronal precursor cells.

Table 1: Overview over proteins involved in JAK/STAT action: JAK1 in combination with STAT1 or 3 regulate proliferation, whereas JAK2 or 3 together with STAT1, 2 or 3 are involved in differentiation. Modified from JAK-STAT 2013; 2:e23282;

	<i>Proliferation</i>	<i>Differentiation</i>
<i>JAKs family</i>	JAK1	JAK2,3
<i>STATs family</i>	STAT1,3	STAT1,2,3
<i>Transcription factor</i>	Mef2-STAT1	MyoD-Mef2
	MyoD STAT3	MyoD-STAT3
<i>Signaling pathway</i>	MEK/ERK	PI3K/AKT
<i>Inducer</i>	LIF	IGF

4.9 Tet-On-System

The TET-On-System is a two-vector system designed for a tight regulation of transgenes in mammalian cells with a minimal dosage of doxycycline (Chao, Chao, Chang, Chiu, & Yuan, 2012; Fellmann et al., 2013). The Tet-On system uses a two-component conditional expression system that requires a reverse tetracycline transactivator (rtTA) and a tetracycline-responsive element (TRE) promoter driving shRNA expression (Gossen et al., 1995; Zuber et al., 2011) and leading to target gene downregulation. A C2 Tet-On cell line is a double stable cell

line containing both, the regulatory and response plasmid. RtTA binds the TRE and activates the transcription of shRNA only in the presence of doxycycline. In this thesis, the retroviral RT3GEP vector (carrying a puromycin selection cassette, GFP as a fluorescent marker and T3G as a Tet responsive element promoter) with EcoRI and XhoI shRNA insertion sites is chosen to function as the Tet regulatory element (Fellmann et al., 2013). GFP is co-expressed upon doxycycline stimulation and serves as a control for the efficiency of tet-induced expression (see section 5.6.10).

4.10 Wnt proteins

The formation of a neuronal network or a specific synapse involves precise and coordinated activation of several signaling pathways and their molecules. Wnt proteins are involved in a wide range of critical developmental cell functions, such as cell division, migration and synaptogenesis. In neuronal development they play a crucial role in axon pathfinding, connectivity, dendritic development/ arborization and synaptogenesis. Wnts are secreted, lipid-modified glycoproteins that are highly conserved among metazoans and are a large family of, in humans, 19 isoforms. The term 'Wnt' itself derives from the *Drosophila* gene *wingless* (*wg*) and the vertebrate gene *Int-1*. It has already been shown 40 years ago, that *wg* is indispensable in early embryonic patterning. Wnts are modulating the formation of the NMJ by affecting the differentiation of pre-/ and postsynaptic components, especially the distribution and clustering of AChRs on the muscle membrane. Wnts are controlling the expression of several myogenic regulator factors (MRFs), such as MyoD, Myf5 and Myogenin, thus regulating the differentiation of myoblasts. They transduce signals through Frizzled receptors and co-receptors Lrp5/6 (low density lipoprotein receptor-related protein 5 and 6), which have an extracellular domain with a very high similarity to the domain in Lrp4. However, a definite binding of Wnts to Lrp4 still remains to be verified (He, Semenov, Tamai, & Zeng, 2004). Different pathways triggered by Wnt have been demonstrated to affect either positively or

negatively the differentiation of pre- and postsynaptic specializations to shape the embryonic development of the NMJ.

The β -catenin or canonical pathway (Figure 11a_{ii}) is the best understood cascade where Wnt binds to its Frizzled receptor (Fz) and the coreceptor Lrp5/6 and activates downstream target gene expression. Binding to these receptors recruits Dishevelled (Dvl), a scaffolding protein required for all Wnt pathways. Its phosphorylation recruits the Axin complex, which inhibits the serine-threonine kinase Glycogen synthase kinase 3 β (GSK3 β). This leads to inhibition of β -catenin phosphorylation and its subsequent accumulation in the cytoplasm. Furthermore, β -catenin translocates into the nucleus and activates target gene expression by T cell factor/ lymphoid enhancer factor (TCF/LEF)-mediated transcription. In the absence of Wnt proteins (Figure 11a_i), the β -catenin level remains relatively low by the action of the so-called 'destruction complex' formed by the scaffolding protein Axin, adenomatous polyposis coli (APC) and the enzyme GSK3 β . This complex phosphorylates β -catenin stimulating its destruction by the proteosomal pathway. Wnt-Fzd-interaction is recognized by the activated Dvl protein.

In the planar cell polarity pathway (PLP, Figure 11b) the Wnt-Fz dependent recruitment of Dvl leads to activation of small GTPases, such

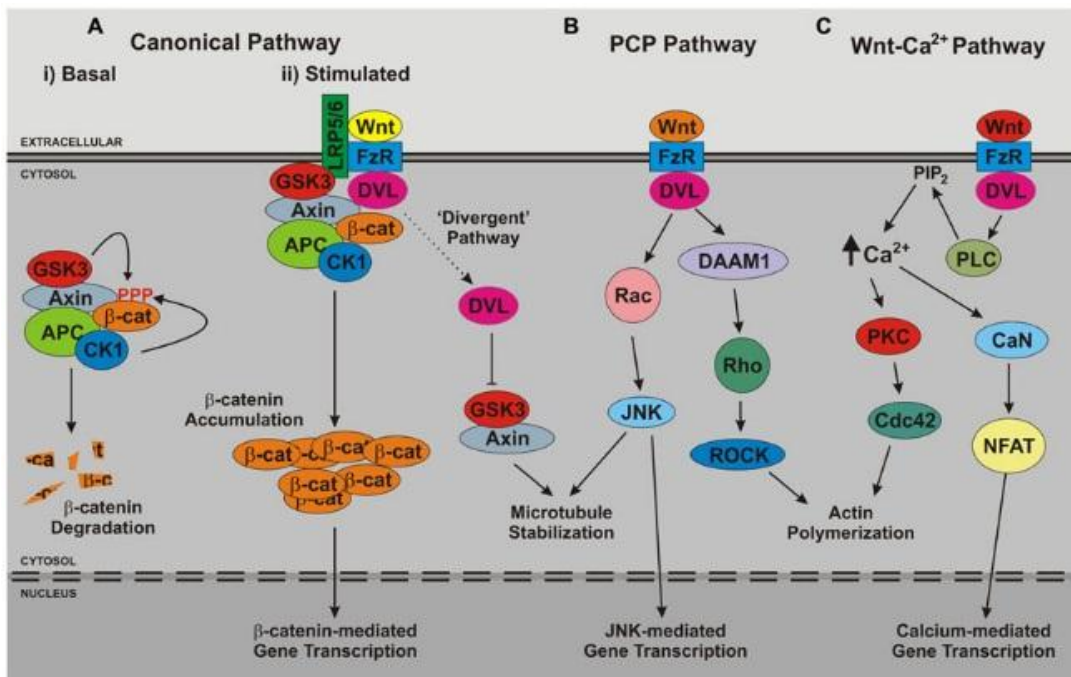


Figure 11: **Overview of Wnt signaling pathways.** The three major branches of Wnt signaling – (A) the canonical, (B) planar cell polarity (PCP) and (C) Wnt-Ca²⁺ – pathways are illustrated. Reviewed in (Daniel C. Berwick & Kirsten Harvey, 2013)

as Rho and Rac, which subsequently activate the c-Jun N-terminal kinase (JNK). This kinase either signals to the nucleus triggering target gene activation or it modifies the cytoskeletal stability via phosphorylation of MAPs (MAP1B, Tau, MAP2) and actin regulator proteins. Dvl also activates Dvl-associated activator of morphogenesis 1 (Daam1) controlling cell and tissue polarity.

The third pathway is *the calcium pathway* (Figure 11c) where Dvl activates downstream trimeric G-proteins and the enzyme phospholipase C (PLC). PLC hydrolyzes PIP₂ to produce IP₃ and DAG, which increases the intracellular calcium due to activation of IP₃ receptor and activates calcium/calmodulin dependent protein kinase II (CaMKII) and phosphatase calcineurin. Some of these enzymes regulate the transcription factor NF-AT, promoting the expression of target genes.

4.10.1 Wnt in Prepatterning, NMJ formation and AChR clustering

The fact that AChR clusters already appear in the central muscle region before innervation by a motor nerve terminal and that some activation pathways of Wnt signaling interfere with MuSK signaling, set the focus onto Wnt proteins and how they might be involved into prepatterning and NMJ formation. It was shown that agrin mutant mice exhibit normal prepatterning but the formation of larger AChR cluster, such as after innervation was inhibited. Separate studies discovered that the CRD of MuSK shows high similarities to the Frizzled receptor CRD, a human Wnt binding domain (Glass et al., 1996; Luo et al., 2002; Valenzuela et al., 1995). The first hint that Wnt proteins might be involved was provided by studies that found an interaction between MuSK and Dvl (Jing, Lefebvre, Gordon, & Granato, 2009). More precisely, suppression or inhibition of Dvl or disruption of Dvl-MuSK interaction inhibits agrin- and neuron-induced AChR clustering. It reduces the amplitudes of spontaneous synaptic currents and their frequency. Dvl signaling seems important for both, post- and presynaptic differentiation. Additionally, the Dvl adaptor APC was shown to regulate AChR clustering (J. Wang et al., 2003). Agrin promotes APC-AChR β subunit interaction. Through the ability of APC interacting with actin and microtubules, it is able to link AChRs to the cytoskeleton and to localize them to the NMJ. Separate studies by Zhang (B. Zhang et al., 2012) and Dobbins (Dobbins, Luo, Yang, Xiong, & Mei, 2008) suggested that β -catenin regulates AChR clustering by bridging AChR and Rapsyn with α -actinin-associated cytoskeleton.

Wnt signaling and postsynaptic development at the vertebrate NMJ is very complex. Experiments using the Wnt antagonist secreted Frizzled related protein 1 (Sfrp1) have shown that muscle exposed to the inhibitor show decreased prepatterning and AChR clustering (using Wnt4, Wnt11 and Wnt3). This strengthen the hypothesis that endogenous Wnt regulates postsynaptic assembly (Henriquez et al., 2008). Wnt4, 9a and 11 are able to bind MuSK and Wnt4 and 11

additionally activate it even without the presence of agrin. Additionally, mRNA expression of Wnt4, 9a and 11 was demonstrated in muscle cells, indicating a role in NMJ formation. These Wnts initiate Dvl-dependent canonical Wnt-pathway to induce clustering. However, the effect of Wnt and agrin is not additive during AChR clustering and is less effective compared to agrin (Strochlic et al., 2012).

Little is known about the action and function of Wnt in AChR clustering and NMJ formation. In 2012, Strochlic (Strochlic et al., 2012) reported the crucial role of Wnt4 in vertebrate junction formation. Wnt4 is primarily expressed in early embryogenesis, when the first nerve-muscle contacts are formed, it binds to the extracellular CRD domain of MuSK and increases MuSK phosphorylation levels. Wnt4^{-/-} mutant mouse embryos showed innervation defects, nerves bypassing AChR clusters and 30% of unapposed nerve terminals. Experiments with cultured myotubes revealed an increased AChR cluster number in Wnt4 overexpressing myotubes and an increased number in Wnt4 loss of function tests.

There are different models for postsynaptic development in different species. In zebrafish, the Wnt11r or Wnt4b ligands are expressed from tissues adjacent to the newly formed muscle fibers. AChR prepatterning requires Wnt11r and Wnt4a. Only the combined knockout of both Wnts causes complete loss of aneural AChR clusters. Additionally, Wnt4a and Wnt11a are shown to stimulate MuSK translocation from muscle surface to recycling endosomes (Gordon, Gribble, Syrett, & Granato, 2012). Wnt4b and Wnt11r activate MuSK-dependent AChR cluster prepatterning in myotubes and the guidance of motor axon. MuSK is translocated to endosomes in the middle region of the muscle fiber and assembles a complex with scaffolding proteins such as Diversin, Rho A and Daam1 to position aneural AChR clusters in the central muscle band, guiding the arriving motor axon (B. Zhang et al., 2008). An important example of the interaction between Wnt- and agrin-pathway in postsynaptic NMJ differentiation is Wnt3. Wnt3 activates, prior to innervation, first the small GTPase Rac1 which rapidly induces

the formation of unstable microclusters. These microclusters are aggregated into stable, bigger clusters after agrin-dependent activation of Rho (Henriquez et al., 2008).

One interesting finding is the inhibitory effect of β -catenin on AChR clustering (Wang et al., 2013). Wnt3a is expressed by the developing skeletal muscle and its Wnt/ β -catenin pathway inhibits AChR clustering but promotes presynaptic behavior via a retrograde signal. In this case, Wnt3a activates the β -catenin pathway that induces the dispersal of AChR clusters through inhibition of Rapsyn expression. Specific ablation or stabilization of β -catenin in muscles, but not in motor neurons, results in presynaptic defects showing that a still unknown retrograde signal exists for presynaptic differentiation (J. Wang et al., 2008).

4.11 Aim of the study

The main goal of this Master's Thesis was to provide further insight into the molecular mechanisms of MuSK activation, its downstream signaling and role in AChR clustering. This work is divided into two main projects: The first part was to establish stably expressing C2C12 Tet-ON cells where expression of proteins can be downregulated upon doxycycline stimulation. The focus was set on the following 4 proteins: Lrp4, EB3, Dynamin-2 and FAK.

The second part aimed to examine the role of Wnts during MuSK signaling. For this, I used a heterologous cell system to express and purify Wnt proteins and I performed co-immunoprecipitation/co-localization experiments to study Wnt/MuSK interaction.

The main questions of my study were:

1. Determine the role of cytoskeletal-associated protein in AChR clustering
 - a. Establishment of stable expressing C2 Tet-ON cell lines

- b. Testing RNAi-mediated downregulation with biochemistry methods and assaying the effect on AChR clustering
2. Wnt and their association with MuSK
- a. Examine the interaction between Wnt and MuSK
 - b. Optimization of Wnt expression and purification

5 Materials and Methods

5.1 Chemicals and Reagents

5.1.1 List of chemicals and reagents used in molecular and biochemistry methods

1M BES	Roth
1,4-diazabicyclo [2.2.2] octane (Dabco)	Roth
10x loading dye	Fermentas
1M Na ₂ HPO ₄	Roth
2.5M CaCl ₂	Roth
40% Acrylamide (Rotiphorese Gel 40)	Roth
5M NaCl	Roth
Acetic acid	Roth
Agarose	Roth
Alexa 594 and 555 conjugated α -BGT (IHC 1:500)	Invitrogen
Ammoniumperoxidisulfate (APS)	Roth
Ampicillin	Sigma-Aldrich
Aprotinin	Roth
Bovine serum albumin (BSA)	PAA
Bromophenol blue	Roth
Calcium chloride (CaCl ₂)	Roth
CHAPS	Roth
Coomassie	Roth
DH 10 <i>E.coli</i> strain	Invitrogen
Dimethylsulfoxide (DMSO)	Roth
Dithiothreitol (DTT)	Sigma-Aldrich
Dulbecco 's modified Eagle 's medium (DMEM)	Sigma Aldrich
DMSO (comp. Bacteria)	AppliChem
dNTPs	ThermoScientific
Ethanol (EtOH)	Merck
Ethidium bromide (EtBr)	Roth
Ethylene glycol bis (2-aminoethyl)-tetraacetic acid	Roth
Ethylene-diamine-tetraacetic acid (EDTA)	Roth
EtOH abs	Aust-Alco
Fetal bovine serum (FBS)	Gibco
G, B, R, O 10x Buffer Restriction Enzymes	ThermoScientific
Gelatine 0,2% in PBS	Sigma Aldrich
Gelatine from porcine skin	Sigma Aldrich
Gene ruler 1kb DNA ladder	Fermentas
Gentamycin (30-50 μ g/ml)	Roth

Glycerol	Roth
Glycine	Sigma Aldrich
Hank´s buffered salt solution (HBSS)	Lonza
HEPES	Roth
Horse serum (HS)	Invitrogen/Gibco
Hydrochloric acid (HCl)	Roth
Imidazole	Sigma Aldrich
Immobilon TH-P PVDF nylon membrane 0.45µm	Millipore
Isopropanol	Roth
Kanamycin	Roth
Lysogeny broth (LB)	Roth
Leica immersions oil	Leica
Leupeptin	Roche
Lumi-Light western blotting substrate	BioRad
Magnesium chloride (MgCl ₂)	Fluka
Magnetic beads (SureBeads Protein A)	BioRad
Methanol (MeOH)	Roth
MgCl ₂	Roth
MgSO ₄	Roth
Milkpowder	Roth
Mowiol 4-88	Roth
Neural agrin (4.8)	Herbst and Burden, 2000
Ni-NTA Resin beads	GE Healthcare
Nonidet P-40 or Octylphenoxypolyethoxyethanol	Fluka, Sigma ALdrich
Page ruler prestained protein ladder (10-170 kDA)	Fermentas
Paraformaldehyde (PFA)	Fluka
PBS	Sigma Aldrich
PEG	Sigma Aldrich
Penicillin Streptomycin	Sigma Aldrich
Pepstatin-A	US Biological
Phenol/Chloroform	Roth
Phenylmethanesulfonylfluorid (PMSF)	Roth
PoliAcrylamid Rotiphorese Gel 40	Roth
Potassium chloride (KCl)	Roth
Potassium dihydrogen phosphate (KH ₂ PO ₄)	Roth
Pre-clearing beads (Pierce Control Agarose Resin)	ThermoScientific
Protein A Agarose Beads	Roche
Protein G Agarose Beads	Roche
Page Ruler Prestained Protein Ladder	ThermoScientific
Page Ruler Plus Prestained Protein Ladder	ThermoScientific

Puromycin	Roth
RIPA buffer	Assay buffer
SAP buffer	ThermoScientific
SDS pellets	Roth
Silver Nitrate	Roth
Sodium azide (NaN ₃)	Sigma-Aldrich
Sodium chloride (NaCl)	Roth
Sodium dodecyl sulfate (SDS)	Serva GmbH
Sodium fluoride (NaF)	Sigma-Aldrich
Sodium hydrogen phosphate dihydrate	Roth
Sodium hydroxide (NaOH)	Roth
Sodium orthovanadate	Sigma-Aldrich
Supersignal Western Blot Substrate	Millipore (Roth)
T4 ligase buffer	ThermoScientific
Tango Buffer	ThermoScientific
Tetramethylethylene diamine (TEMED)	Roth
Triethanolamine (TEA)	Fluka
Tris base	Sigma Aldrich
Tris-HCl	Roth
Triton X-100	Roth
Trypsin EDTA	Sigma Aldrich
Trypsin EDTA without phenolred	Sigma Aldrich
TSB	Sigma Aldrich
Turbofect Reagent	ThermoScientific
Tween 20	Promega
Unique Buffer	ThermoScientific
Whatman 3mm filter paper	Roth
β-glycerophosphate	Sigma-Aldrich
β-Mercaptoethanol	Roth

5.1.2 List of supplied lab-utensils

1000µl pipette	Eppendorf / Gilson
10cm dish	Greiner
10ml serological pipette	StarLab
12 well plate	NUNC
15 ml Falcon	StarLab
20µl pipette	Eppendorf / Gilson
200µl pipette	Eppendorf / Gilson
24 well plate	IWAKI
25ml serological pipette	StarLab
3.5cm dish	Greiner
50ml falcon	GE Healthcare
50ml serological pipette	StarLab

5ml serological pipette	StarLab
6 well plate	Greiner
6cm dish	Greiner
Agarose Gel Chamber	BioRad
Blotting paper	Roth (1.5mm, 0.35mm)

5.2 Antibodies and Toxins

5.2.1 Primary Antibodies and Toxins

Name	used dilution	Supplier
AChRa mouse (monoclonal)	1:250	BD Biosciences
FAK rabbit (monoclonal)	1:1000	Abcam
biotin-BGT	1:500	Molecular Probes
BGT-555, BGT-594	1:500	
anti-clathrin (goat)	1:300	Santa Cruz
c-myc clone 9E10 (mouse monoclonal)	1:300	Sigma
Dynamin	1:2000	BD Biosciences
GFP (B-2, monoclonal)	1:1000	Santa Cruz
HA (mouse monoclonal)	1:300	Cell Signaling
HA (rabbit)	1:300	Sigma
His (mouse)	1:1000	Sigma
Lrp4 207/27 extracellular (mouse)	1:1000	UC Davis made in Steve Burden Lab
MuSK 94277 (rabbit)	1:1000	Cell Signaling
Myc (rabbit)	1:1000	Cell Signaling
Phalloidin	1:500	
T7 (monoclonal mouse)	1:10000	Novagen
Tubulin B512 (mouse)	1:2000	Sigma

5.2.2 Secondary Antibodies and Others

Name	Vendor	Dilution
anti-mouse 488	JIR	1:1000
anti-mouse 594	JIR	1:1000
anti-mouse 649	JIR	1:800
anti-mouse Cy3	JIR	1:1000
anti-rabbit 488	JIR	1:400
anti-rabbit 649	JIR	1:1000
streptavidin-Cy3	JIR	1:1000
streptavidin 647	JIR	1:1000
anti-goat 647	JIR	1:1000
anti-goat HRP	JIR	1:5000
anti-mouse HRP	JIR	1:5000

anti-rabbit HRP	JIR	1:5000
anti-rat HRP	JIR	1:5000

5.3 Solutions and Buffers

5.3.1 Commonly used Solutions and Buffers for biochemical and molecular biology methods

<i>Glycerolstock (bacteria)</i>
800 µl liquid bacteria culture
200 µl glycerol
→ freeze -80 °C

<i>LB plates</i>
25 g LB
15 g Agar
→ ad 1000 ml ddH ₂ O

<i>NP-40 Lysisbuffer</i>	<i>stock</i>	<i>mix</i>
5 mM EGTA	0,5 M	1 ml
50 mM NaCl	5 M	1 ml
30 mM TEA pH7,5	1 M	3 ml
50 mM NaF	1M	5 ml
ddH ₂ O		ad 100 ml
5 mM NP40 (should be added the last)	100%	1 ml

<i>Proteinase Inhibitor-Stocks</i>	<i>stock</i>	<i>dilute in</i>	<i>use</i>
Leupeptin	1 mg/ml	ddH ₂ O	1/1000
Pepstatin	1 mg/ml	ddH ₂ O	1/1000
Aprotinin	0,5 mg/ml	EtOH	1/500
PMSF	100 mM	EtOH	1/500
Sodium Orthovanadate	200 mM	ddH ₂ O	1/200
β-Glycerophosphate		ddH ₂ O	1/1000

<i>10x PBS, pH~7,3</i>	<i>MW g/mol</i>	<i>conc.</i>	<i>gramms</i>
NaCl	58,44	1,37 M	80
KCl	74,56	27 mM	2
Na ₂ HPO ₄ x2H ₂ O	177,99	43 mM	7,65
KH ₂ PO ₄	136	14 mM	2
ddH ₂ O			ad 1000 ml

<i>TSB Buffer for competent bacteria</i>	<i>final conc</i>	<i>stock</i>	<i>dilution</i>	<i>ddH₂O ad 10 ml</i>
PEG	10%	50%	1:5	2 ml
DMSO	5%	100%	1:20	0,5 ml
MgCl ₂	10 mM	1 M	1:100	0,1 ml
MgSO ₄	10 mM	1 M	1:100	0,1 ml

<i>5x Running Buffer SDS-PAGE (TANK)</i>	<i>10x Running Buffer SDS-PAGE</i>	<i>10x Stacking Buffer SDS-PAGE</i>
30,1 g Tris Base	90,8 g Tris Base	0,43 g Tris Base
144 g Glycine	10,9 ml HCl	15,12 g Tris -Cl
10 g SDS	ddH ₂ O ad 500 ml	ddH ₂ O ad 200 ml
ddH ₂ O ad 2 L	pH ~8,8	pH~6,8

<i>4x SDS loading buffer for SDS-PAGE</i>	<i>concentration</i>	<i>stock</i>	<i>Mix (10 ml total volume)</i>
ddH ₂ O			0,6 ml
Tris-Cl pH6,8	240 mM	1 M	2,4 ml
β-Mercaptoethanol	8%		1 ml
SDS	4%	20%	2 ml
Glycerol	40%	100%	4 ml
Bromphenolblue			tip of a spatle

<i>10x TBS-Tween</i>	<i>stock conc.</i>	<i>10x conc.</i>
100 ml Tris-Cl pH8	1 M	100 mM
87,7 g NaCl		1,5 M
5 ml Tween	100%	0,50%
ddH ₂ O ad 1 L		

<i>50x TAE (agarose gels)</i>
242 g Tris Base
57,1 ml acetic acid
100 ml 0,5 M EDTA pH8
ddH ₂ O ad 1 L

<i>Western blot blocking solution</i>	5% milk powder or BSA in 1x TBS-T
<i>Western blot stripping buffers</i>	0,2 M NaOH or 10% acetic acid in ddH ₂ O

5 Materials and Methods

PAA Gels	<i>running gel</i>			
	6%		7,5%	
total volume [ml]	10 (1 gel)	20 (2 gels)	10	20
40% AA mix [ml]	1,5	3	1,88	3,76
1,5M Tris/0,5M HCl [ml]	2,5	5	2,5	5
ddH ₂ O [ml]	5,85	11,7	5,4	10,8
10% SDS [μ l]	100	200	100	200
APS [μ l]	50	100	50	100
TEMED [μ l]	10	20	10	20

PAA Gels	<i>running gel</i>			
	10%		12,5%	
total volume [ml]	10	20	10	20
40% AA mix [ml]	2,5	5	3,1	6,2
1,5M Tris/0,5M HCl [ml]	2,5	5	2,5	5
ddH ₂ O [ml]	4,8	9,6	4,2	8,4
10% SDS [μ l]	100	200	100	200
APS [μ l]	50	100	50	100
TEMED [μ l]	10	20	10	20

PAA Gels	<i>stacking gel</i>	
	5%	
total volume [ml]	5 (2 gels)	10 (4 gels)
40% AA mix [ml]	0,625	1,25
0,02M Tris/0,48M Tris-Cl [ml]	1,25	2,5
ddH ₂ O [ml]	3,025	6,05
10% SDS [μ l]	50	100
APS [μ l]	50	100
TEMED [μ l]	5	10

<i>Silver staining of proteins after PAA gel electrophoresis</i>	
Fixation solution	50% MeOH, 10% acetic acid
Wash solution	50% MeOH
Sensitizing solution	0,02% w/v Na ₂ S ₃ O ₃
Silver stain	0,1% w/v AgNO ₃
Developing solution	2% w/v Na ₂ CO ₃ , 0,04% H ₂ CO ₄
Stop solution	10% acetic acid

<i>His-Wnt purification with Ni-NTA beads</i>	
Washing buffer 1	1% CHAPS, 1 mM Imidazole in PBS
Washing buffer 2	0,3 M NaCl, 0,5% CHAPS, 1 mM Imidazole
Elution buffer 1	300 mM Imidazole, 0,5% CHAPS
Elution buffer 2	500 mM Imidazole, 0,5% CHAPS

5.3.2 Media components for cell culture methods

<i>Freezing medium</i>	GM +10% FBS + 10% DMSO
<i>C2- Growth medium</i>	15% FBS and 1% penicillin/streptomycin in DMEM, stored at 4 °C
<i>C2- Differentiation medium</i>	2% Horse serum (Sabourin & Rudnicki) and 1% pen/strep in DMEM, stored at 4 °C
<i>GM for heterologous cells (HEK, Cos7, CHO. phoenix)</i>	10% FBS and 1% penicillin/streptomycin in DMEM, stored at 4 °C

5.4 Plasmids and Primers**5.4.1 Plasmid List**

<i>Plasmid</i>	<i>Description/cloning</i>	<i>Source/Reference</i>
pEGFP-N1	4,7kb, CMV promoter and MCS N-terminal of EGFP, SV40 ori, neomycin selection marker, kanamycin resistance	Clontech
pcDNA 3.1 (5,4kbp); pcDNA 3.1/myc-His A (5,5kbp)	5,4kbp, Amp resistance, neomycin selection marker for stable cell lines, BGH polyA, SV40ori (eposomal replication), CMV promoter	Invitrogen
pcDNA 3.1/his A-Wnt 4, Wnt 9a and Wnt 11	pcDNA 3.1/his A vector with EcoRI/XbaI insertion sites of mouse Wnt cDNAs of Wnt 4, 9a and 11, single tag his,	Dr. Ruth Herbst, Center for Brain Research, Vienna
pcDNA 3.1/myc-His A- Wnt 4, Wnt 9a and Wnt 11	pcDNA 3.1/myc-his A vector (5,5kbp) with EcoRI/XbaI insertion sites of mouse Wnt4, 9a and 11, Wnt cDNA cut out from pcDNA3.1/his A produced by Dr. Ruth Herbst ,double tag myc-his,	Sandra Parzer
pcDNA 3.1/HA-MuSK	pcDNA 3.1 (5,4 kbp) vector containing HA-MuSK, C-terminally tagged MuSK, Amp resistance	D.Hantai, Inserm Paris, (Chevessier et al., 2004)
Lrp4-GFP	pEGFP-N1 vector (4,7kb, x HindIII/SalI) containing Lrp4 (5,7kb), x HindIII/ XhoI)	Dr. Ruth Herbst, Center for Brain Research, Vienna (Luiskandl, Woller, Schlauf, Schmid, & Herbst, 2013)
Dyn1-HA	Prk5 vector containing cDNA Dynamin-1 (x BamHI/HindIII)	Prof. Freissmuth, Medical University of Vienna

Dyn2-GFP	Dynamin-2 cDNA (2,6 kb) introduced into peGFP- N1 vector (4,7 kb), restriction sites: HindIII/EcoRI, total 7,3kb	Dr. McNiven, Mayo Clinic, Arizona, (Ochoa et al., 2000)
RT3-GEP	puromycin selection cassette, GFP as fluorescent marker, T3G as Tet responsive element promoter, EcoRI/XhoI shRNA restriction sites	(Fellmann et al., 2013)
Dnm2.838/ 1316 Ptk2.352/ 2316 Lrp4.1058/ 1346/ 1489 Mapre3.423/ 1355	RT3-GEP vector containing desired shRNA sequences (100 bp), cloning sites: EcoRI/XhoI, puromycin selection marker, GFP fluorescent marker	Sandra Parzer, Bahar Camurdanoglu, Center for Brain Research, Vienna

5.4.2 List of Primers

<i>Primer</i>	<i>Sequence</i>	<i>Reference</i>
miRE- Xho-fw	5'- TGA ACTCGAGAAGGTATATTGC TGT TGACAGTGAGCG-3'	Matthias Tomschik, Bahar Camurdanoglu (unpublished data 2015)
miRE-Eco Oligo-rev	5'- TCTCGAATTCTAGCCCCTTGAAG TCC GAGGCAGTAGGC-3'	Matthias Tomschik, Bahar Camurdanoglu

5.5 Cell Culture Methods

5.5.1 Freezing Cells

The cells are trypsinized, centrifuged (5 min, 15000 rpm) and resuspended in 1 ml of freezing medium per cryovial. Depending on the cell type, cells are frozen in their corresponding growth medium supplied by 10% FBS and 10% DMSO and immediately stored at -80 °C.

5.5.2 Thawing Cells stored at -80°C

Frozen cells in cryovials are quick-thawed in a waterbath heated to 37 °C. They are transferred into a 15 ml falcon tube and slightly shaken while adding normal growth medium. A centrifugation step (5 min, 15000 rpm) is followed by the removal of the supernatant, resuspension in growth medium and their dissemination onto a 10 cm culture dish. Cells are maintained in growth medium at 37 °C and 5% CO₂.

5.5.3 Splitting cells

After trypsinization, resuspension and centrifugation of cells the supernatant is removed and followed by the resuspension of the pellet. The amount of growth medium used for resuspension varies between 5 ml and 10 ml per 10 cm dish, depending on cell type and cell number. 10 µl out of the resuspension solution were taken for cell-counting with a hemocytometer (Neubauer chamber) and determination of cell number with the following formula:

$$\text{density of cells} = \frac{\# \text{ of cells} * 10000}{\# \text{ of square} * \text{ dilution}}$$

After determination of cell number, the desired density was plated onto different cell culture dishes. For a 3,5 cm about 0,3x10⁶ cells are seeded. For a 6 cm 0,8x10⁶ and for a 10 cm 2,2x10⁶ seeded cells are suitable.

5.5.4 Proliferation of mouse C2C12 muscle cells

C2C12 cells were seeded on 0,2% gelatine coated 10 cm dishes or 12-well plates in desired densities, maintained in GM at 37 °C and 5% CO₂ and split every 2 or 3 days at approximately 80% confluency. It is important to split before the myoblasts get too dense and start to align which indicates subsequent fusion to myotubes.

Stable C2 TET-ON cell lines carrying a neomycin (G418) and puromycin resistance were maintained and selected with G418 in a concentration of 200 µg/ml and puro 2 µg/ml in the growth medium.

5.5.5 Differentiation of muscle cells

For fusion of myoblasts and formation of multinucleated myotubes C2C12 cells were plated onto 0,2% gelatine (0,2% gelatine in 1x PBS) coated 3,5 cm, 6 cm or 12-well plates. At approximately 80-85% confluency differentiation was started by switching to differentiation medium (DM) and maintained 3-5 days at 37 °C.

5.5.6 Doxycycline start

Doxycycline induced shRNA expression in stable C2 TET-ON cell lines was started one day after differentiation start with a concentration of 100 ng/ml.

5.5.7 Transient calcium phosphate transfection

Cells were plated 12 h before transfection on 6-well plates with a density of $5,5 \times 10^5$. At the day of transfection, 2xBBS and 0,25 M CaCl₂ were thawed at RT. 20-25 µg of expression plasmid DNA was aliquoted into 6ml round bottom polystyrene tubes. 175 µl of 0,25 M CaCl₂ (875 µl for a 10 cm dish) was added to the DNA and mixed. 175 µl of 2xBBS (875 µl for 10 cm) was added dropwise while vortexing the polystyrene tube. The transfection mix was incubated for 11-13 min at RT to allow the precipitation of DNA and calcium phosphate. After the incubation time,

the DNA was added dropwise onto the prepared cells. Medium change was performed 10 h after transfection and 2 days after transfection the cells were ready for lysis and further processing.

5.5.8 Transient Turbofect transfection

Cells were seeded one day before transfection on a 6 cm dish with a density of 8×10^5 cells/6 cm dish. Transfection was performed with a transfection mix containing: 4 μ g DNA, 400 μ l DMEM and 8 μ l Turbofect reagent in a total volume of 5 ml GM. DNA, DMEM and Turbofect were combined in a round bottom, polystyrene tube, vortexed, incubated for 13 min at RT and added dropwise onto cells. After incubation of 1 day at 37 °C with 5% CO₂ the cells were ready for further processing.

5.5.9 Stable transfection of CHO cells with Wnt4, 9a and 11

CHO cells were seeded on 10 cm dishes and transfected with his-tagged Wnt via calcium phosphate method. Cells were treated with 2 μ g/ml puromycin and 400 μ g/ml G418 for 1 week for selection. Subsequently, clonal selection was performed and the cells were further processed according to the protocols.

5.5.10 Stable Transfection Method with retroviral infection

The packaging phoenix cell line was used for stable transfection of C2 myoblasts with shRNAs for downregulation experiments. Therefore, phoenix cells were seeded on 3,5 cm dishes containing GM a day prior to transfection. The next day, phoenix cells were transfected with Tet-ON vectors containing the desired shRNA via calcium phosphate method. The cells were then producing group-specific antigen (gag), reverse transcription polymerase (pol) and envelope proteins (env) to construct viral particles containing transfected DNA. The medium of phoenix cells was changed the next day, the same day C2C12 target cells were seeded $0,5 \times 10^5$ on 0,2% gelatine-coated 3,5 cm dishes. Virus containing

medium was collected 3 days after transfection, centrifuged with 3000 rpm for 10 min, mixed with 5 ng/ml polybrene and immediately used for C2C12 cell infection. After 3 h incubation of C2C12 cells, the virus containing medium was replaced with normal corresponding GM. 24 h later the cells were split and seeded on 0,2% gelatin coated 10 cm dishes and maintained in GM supplemented with 200 µg/ml G418 and 2 µg/ml puromycin for selection of infected cells. Clones were isolated (see section 5.5.11) and cells were further processed according to the protocols.

5.5.11 Clonal selection of C2 cells

This method was used to create a cell population out of a single, stable transfected cell. C2C12 cells were seeded onto 10 cm dishes with 250 cells per dish and cultivated in GM supplemented with 200 µg/ml G418 and 2 µg/ml puromycin for approximately 1 week, until the first single separated colonies were visible. Each colony was marked and transferred- after washing with PBS and trypsinization -to one well of a 12-well plate. At confluency of 80%, each colony was then split to 6 cm (3×10^5 cells) and 0,2% gelatine-coated 3,5 cm dishes (for each 12×10^4 cells) for differentiation (+/-doxycycline). Fully differentiated myotubes were then stained for AChR clusters (see section 5.8) or lysed for Western Blot analysis (see section 5.7). Well growing clones were further kept and cultivated on the 6 cm dish or frozen.

5.5.12 Agrin stimulation

Agrin stimulation of transiently and stably transfected C2C12 cells was performed after full differentiation to myotubes. Therefore, Agrin 4.8 was applied in a concentration of 12 µl/ml differentiation media for 7-8 h and followed by cell stainings according to the cell experimental settings.

5.6 Molecular biology DNA methods

5.6.1 DNA linearization, purification and further precipitation

For easier stable transfection of cells, sometimes linearized DNA is used. Therefore an enzyme, which cuts the desired plasmid only once, had to be used. The amount of cut DNA depends on the amount of DNA, which is needed to perform the desired transfections. 1x Buffers with 1 unit restriction enzyme in a total volume of 20 μ l and incubation at 37 °C for 3 h was the working protocol.

The digestion was followed by DNA purification with Phenol/Chloroform to remove the restriction enzymes. The volume was filled up to 50 μ l and 1 vV of Phenol/Chloroform was added (50 μ l). The vial was mixed, inverted until the DNA-Phenol/Chloroform mix was turning milky. The final step of the purification was 5 min of centrifugation.

After the purification step, the DNA has to be precipitated. 1,5 to 3 vV 0,3 M NaAc/EtOH was added (with a digestion volume of 20 μ l, 60 μ l were used) which is followed by a freezing step of 30 min at -20 °C and 10 min centrifugation with 13000 rpm. The DNA was resuspended in 70% EtOH, centrifuged again for 10 min and the pellet was dried in an Eppendorf-tube with an open lid at RT. After resuspension in 20 μ l Tris-buffer/normal Elution buffer and concentration determination with Nano-Drop, the DNA can be used for transfection or frozen and stored at -20 °C.

5.6.2 Generation of competent bacteria

One day before starting the overnight culture, the bacteria (E.Coli, DH10) have to be streaked on an agar plate without antibiotics and incubated overnight at 37 °C. The next day, start of the primary overnight culture with 1 colony in 3 ml of plain LB medium without any antibiotics. The next day, 1 ml of the primary culture was taken and further incubated in a total volume of 100 ml. After 2-4 h shaking (220 rpm, 37 °C), the growth of the bacteria was stopped by keeping the beaker on ice when OD₆₀₀ measurements reached to 0,3-0,6.

Afterwards, the whole volume was centrifuged 5 min, 5000 rpm, 4 °C and the pellet was resuspended in 10 ml of TSB buffer (recipe see section 5.1.1) , aliquoted and stored at -80 °C.

5.6.3 Transformation efficiency of competent bacteria

To check the transfection efficiency of newly generated competent bacteria, a control transformation with the empty, Ampicillin resistant puc19 vector was performed. Therefore 0,1 ng of puc19 was used, the negative control does not contain any additional DNA and the volume was filled up with 40 µl ddH₂O and 10 µl 5xKCM buffer to a total volume of 50 µl. The transformations were plated onto Amp50 plates (50 µg/ml) and incubated overnight. The next day, there should be colonies only on the positive control plate. To determine their efficiency the colonies per plate are counted and the following equation was used to determine the number of transformants:

$$\# \text{ of transformants} = \left(\frac{\# \text{ colonies per plate}}{\text{ng of plated DNA}} \right) \times 1000 \text{ ng}/\mu\text{g}$$

5.6.4 Digestion/ Klenow fill-in and Dephosphorylation

All used enzymes, buffers and reagents were supplied by Fermentas or New England Biolabs and used as suggested by the manufacturer. Digestions were mostly carried out in a 20 µl volume using 0,5-1 unit of restriction enzyme solution and approximately 0,5-1 µg of DNA. The restriction components were gently mixed and incubated at 37 °C for 2-3 h.

If required, 5' sticky end-fill-up was performed using Klenow polymerase resulting in blunt ends. 1 µl Klenow polymerase (5 u/µl, Fermentas) was added directly into the restriction mix together with 0,5 µl 10 mM dNTPs. The vial was spinned, incubated 30 min at 37 °C with subsequent 10 min Klenow heat inactivation at 75 °C.

In case of vectors having blunt ends to prevent its religation, the 3' or 5' phosphate group of the vector was removed. Therefore, 3 µl 10x SAP buffer and 1 µl SAP (shrimp alkaline phosphatase, Fermentas) were added directly after restriction in 20 µl digestion mix. Followed by 37 °C, 30 min incubation and 15 min heatinactivation of the enzyme at 65 °C. The vial was then directly used for further ligation.

5.6.5 Electrophoretic separation of digested DNA and elution

After enzymatic digestion, overhang fill-in/removal or dephosphorylation, the reaction product was run (110 V) on 0,7-2% agarose gels in 1x TAE buffer, with 2 µl of Ethidium Bromide per 50 ml of gel and with a suitable marker size, depending on the size of the used DNA. After complete separation of the DNA fragments, a gel slice containing the desired band was cut out and the DNA was isolated using a GeneJet™ Gel Extraction Kit (Fermentas) according to the protocol. DNA was eluted in 50 µl supplied Tris-/Elution buffer when stored in the fridge and used as a stock or eluted in ddH₂O when directly used afterwards for ligation. Concentration of the eluted DNA was estimated loading 1 µl onto an agarose gel and comparing it with bands of known concentrations such as with 1 kb or 100 bp DNA ladder.

5.6.6 DNA Ligation

Ligation reaction was carried out in a 20 µl volume with enzymes and buffers supplied by Fermentas. After digestion, vector and insert were ligated mostly in a ratio of 1:3 (smaller inserts <500bp were used 1:5) depending on their length (see following equation).

$$\frac{Vector [ng] * Insert [ng]}{Vector [kb]} * molar\ ratio \left[\frac{Insert}{Vector} \right] = used\ Insert [ng]$$

The ligation was performed combining calculated vector/insert volume with 2 µl 10x T4 Ligase buffer, 1 µl T4 DNA Ligase (5u/µl, Fermentas) and H₂O filled up to 20 µl. After an incubation time of 2-5 h at RT, the

ligation mix was transformed into competent bacteria as described in the following section.

5.6.7 Transformation of competent bacteria with DNA

For the *transformation of plasmid DNA* 1 μ l DNA, 10 μ l 5x KCM buffer, 40 μ l ddH₂O and 50 μ l quick thawed competent bacteria (E.Coli strain DH10) were mixed and incubated on ice for 30 min. Followed by a 2 min heat shock at 42 °C, adding of 900 μ l LB medium and incubation at 37 °C for 30 min. Finally, 150 μ l of bacteria bacteria plated on selective LB agar plates.

For *transformation of a ligation mix* (ligation of vector-insert fragments) the protocol was the same, the volumes were changed. The full volume of the ligation mix (20 μ l) was taken, combined with 20 μ l 5x KCM buffer, 60 μ l ddH₂O and 100 μ l of competent bacteria, was pelleted (max. 11.000 rpm), resuspended in 150 μ l of the supernatant and plated on selective LB agar plates..

5.6.8 Plasmid Mini/Midi/Maxi preparations

Plasmid preparation kits are used for small and large scale plasmid preparations. For an overnight culture of a single transformed bacterial culture, one colony was picked with a pipette tip and inoculated in LB medium depending on the needed amount of DNA. Overnight cultures were grown in 3 ml – 100 ml LB supplemented with antibiotics (Ampicillin 50 mg/ml, Kanamycin 30 mg/ml). After pelleting in a table-top centrifuge plasmids were isolated using a Miniprep, Midiprep or Maxiprep kit supplied by Invitrogen, Fermentas or Qiagen. All steps were carried out as suggested by the manufacturer.

5.6.9 DNA Sequencing

To confirm correct ligations or incorrect mutations, samples were sent to be sequenced by Microsynth AG via a Barcode Economy Run Service.

Primers were selected from a supplied standard primer list or the desired primer was added in a concentration of 3 pM. The sample contained 1,2 µg DNA in ddH₂O in a total volume of 15 µl.

5.6.10 Oligo annealing, PCR and sub-cloning of shRNAs for RNAi

Oligos were annealed and PCR was performed. ShRNAs were digested with *EcoRI* and *XhoI* and inserted into the RT3-GEP/Tet-ON vector (Figure 12).

Protocol annealing oligos of siRNAs: 3 µg of sense oligo, 3 µg of antisense oligo combined with TE Buffer added up to 50 µl in a PCR tube were mixed and the linker program was applied. 1 µl of the annealed primers (100 bp) was diluted 1:1000 in ddH₂O and used for further PCR processing (annealing temperature was adjusted according to the primer T_m° of the product sheet).

PCR protocol: PCR was amplified using the primers miRE-Xho-fw (5'-TGAACTCGAGAAGGTATATTGCTGTTGACAGTGAGCG-3') and miRE-EcoOligo-rev (5'-TCTCGAATTCTAGCCCCTTGAAGTCCGAGGCAGTAGGC-3'). 38,5 µl ddH₂O, 1 µl Pfu Pol, 5 µl Pfu Buffer +MgSO₄, 1 µl 10 mM dNTPs, 2,5 µl annealed oligos, 1 µl 10 µM miR-EcoRI and 1 µl 10 µM miR-XhoI were mixed in a total volume of 50 µl and PCR was performed in a thermocycler. Cycling parameters were 95 °C for 5 min; 30 cycles of 95 °C for 25 sec, 56 °C for 25 sec, and 72 °C for 30 sec; 72 °C for 5 min.

PCR cleanup kit: PCR cleanup was performed as suggested by the supplier Fermentas Thermo Scientific and eluted in 30 µl ddH₂O. 1/10 of the eluted PCR product (3 µl) was loaded on 2% agarose gel to test if the PCR was successful.

Sub-cloning of vector and inserts: RT3-GEP vector and desired shRNA inserts were cut with *XhoI* and *EcoRI* in 20 µl total volume for 2 h at 37 °C, loaded on a 2% agarose gel, cut out and eluted in 20 µl

ddH₂O. Ligation was performed in 20 µl total volume with 15 ng of inserts and 50 ng (100 bp) of vector (8,1 kbp) for 3 h at RT.

Table 2: Summary of used siRNAs and their target protein recognition sites

shRNA ID	97mer oligo	mRNA target site
Dnm2.1316	TGCTGTTGACAGTGAGCGCAAGATGGAGTTTGAT	AAAGATGGAGTTT GATGAGAAA
	GAGAAATAGTGAAGCCACAGATGTATTTCTCATC	
	AAACTCCATCTTTTGCCTACTGCCTCGGA	
Dnm2.838	TGCTGTTGACAGTGAGCGACAGGGATGTCCTGGA	CCAGGGATGTCC TGGAAAACAA
	AAACAATAGTGAAGCCACAGATGTATTGTTTTCCA	
	GGACATCCCTGGTGCCTACTGCCTCGGA	
Mapre3.1355	TGCTGTTGACAGTGAGCGACAGCAGCTGTATATT	CCAGCAGCTGTAT ATTTGACAA
	TGACAATAGTGAAGCCACAGATGTATTGTCAAAT	
	ATACAGCTGCTGGTGCCTACTGCCTCGGA	
Mapre3.423	TGCTGTTGACAGTGAGCGCCCCGTAGAGAAGTTA	TCCCGTAGAGAA GTTAGTGAAG
	GTGAAATAGTGAAGCCACAGATGTATTTCACTAA	
	CTTCTCTACGGGATGCCTACTGCCTCGGA	
Lrp4.1058	TGCTGTTGACAGTGAGCGCGCGACAACAGCGA	TGCGGACAACAG CGATGAAGAA
	TGAAGAATAGTGAAGCCACAGATGTATTCTTCATC	
	GCTGTTGTCCGCATGCCTACTGCCTCGGA	
Lrp4.1346	TGCTGTTGACAGTGAGCGCACGTGCCAGGATGTA	AACGTGCCAGGA TGTAACGAA
	AACGAATAGTGAAGCCACAGATGTATTCGTTTAC	
	ATCCTGGCACGTTTGCCTACTGCCTCGGA	
Lrp4.1489	TGCTGTTGACAGTGAGCGCACCTGTGCTACTGTT	AACCTGTGCTACT GTTTGCCAA
	TGCCAATAGTGAAGCCACAGATGTATTGGCAAAC	
	AGTAGCACAGGTTTGCCTACTGCCTCGGA	

5.6.11 Subcloning in Wnt Isolation Experiments

Wnt experiments including purification and co-immunoprecipitation were first performed with his-tagged Wnt constructs (Wnt4, 9a and 11-pcDNA3.1/hisA). The obtained results and the general protein expression levels were not satisfying. For higher expression and better detection via two different tags the constructs were subcloned into pcDNA3.1/myc-hisA via *EcoRI* and *XbaI*. They were further used for transient HEK transfection, for co-immunoprecipitation, stringency

experiments, immunostainings and stably transfected into CHO cells for detection in lysates, supernatants and for higher purification yields.

5.7 Protein biochemistry methods

5.7.1 Preparation of protein extract from heterologous cells

The whole lysis procedure of HEK-293 cells was carried out on ice. 48-72 h after Turbofect- or Calcium chloride transfection (in 10 cm dishes or 6-well plates), the cells were scraped off the dish, transferred into a 15 ml or 50 ml falcon and centrifuged (5 min, 2500 rpm, 4 °C). Followed by 2 washing steps with ice cold PBS and 2 centrifugation steps (5 min, 2500 rpm, 4 °C). Afterwards, 1 ml (10 cm dish) or 400 µl (1x 6-well) NP-40 lysisbuffer (supplied with inhibitors Pepstatin 1:500, Leupeptin 1:1000, Aprotinin 1:1000, PMSF 1:500) were rotated at 4 °C for 20 min. The cell lysates were then centrifuged at 4 °C with 13400 rpm for 15 min to remove all unwanted cell debris. Immediately afterwards, the supernatant was either totally used for SDS PAGE analysis of target protein expression or divided into a 40 µl aliquot of untreated total lysate (TL, supplied with 4x loading dye and frozen at -20 °C) and the remaining lysate was used for immunoblotting, immunoprecipitation (IP, see section 5.7.3) or frozen in liquid N₂ for storage at -80 °C.

5.7.2 Preparation of cell lysates from C2C12 mouse muscle cells

Myoblasts were cultured on 0,2% gelatine coated 3,5 cm plates. After 5 days of differentiation, the fully differentiated myotubes were washed twice in ice-cold PBS and incubated for 20 min on the shaker at 4°C in 100 µl RIPA buffer supplied with inhibitors (Pepstatin 1:500, Leupeptin 1:1000, Aprotinin 1:1000, PMSF 1:500, β-Glycerophosphate 1:1000 and Orthovanadate 1:200). The adherent cells were then scraped off using a cell scraper, transferred into a prechilled Eppendorf tube, centrifuged at 12.000 rpm and aliquoted or processed like described above in 5.7.1.

5.7.3 Co-Immunoprecipitation of Wnt protein via MuSK in HEK cells

Again, all the steps were carried out at 4°C or on ice. Immediately after lysis and after taking an aliquot of the total lysate (TL, 40 µl), the protein lysate was mixed with protein pre-clearing beads 'Pierce Control Agarose Resin' and rotated 2 h at 4 °C. Meanwhile, the HA-antibody was pre-coupled to the antibody. The HA-antibody was used 1:500 with magnetic beads 'SureBeads™ Protein A' rotating for 2 h as well at 4 °C. After 2 h the lysate was centrifuged for 5 min with maximal speed to get rid of the pre-clearing beads (and the bound unspecific proteins). The coupled-antibody beads were washed 2 times with lysis buffer (without centrifugation in the magnetic rack) and added 1:500 to the lysate and incubated overnight, rotating at 4 °C. The next day, the samples were washed 3 times with 1 ml of lysis buffer supplemented with inhibitors to remove unbound protein. After the last washing step and taking off of the supernatant, 28 µl of 4x loading buffer was added to the protein. The sample was then either frozen at -20 °C or directly loaded onto a polyacrylamide gel for Western Blot analysis.

5.7.4 SDS-Page Gel electrophoresis of proteins

Running and stacking gels were prepared and put into a gel tank with 1x SDS-running buffer. Protein samples from Co-IP containing 4x SDS loading dye were denatured at 95 °C for 5 min, followed by a centrifugation step at full speed for 3 min. Denatured samples were loaded onto the polyacrylamide gels together with the prestained PAGE ruler protein ladder supplied by Fermentas. The gel was started with 100 V until the protein front reached to the running gel and when marker bands started to separate. Then the migration velocity was fastened up to 140 V for approximately 60 min, until the protein bands were separated as desired or the bromophenol blue dye of loading dye entered to the running buffer from the bottom of the running gel.

5.7.5 Western blotting

After SDS-PAGE, the stacking gel was removed and the protein containing running gel equilibrated at 4 °C for 10 min in 1x transfer buffer. A PVDF membrane was activated in absolute MeOH and equilibrated in 1x transfer buffer for 10 min at 4 °C. Proteins separated on the gel were transferred to the activated Millipore PVDF membrane with the standard Trans-Blot® Turbo™ Transfer System for 30 min, 25V. The membrane was rinsed for few minutes shaking in TBS-T and then blocked in TBS-T containing 5% BSA for 2 h at RT or overnight at 4 °C gently shaking. The blocking solution was rinsed away 3 times with TBS-T, followed by incubation of the membrane with the primary antibody diluted in TBS-T containing 5% BSA and 0,1% NaN₃ for 2 h at RT or overnight at 4 °C. The antibody solution was reused several times. The blot was washed 3 times for 10 min with TBS-T and incubated 1 hour at RT with a HRP-conjugated secondary antibody diluted 1:5000 in 5% milk in TBS-T. After 3 times washing in TBS-T for 10 min the membranes were incubated for 5 min with HRP-substrate and visualized by a ChemiDoc Fluorimager System (Bio-Rad).

5.7.6 Stripping and reprobing

In need to detect a different protein on the same blot, the membrane can be stripped and probed again with other specific antibodies. Stripping was done in 0,2 M NaOH for 5 min with subsequent washing with TBS-T, blocking, primary antibody and secondary antibody incubation as already mentioned in section 5.7.5.

5.7.7 Silver staining of proteins in polyacrylamide gels

After electrophoretic separation of proteins in polyacrylamide gels, silver staining is one of the various gel-based proteomics detection methods. It combines a high sensitivity with relatively cheap and simple laboratory procedure. Since it is possible to detect proteins in the very low ng range (<1 ng) (Weiss, Weiland, & Gorg, 2009), it is a clever alternative for

detecting possible his-tagged Wnt proteins secreted in the medium by stably transfected CHO cells (see section 5.7.8). Coomassie staining was tried too but was not sensitive enough for the low amount of Wnt proteins. Silver staining procedure was started (after gel electrophoresis) with a fixation step. The gel was incubated 20 min in 100 ml fixation solution (50% MeOH, 10% acetic acid). Afterwards, 10 min incubation in 100 ml wash solution (50% MeOH) and only 1 min in 100 ml sensitizing solution of sodium thiosulfate (0,02% w/v $\text{Na}_2\text{S}_3\text{O}_3$). Followed by the staining step in silver nitrate (100 ml, 20 min, 4 °C, 0,1% w/v AgNO_3) and 30 sec of 100 ml developing solution (2% w/v Na_2CO_3 , 0,04% H_2CO_4). The developmental step was stopped in 100 ml stop solution (10% acetic acid). Imaging was performed with BioRad ChemiDoc and ImageLab. The stained gel can be stored in ddH₂O without shaking for some months at 4 °C.

5.7.8 Wnt protein purification with Ni-NTA Resin beads

Stably expressing CHO his-Wnt4 and his-Wnt11 cells were grown on 10 cm or 15 cm dishes selected with 400 µg/ml G418. At confluency, they were lysed and the supernatant with the secreted Wnt proteins was harvested. A 50 µl aliquot of the lysates was loaded on a 10% polyacrylamide gel for gel electrophoresis and anti-His immunoblotting. The supernatant was used for His-Wnt isolation via gravity purification with Ni-NTA beads. The harvested supernatant was centrifuged for 10 min at 3000 rpm at 4 °C and filtered through a 0,45 µm syringe filter. 400 µl Ni-NTA beads calculated for 15 ml falcon of supernatant were washed twice in 5 ml PBS and resuspended in PBS/2 mM imidazole. The centrifuged supernatant was then incubated overnight with the resuspended Ni-NTA beads rotating at 4 °C. During this incubation, the beads are binding the His-tagged Wnt protein and trapping it until its elution with imidazole. The next day (the following steps were all carried out at 4 °C), the column was equilibrated with PBS and the supernatant was loaded on the column. The beads have to settle down, which takes about 10 min. The loaded column was washed with 15 ml washing buffer

1 (1xPBS, 1% CHAPS, 2 mM imidazole) and 3 ml of washing buffer 2 (0,3 M NaCl, 0,5% CHAPS, 2 mM imidazole). Elution was performed with 2 ml elution buffer 1 (300 mM imidazole, 0,5% CHAPS) and 1 ml elution buffer 2 (500 mM imidazole, 0,5% CHAPS), with 15 min incubation time before starting the elution. 200 μ l fractions were collected in Eppendorf tubes as well as aliquots of washing buffers and beads after elution for followed western blot analysis and quantification of silver staining.

5.7.9 Antibody and shRNA specificity tests in HEK and C2C12 cells

Firstly, experiments with heterologous cells (HEK 293) and C2C12 cells including negative and loading controls were performed to test antibody specificity and to detect endogenous target protein expression. These cell lines were transiently transfected with Lrp4-GFP, EB3-GFP, Dyn-1-HA and Dyn-2-GFP. The transfected Lrp4-GFP was successfully detected by the antibody α -Lrp4.207_27, which recognizes the external domain of Lrp4 (197 kDa) and via α -GFP (220 kDa). Anti-Lrp4 antibody is able to detect endogenous and transfected Lrp4 in C2 cells. They were distinguished by their distinct molecular size. For detection of EB3-GFP expression α -GFP (67 kDa) was used. Dynamin-1 and Dynamin-2 were detected via α -GFP (130 kDa), α -HA (100 kDa) and α -Dynamin (100 kDa). Anti-Dynamin detected endogenous and transfected protein, whereas α -HA and α -GFP antibodies were specific for the transfected protein. For FAK, α -FAK antibody was positively tested.

5.8 Immunocytochemistry methods

5.8.1 AChR cluster Assay

Cultivated C2 myoblasts (3,5 cm dishes) at differentiation day 5 treated with and without doxycycline were used for labeling of AChRs. Since α -Bungarotoxin (BGT) binds to AChR-alpha subunits, it is used in a fluorophore-conjugated form for cluster assays. After 7 h of Agrin 4.8-stimulation (12 μ l/ml medium) the 3,5 cm dishes were slightly washed once with 1x PBS. The myoblasts were fixed in 500 μ l 4% PFA in PBS

for 10 min and 2 times washed with 1x PBS. Followed by the staining step with α -BGT-Alexa-555 or α -BGT-Alexa-594 (BGT 1:500 in 2% FBS in PBS) for 30 min slightly shaking in 500 μ l staining solution. After 2 washing steps with PBS, the myotubes were mounted in 10 μ l Mowiol with 22 mm square glass cover slip. This procedure was used for Ptk2/FAK transfected C2 cells.

For Mapre/EB3 staining, two more staining steps with Strep-647 (1:1000) and Phalloidin (1:500, f-actin staining) were added to the first BGT-biotin (1:500) step. The 0,2% gelatin coated 3,5 cm dish was therefore washed twice with 1x PBS after BGT incubation for 30 min, incubated 30min with 500 μ l Strep-647 (1:1000) in 2% FBS/PBS, 2x washed in 1x PBS and permeabilized in 0,1% Triton/PBS (500 μ l). Two PBS washing steps were followed with 30 min α -Phalloidin in 1% BSA/PBS (1:500) incubation on the shaker, washed 2 times again with PBS and then mounted in 10 μ l Mowiol as described above.

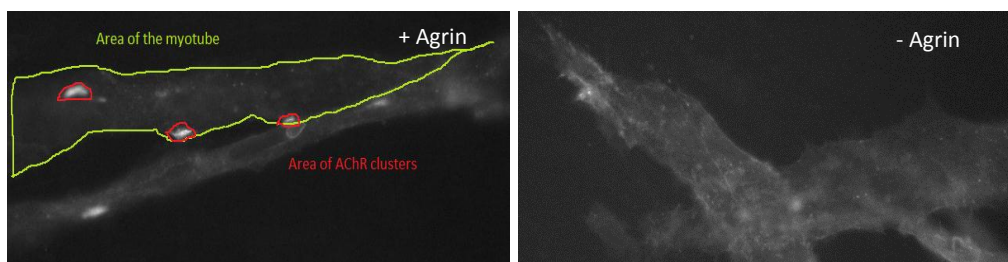


Figure 12: Analyzing cluster assays: Agrin treated myotubes should show AChR clusters indicated in red. Untreated myotubes are unable to form clusters. The area of the myotube where clusters are formed used for quantification is indicated in yellow. Quantification of clusters with ImageJ software.

Immunostained AChR clusters were controlled on a Leica inverted fluorescence microscope with 20x or 63x oil objectives. Quantification of the number of agrin-induced clusters per myotube (larger than 5 μ m) was done using 'ImageJ' software and MSExcel2014. To determine the effect of inhibitors on AChR cluster formation, myotubes were stimulated with agrin 4.8 in the presence or absence of doxycycline (Figure 12).

5.8.2 Clathrin-BGT staining

Clathrin stainings were performed with Clathrin transfected C2 cultivated myotubes at differentiation day 5, treated with and w/o doxycycline (1:100, 40 h) and agrin stimulation (12 μ l/ml) overnight. Cells were washed in PBS, fixed 10 min in 500 μ l 4% PFA/PBS at RT, washed again 2 times in PBS and permeabilized 5 min in 0,2% Triton/PBS. Blocking 30 min at RT in 5% rabbit serum in PBS was followed by 1-2 h primary incubation with BGT (1:500 in 10% FBS/PBS, 300 μ l) and anti-Clathrin (1:300 in 5% rabbit serum in PBS, 300 μ l). Three times washing in PBS and secondary incubation of 1 h at RT in Strep-Cy3 and anti-goat-647 (both 1:100) was followed by three washing steps and mounting in 10 μ l Mowiol. Stainings were controlled by confocal microscopy (20x, 63x oil objectives) and quantification was done with ImageJ.

5.8.3 Tubulin staining

Tubulin staining of Mapre/EB3 positive C2 myoblasts, cultivated on 3,5 cm dishes was performed with the same procedure like Clathrin staining mentioned in 5.8.2, but with different incubation times of primary and secondary antibodies. Primary incubation was performed with BGT (1:500) and anti-tubulin (1:2000) for 1-2 h and secondary incubation for 1 h at RT with strep-Cy3 and anti-mouse-647 (both 1:1000). Tubulin was fixed with 4% PFA/PBS for 10 min at 37 °C (and not at RT like for Clathrin stainings).

5.8.4 Colocalization stainings of Cos-7 cells with Wnt, MuSK and Lrp4

14 coverslips were distributed in a 10 cm dish where $1,2 \times 10^6$ Cos-7 cells were seeded on and incubated overnight at 37 °C in growth medium (DMEM supplemented with 10% FBS and 1% Pen/Strep). The next day the coverslips were carefully transferred into a 12-well dish in 2ml GM per well. The Cos-7 cells were then subsequently transfected with

turbofect (1 µg DNA, 100 µl DMEM, 2 µl Turbofect, 15 min incubation) and kept growing for 12 more h. The next day, total and surface stainings were done. Total staining refers to the whole amount of protein in the cell due to an extra permeabilization step between fixation and blocking. Surface staining displays only the proteins on the cell surface.

For surface staining, the cells were starved for 30 min with normal DMEM at 37 °C, carefully rinsed with PBS and 10 min fixed with 4% PFA at RT. 30 min blocking in PBS/10% FBS, 1 hour incubation of primary Antibody in PBS/10% FBS in wet chamber at RT and three times washing with PBS for each 5 min is followed by 1 hour incubation with secondary antibody in PBS/10%FBS in the well. Three times washing, 15 min incubation with DAPI, three times washing again and mounting in 10 µl Mowiol complete the surface staining procedure. For total stainings, 5 min permeabilization step was introduced between fixation and blocking with 0,1% Triton/PBS.

Table 3: Overview of Cos-7 cell stainings and used antibodies and dilutions; different staining procedures were performed with different antibody combinations

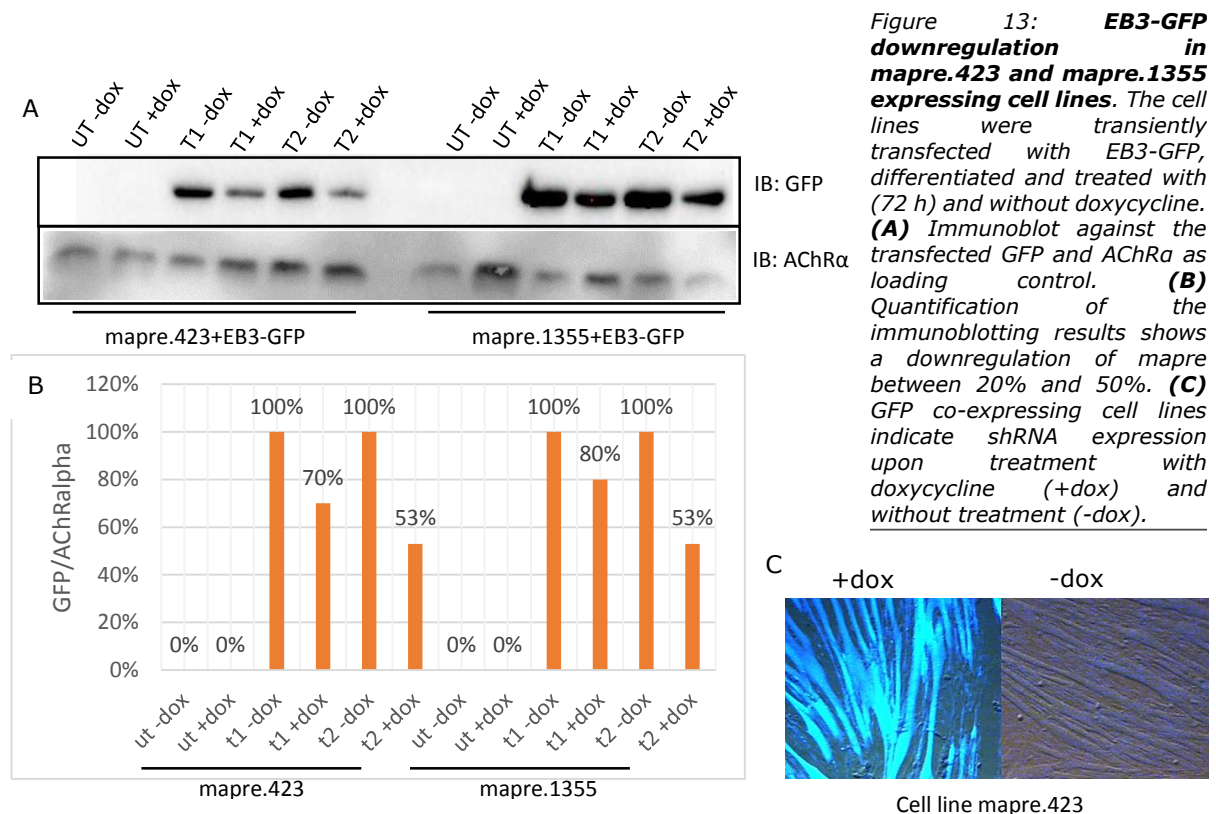
<i>constructs</i>	<i>stainings</i>
<i>Wnt4, 9a, 11</i>	Anti-myc (1:300)+ anti-mouse 488 (1:1000)
	Anti-myc (1:300)+ anti-mouse 649 (1:800)
HA-MuSK + Wnt4, 9a, 11	Rabbit anti-HA (1:300) + anti-rabbit b649 (1:1000)
	Rabbit anti-HA (1:300)+ anti-rabbit alexa488 (1:400)
	Mouse anti-myc (1:300) + anti-mouse 594 (1:1000)
	Mouse anti-myc (1:300)+ anti-mouse 649 (1:800)
HA-MuSK + Wnt4, 9a, 11 + Lrp4-GFP	Rabbit anti-HA (1:300) + anti-rabbit 649 (1:1000)
	Mouse anti-myc (1:300)+ anti-mouse 649 (1:800)
	Mouse anti-myc (1:300) + anti-mouse 594 (1:1000)
HA-MuSK + Lrp4-GFP	Rabbit anti-HA (1:300) + anti-rabbit 649 (1:1000)
HA-MuSK	Rabbit anti-HA (1:300) + anti-rabbit 649 (1:1000)
	Rabbit anti-HA (1:300)+ anti-rabbit alexa488 (1:400)
UT	Mouse anti-myc (1:300)+ anti-mouse 594 (1:1000)
	Rabbit anti-HA (1:300)+ anti-rabbit 649 (1:1000)
	Anti-rabbit 649 (1:1000)
	Anti-mouse 594 (1:1000)

6 Results

6.1 RNAi-mediated downregulation of proteins in mouse C2 muscle cells

6.1.1 EB3 downregulation in mapre.423 and 1355 expressing C2 cell lines transiently transfected with EB3-GFP

EB3 is a microtubule plus-end-associated protein, binding to APC (adenomatous polyposis coli complex) and involved in microtubule capturing, AChR clustering, muscle cell elongation and fusion. Mouse C2 muscle cells, modified to carry Tet-ON-system were produced and provided by M. Tomschik (unpublished data 2015, Center for Brain Research). These C2 cells were retrovirally infected with vectors targeting EB3 for downregulation, tested for differentiation and GFP expression in doxycycline treated cells indicating shRNA expression. In order to test the downregulation of EB3, stable mapre.423 and mapre.1355 shRNA expressing C2 cell lines were transiently transfected with EB3-GFP. 12-15 h post-transfection, differentiation medium supplemented with doxycycline (100 ng/ml) was added and maintained



for 72h. Differentiated myotubes were lysed at day 5 after start of differentiation in RIPA buffer and used for biochemical analysis. Figure 13 shows the shRNA-mediated knockdown of EB3-GFP. Transfected EB3 was detected via its GFP tag using anti-GFP antibody. The way of detecting EB3 through its GFP-tag was chosen because of, at this time, unavailability of anti-EB3 antibody. AChR α is used as loading control and differentiation marker, since it is upregulated as soon as myotubes are formed. The addition of doxycycline allows expression of the shRNA, which binds specifically to the complementary mRNA of the desired target protein and leads to its downregulation. This is illustrated in Figure 13A, using mapre.423 and mapre.1355 stably expressing C2 cell lines in two different transfection experiments performing immunoblot against GFP and AChR α . The analysis of transfection 1 (T1) indicates a downregulation efficiency of approx. 20-30%, whereas transfection 2 (T2) shows an about 50% lower level of EB3 expression. As expected, untransfected samples (UT) show no signal. Quantification of signals (Figure 13B) was performed using results of anti-GFP normalized against anti-AChR α . Samples without doxycycline treatment were set to 100%. Expression of shRNA can be visualized by GFP expression (Figure 13C). Due to the vector design of the Tet-ON-system, GFP is co-expressed upon doxycycline treatment and shRNA expression.

6.1.2 Downregulation of endogenous Lrp4 in Lrp4.1058 expressing C2 cell lines

Mouse muscle C2 Tet-ON cells were retrovirally infected with vectors targeting Lrp4. After doxycycline treatment (100 ng/ml) of 72 h of stably shRNA Lrp4.1058 expressing cells, cells were screened for differentiation and GFP expression. GFP expressing fully differentiated myotubes indicate successful shRNA expression (Figure 14E). Cells were lysed at differentiation day 5 and immunoblotting against Lrp4 (external domain, 200 kDa), AChR α and the ubiquitously expressed controls Actin and Dynamin were performed.

In Figure 14A and B immunoblotting results and their quantification with three different controls are shown. Actin acts as ubiquitously expressed loading control for protein amount and AChR α as loading control for myotube formation. Immunoblot using Lrp4.207_27 antibody recognizes the extracellular domain of Lrp4 (Figure 14B). Figures 14A, C and D represent the quantification of protein expression of the signal of endogenous Lrp4 normalized with actin, AChR α and Dynamin, respectively. A mean downregulation of Lrp4 of approx. 40% can be reported. Since immunoblot using Lrp4 shows low signal intensity for T0

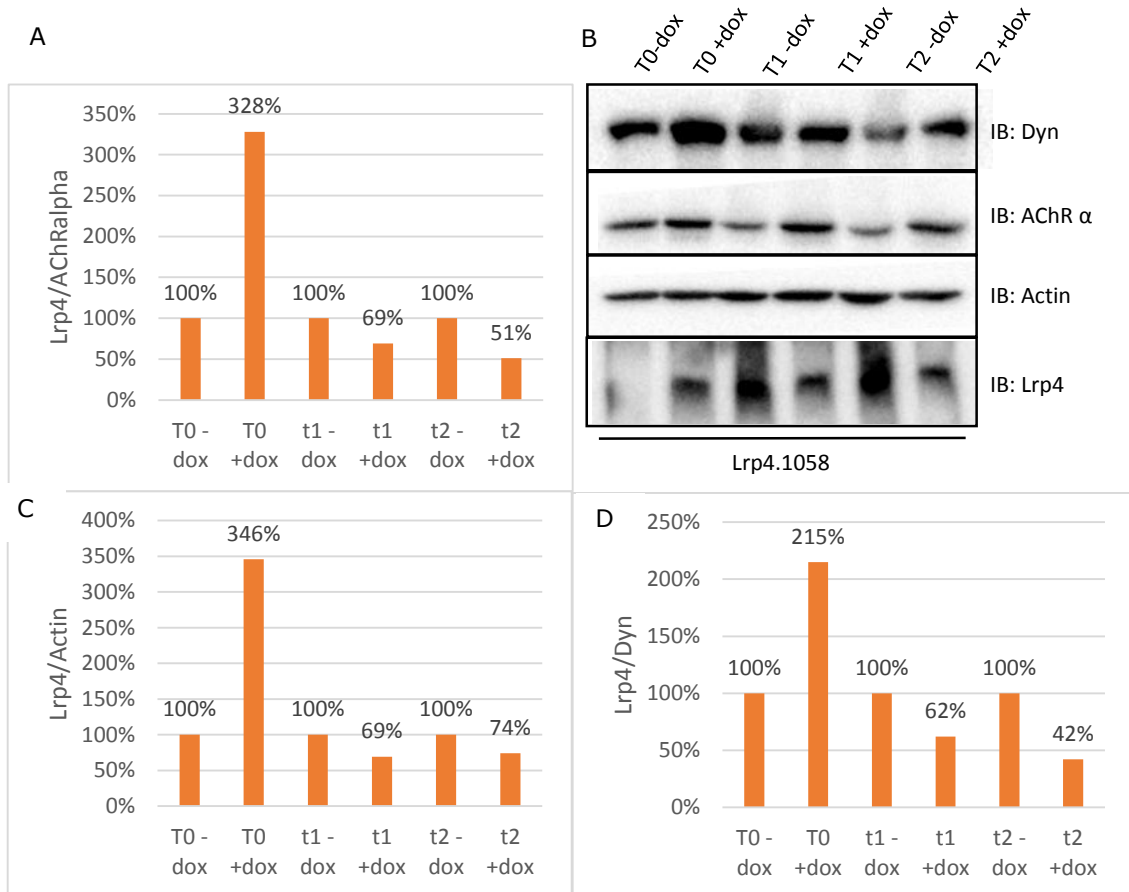
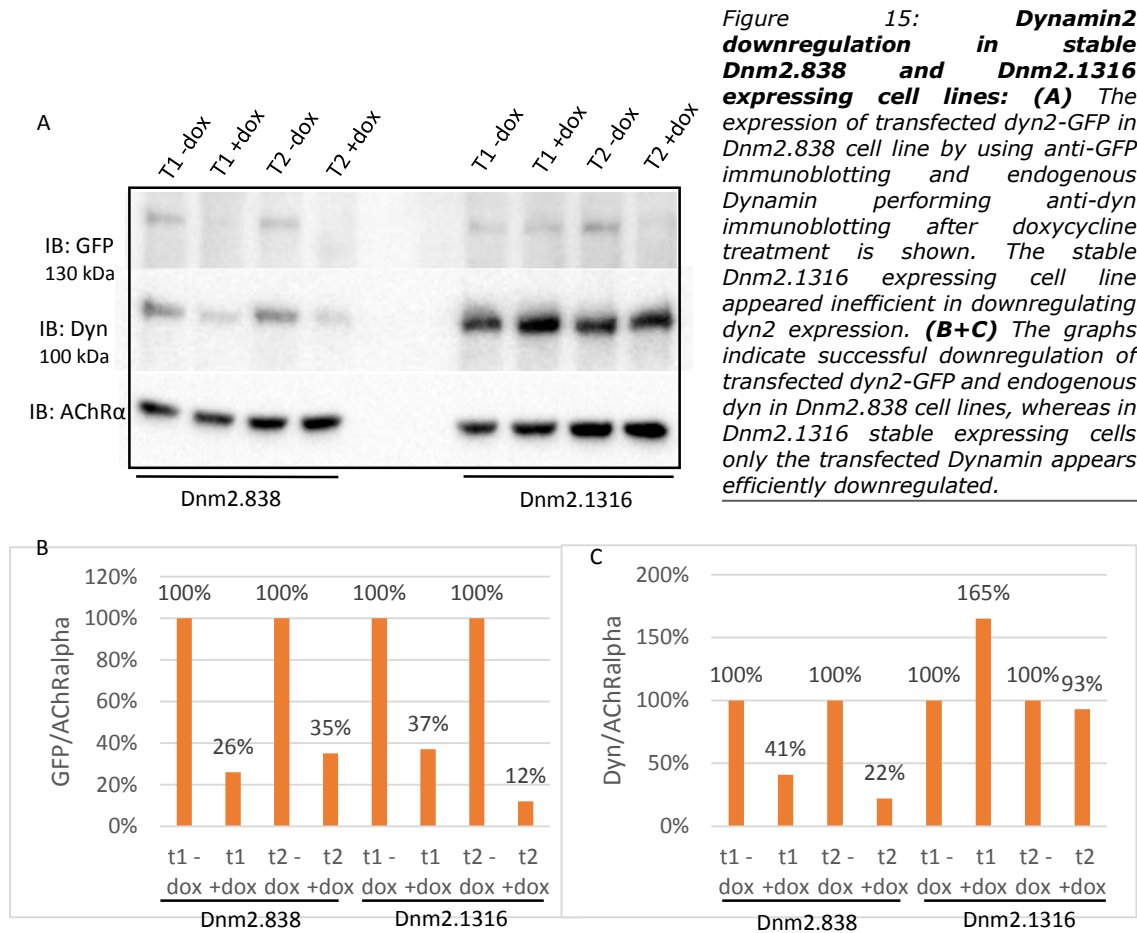


Figure 14: RNAi-mediated depletion of Lrp4 in C2 cell lines: Stable Lrp4.1058 expressing C2 cell lines were differentiated with medium supplemented with and without doxycycline. Cells were tested for differentiation and GFP expression and lysed 5 days after differentiation start. **(B)** Biochemical analysis by blotting against Lrp4, Dyn, AChR α and Actin; **(A,C,D)** Normalization of endogenous Lrp4 against AChR α , Dynamin and Actin results in a graph showing the percentage of protein expression with and without doxycycline treatment. A downregulated protein expression in doxycycline treated cells can be seen. **(E)** Efficient GFP co-expression upon shRNA expression induced by doxycycline. +/-dox: with/without doxycycline treatment

cells without doxycycline treatment, the quantification graphs give an unspecifically high signal at T0 with doxycycline treatment.

6.1.3 RNAi-mediated depletion of transfected Dynamin-2 in C2-Tet cells

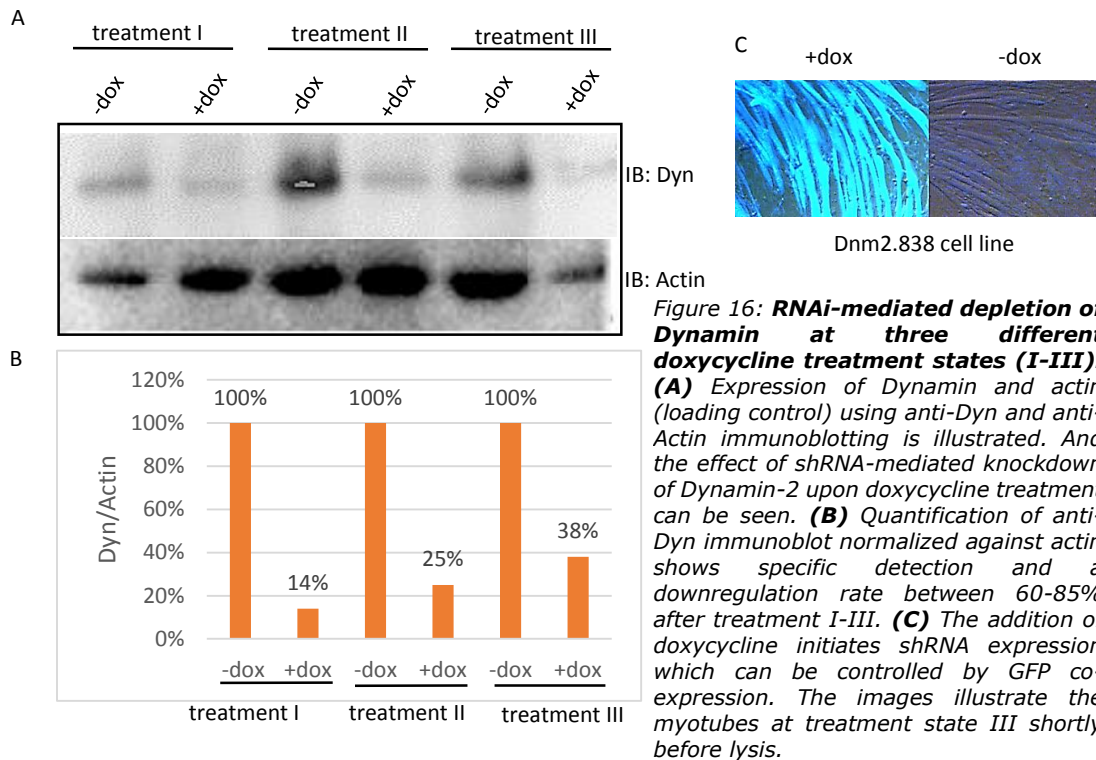
C2-Tet-ON cells were retrovirally infected with a vector targeting Dynamin2, tested for differentiation and GFP expression in doxycycline treated cells indicating shRNA expression. Stably Dnm2.838 and Dnm2.1316 expressing cell lines were transiently transfected with Dyn2-GFP in order to test the knockdown of transfected and endogenous Dynamin. 12-15 h post transfection, doxycycline (100 ng/ml) was added and the cells were screened for differentiation and GFP expression before lysis on differentiation day 5. Lysates were analyzed by immunoblotting against Dyn and GFP. Dynamin is a protein of about 100 kDa size and Dyn2-GFP was detected at about 130 kDa. Anti-Dyn detects transfected and endogenous protein (with different sizes of 100 or 130 kDa) whereas α -GFP recognizes only the transfected protein. Figure 15A-C illustrates the quantification of Dyn-GFP downregulation in Dnm2.838 and Dnm2.1316 stable cell lines. Anti-Dyn immunoblotting (Figure 15A) is supposed to detect endogenous Dynamin at approximately 100 kDa and transfected Dynamin using anti-GFP immunoblotting at about 130 kDa. However, the transfected Dyn2-GFP at 130 kDa could not be detected using anti-Dyn antibody. Dyn-GFP was detected using anti-GFP antibodies. The stable Dnm2.1316 expressing cell line appeared inefficient in downregulating endogenous Dynamin and transfected Dyn2 expression. The graph in figure 15B shows an average knockdown rate of transfected Dynamin of approximately 77% in both cell lines using anti-GFP antibody. Using anti-Dyn antibody, a downregulation could be reported only in Dnm2.838 expressing cell lines.



6.1.4 RNAi-mediated downregulation of endogenous Dynamin in stably Dnm2.838 expressing C2 cells using different doxycycline treatments

Cells stably expressing Dnm2.838 were treated with doxycycline (100 ng/ml) for different time periods: Timepoint (I) refers to the adding of doxycycline to myoblasts and their lysis after 72 h of doxycycline incubation, whereas (III) stands for the addition of doxycycline to fully differentiated myotubes at day 5 and lysis of myotubes after 72 h of doxycycline. (II) is a timepoint inbetween, where doxycycline is added for 72 h one day after the start of differentiation medium. The cells were lysed and biochemically analyzed by immunoblotting using antibodies against Dynamin and actin, respectively. Dynamin downregulation was quantified using actin as loading control. Figure 16 shows that Dynamin-2 is efficiently downregulated in all experimental settings. Treatment I appeared most efficient in downregulation (86% of downregulation),

whereas treatment III shows the highest protein expression despite doxycycline treatment (62% downregulation).



6.1.5 RNAi-mediated depletion of FAK in C2 cells

Mouse C2C12 muscle cells, modified to carry a Tet-ON-system were retrovirally infected with vectors targeting FAK for RNAi-mediated downregulation. C2 cell lines stably expressing Ptk2.352 and Ptk2.2316 shRNAs were differentiated, treated with doxycycline (100 ng/ml), screened for GFP expression and lysed at day 5 of differentiation. The lysates were biochemically analyzed performing immunoblotting against FAK (focal adhesion kinase) and AChRa. AChRa was used as a differentiation marker and loading control in two independent experiments (E1 and E2). In Figure 17A and B the successful downregulation of a mean of 70% is shown by immunoblotting with α FAK antibody.

Taken together, cell lines Ptk2.352, Ptk2.2316 and Dnm2.838 are efficient in downregulating FAK and Dyn2 for more than 50%, respectively. In experiments targeting Lrp4, a downregulation rate of approx. 40% can be reported using Lrp4.1058 stable expressing cell line. Further experiments will determine whether MuSK phosphorylation, downstream signaling and AChR clustering are affected by the downregulation of the used target proteins.

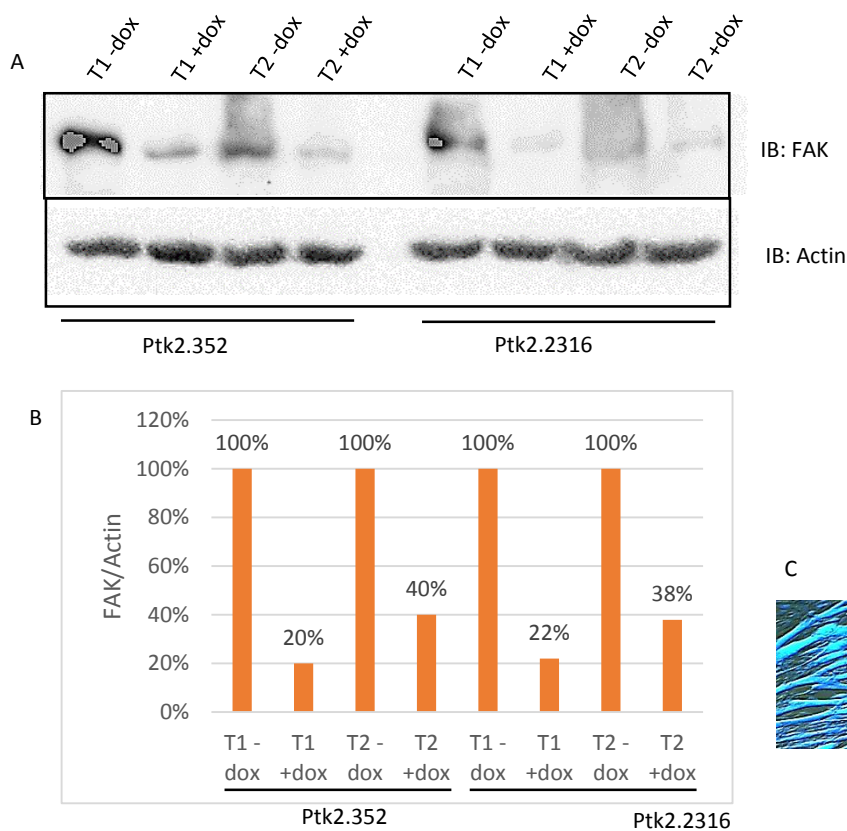


Figure 17: Efficient RNAi-mediated downregulation of FAK in Ptk2.352 and Ptk2.2316 stable expressing C2 cell lines: (A) Lysates of Ptk2.352 and Ptk2.2316 expressing C2 cells were probed with antibodies against FAK and actin, respectively. (B) Quantification of FAK signals normalized against Actin shows a mean downregulation of FAK expression of 70%. (C) GFP expressing cells indicate shRNA expression upon treatment with doxycycline (+dox).

6.2 Assaying AChR cluster formation in C2 cells expressing shRNAs against Lrp4 and FAK

6.2.1 The effect of RNAi-mediated Lrp4 depletion on AChR clustering

Here we wanted to study the effect of Lrp4 downregulation on AChR clustering. Since Lrp4 is a keyplayer in Agrin binding and MuSK activation (Barik, Lu, et al., 2014; B. Zhang et al., 2008), we asked whether a depletion leads to a significant decrease in AChR cluster formation. Stable Lrp4.1058, Lrp4.1346 and Lrp4.1489 expressing and fully differentiated C2 myotubes were treated 72 h with and without doxycycline, stimulated 7 h with agrin and incubated with Alexa-555-coupled bungarotoxin α BGT. To determine effects on AChR clustering,

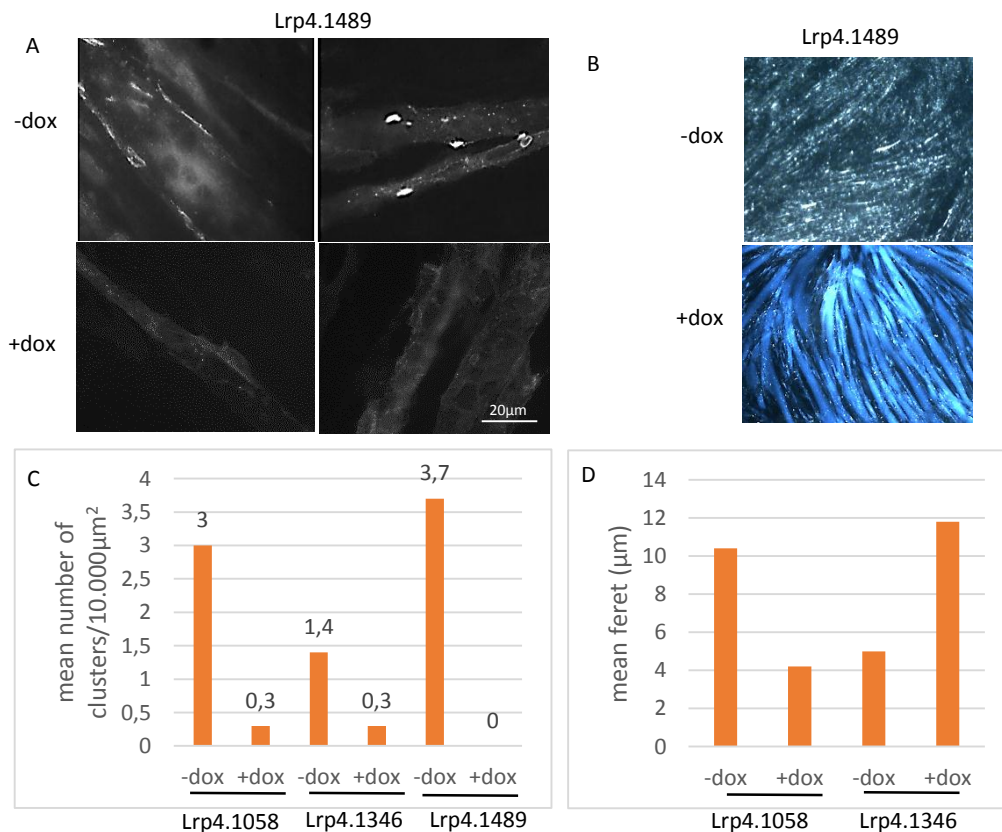


Figure 18: RNAi-mediated depletion of Lrp4 impairs AChR clustering: Stable Lrp4.1058, Lrp4.1346 and Lrp4.1489 expressing C2-Tet myotubes were treated 72 h with doxycycline, stimulated 7 h with agrin and incubated with BGT-555. Subsequently, the mean number (**B**) and the mean Feret's diameter (**C**) of AChR clusters were quantified. (**B**) The reduced number of AChR clusters in the presence of dox indicates a successful knock-down of Lrp4; (**A**) Images show reduced number of AChR clusters in Lrp4 depleted myotubes with doxycycline treatment. (**D**) Mean Feret's diameter of clusters vary. Lrp4.1058 cells with doxycycline treatment develop smaller clusters than untreated cells. However, Lrp4.1346 cells increase their mean Feret's diameter after doxycycline treatment.

20 images were taken and the average number of clusters and the mean Feret's diameter of AChR clusters bigger than 5 μm were quantified (for detailed description of microscopic analysis, objectives, etc. see section 5.8.1). Figure 18 summarizes one experiment of Lrp4.1058, Lrp4.1346 and Lrp4.1489, respectively. The cell lines Lrp4.1346 and Lrp4.1489 were produced and provided by Bahar Camurdanoglu (unpublished data). The effective RNAi-approach in both cell lines was demonstrated. The reduced number of AChR clusters (Figure 18B) in the presence of doxycycline indicates that Lrp4 was successfully downregulated. Figure 18A shows representative images of myotubes stained with $\alpha\text{BGT-Alexa 555}$. Images were analyzed using ImageJ. Myotubes of all cell lines treated with doxycycline formed less AChR clusters than untreated myotubes. Feret's diameter varied between cell lines (Figure 18C). Cell line Lrp4.1058 formed clusters reduced in Feret's diameter after treatment with doxycycline, whereas clusters in Lrp4.1346 expressing cells showed an increased Feret's diameter.

6.2.2 Downregulation of FAK and its effect on AChR clustering

Stably Ptk2.352 and Ptk2.2316 expressing C2 cell lines were differentiated, treated with doxycycline and tested for differentiation and GFP expression (Figure 19B). Fully differentiated myotubes treated 72 h with doxycycline, were stimulated 7 h with agrin and incubated with $\alpha\text{BGT-Alexa 555}$. The mean number and the mean Feret's diameter of clusters were quantified out of 20 images to examine the effect of FAK downregulation on AChR clustering. AChR clusters were visualised with a 63X objective, counted and measured. Figure 19A shows representative images of myotubes stained with $\alpha\text{BGT-Alexa 555}$ analyzed with ImageJ (Figure 19C-D). Stained myotubes show varying results concerning cluster formation. Note that both cell lines show a downregulation of FAK of about 70% in section 6.1.5. Ptk2.352 expressing cell line formed more AChR clusters upon dox treatment than untreated cells, whereas Ptk2.2316 expressing cells showed decreased AChR clustering and an increased Feret's diameter of clusters.

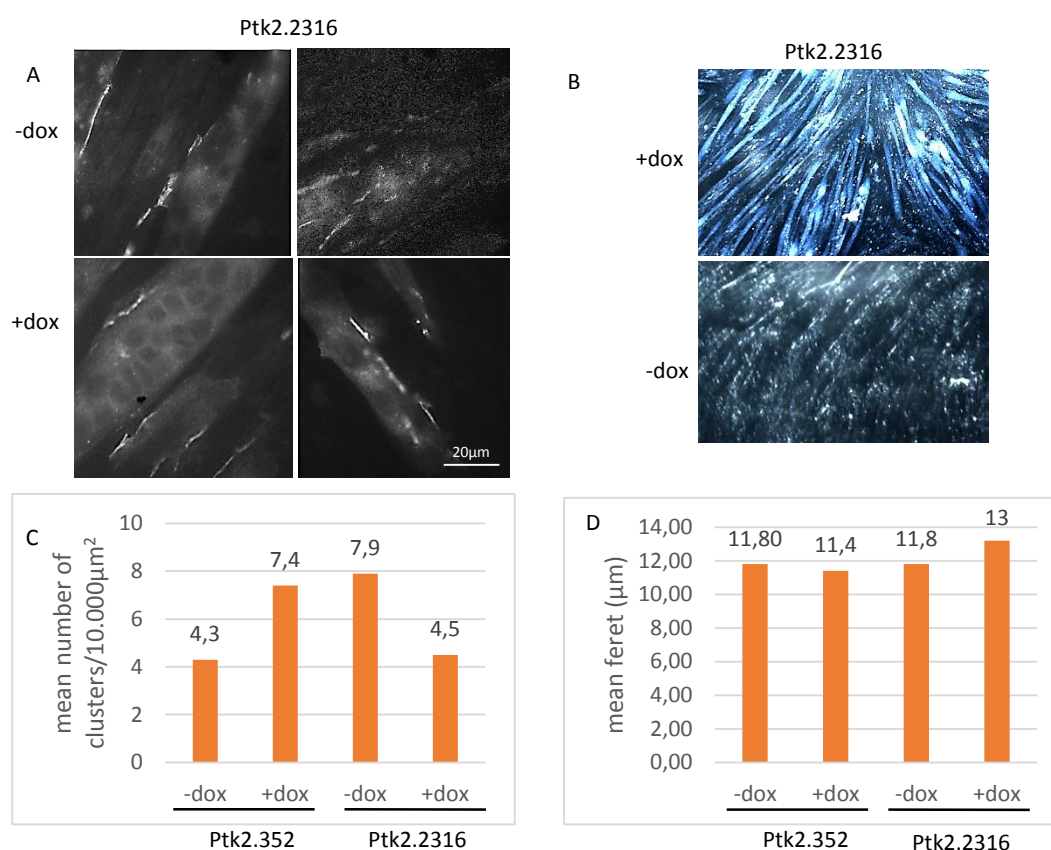


Figure 19: The effect of shRNA-mediated depletion of FAK on AChR clustering: Stable Ptk2.352 and Ptk2.2316 expressing C2-Tet myotubes were treated 72 h with doxycycline, stimulated 7 h with agrin and incubated with αBGT-Alexa 555. Subsequently, the mean number and the mean Feret's diameter were quantified. **(A)** Images of myotubes show no effect of FAK downregulation on AChR clustering. **(B)** Visualization of GFP expressing myotubes upon doxycycline treatment indicate co-expressed shRNA. **(C,D)** Although FAK showed a downregulation of 70% in section 6.1.5, cluster numbers and mean Feret's diameter of clusters do not seem to be affected by FAK downregulation and show varying results.

6.3 Studying Wnt during MuSK signaling

Numerous studies have shown that Wnt proteins are involved in MuSK signaling, prepatterning and NMJ formation (Henriquez et al., 2008; Strochlic et al., 2012; B. Zhang et al., 2012). The focus of the second part of this Master's Thesis was set on studies on the interaction between MuSK and Wnt proteins and their purification. The aim was to establish a heterologous cell line stably expressing Wnt4, 9a and 11 proteins. The isolation of Wnt protein with a gravity purification method using Ni-NTA Resin beads (see section 6.3.1) was performed. In addition, Wnt specificity for MuSK binding was investigated in section

6.3.2 and co-localization studies of MuSK and Wnt proteins were performed (see section 6.3.3).

6.3.1 His-Wnt protein purification with Ni-NTA Resin beads

We aimed the purification of Wnt protein for further stimulation experiments with C2 cells and investigation of the effect on AChR cluster formation. Therefore, CHO cells were stably transfected with his-tagged Wnt4, Wnt9a and Wnt11. After transfection the cells were clonally selected with puromycin. Elected clones were grown until they reached 90% confluency and the supernatant was collected for further biochemical analysis. Due to unefficient protein expression levels in stably Wnt4 and Wnt9a expressing cell lines, experiments were started with Wnt11 cells.

His-tagged Wnt11 containing conditioned medium of stably transfected CHO cells was harvested, centrifuged and isolated via gravity purification using Ni-NTA Resin beads. The beads were washed, equilibrated (2 mM Imidazole) and incubated with the sample overnight rotating at 4 °C. The next day, the column was loaded, the protein was eluted with two washing and elution steps supplemented with imidazole (see section 5.1.1 for used buffers and section 5.7.8 for procedure) and fractionated in 200 µl aliquots. The collected fractions (5 fractions for 500 mM imidazole, 8 fractions for 300 mM imidazole in elution buffer) were separated by SDS-PAGE and subjected to silver staining (see section 5.7.7) and immunoblotting. Total cell lysates were used to check Wnt expression in transfected CHO cells. Wnt proteins have a size of about 42 kDa. Silverstaining analysis in Figure 21 shows the imidazole-dependent time point when the protein separates from the beads. Elution with buffer containing 500 mM imidazole is faster and more robust than with 300 mM imidazole. The whole amount of protein is collected in the first two fractions, whereas the buffer containing less imidazole leads to slow release of the protein. Consequently, protein is present at low concentration in several fractions.

The quantity of Wnt protein was estimated by comparing signals to 10 ng and 100 ng BSA control bands. Unfortunately, the concentration of Wnt protein was not high enough to be further used. The fraction with the highest protein concentration (Figure 20) contained approximately 100 ng of Wnt11. Hannoush et al. (Hannoush, 2008) and Fuerer et al. (Fuerer, Habib, & Nusse, 2010) suggested a Wnt concentration of at least 100-400 ng/ml for experiments stimulating differentiated C2C12 myotubes. To improve the expression rate of Wnt protein, another stably expressing CHO cell line with tandem-tagged Wnt-myc-his under the control of the PGK promoter was established and tested for their amount of protein expression in total lysates and the supernatant. Unfortunately, the protein yield was not increased (Data not shown).

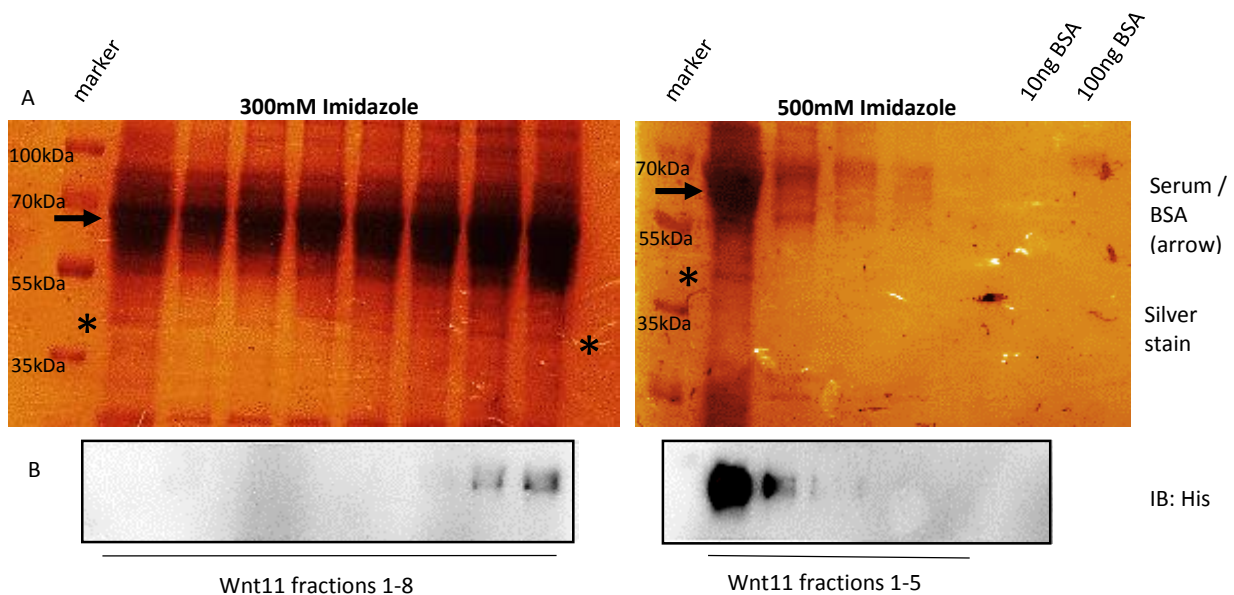


Figure 20: Silver staining and immunoblot analysis of purified his-Wnt11 fractions. Eluted with buffer containing 300mM or 500mM imidazole. The asterisks indicate Wnt at 42 kDa. As a help, estimating the quantity of Wnt protein, 10ng and 100ng BSA was loaded. **(A)** Imaging of performed silverstaining of Wnt11 protein eluted with two different buffer conditions. Elution buffer containing 500mM Imidazole concentrates the protein in the first fraction, whereas the buffer supplemented with 300mM Imidazole elutes the protein in later fractions. BSA artifacts are represented as a big band at 70 kDa (arrow). **(B)** Immunoblotting of eluted fractions and probing against His indicates timepoints and fractions of protein elution comparable to silverstaining analysis.

6.3.2 Examining Wnt - MuSK interaction using co-immunoprecipitation

It has previously been shown that Wnts interact with MuSK and play a role in vertebrate NMJ formation. In 2012, Strohlic et al. (Strohlic et al., 2012) reported the interaction of Wnt4 with MuSK-CRD and activation of MuSK by Wnt4 performing co-immunoprecipitations. Similarly, recombinant Wnt9a and Wnt11 were found to stimulate AChR clustering (B. Zhang et al., 2012).

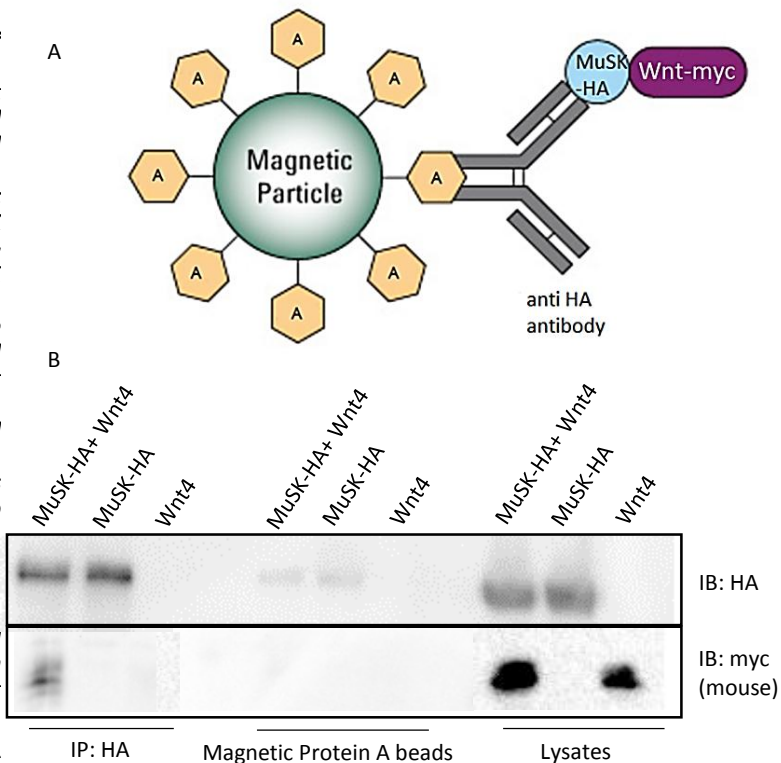
Here, we wanted to study Wnt4, 9a and 11 interaction with MuSK using co-immunoprecipitation. Wnt4, 9a and 11 recognize the frizzled-like cysteine-rich domain (CRD) of MuSK. Cells were transiently co-transfected with MuSK-HA and Wnt4-myc or transfected with MuSK-HA or Wnt4-myc respectively. Cells were lysed 12 h later. Lysates were incubated 2 h with pre-clearing beads while pre-coupling of anti-HA antibody with protein-A magnetic beads. Pre-cleared lysates and coupled beads-antibody mix was incubated overnight and separated by SDS-PAGE. As a control, samples incubated overnight with magnetic protein-A beads only were used.

Figure 21 shows a representative image of anti-HA and anti-myc immunoblotting after HA-immunoprecipitation. Wnt was successfully trapped by MuSK and detected performing anti-myc immunoblotting. Wnt protein binds MuSK-HA, which is captured by anti-HA antibody coupled beads. Figure 21 illustrates the successful detection of MuSK-interacting Wnt protein. Total lysates show equal expression levels of single and co-transfected proteins. The middle column represents lysates only incubated with protein-A magnetic beads without HA antibody. The magnetic protein A beads show some unspecific binding to HA-MuSK but the resulting MuSK signaling is much weaker than in the presence of HA antibody. No unspecific binding to Wnt was detected.

The successful detection of MuSK-Wnt4 interaction resulted from an extensive troubleshooting to reveal ideal experimental settings (Data not shown). Firstly, transfection methods (turbofect, calcium phosphate)

and different types of cells (HEK, Cos-7) were tested on their efficiency of transfection and Wnt and MuSK protein expression. Different tags (myc, myc-his,), their site of tagging (N-/C-terminal of the protein) and whether protein expression is affected was tested. Anti-HA-, anti-MuSK- and anti-myc co-immunoprecipitations were analyzed according to their efficiency and the antibodies used for immunoblotting of MuSK and Wnt proteins were tested. Available antibodies detecting MuSK were anti-MuSK-94277 and anti-HA. Wnt was detected by anti-myc. Co-immunoprecipitation using anti-HA to detect MuSK and anti-myc for the detection of Wnt protein were the best experimental combination. Further conditions including bead types (protein A agarose beads, protein A magnetic beads) to overcome unspecific binding of beads to the protein, lysis buffer (RIPA, NP-40) and washing conditions (NaCl concentration) to increase stringency were extensively tested. DNA ratio in co-transfections played an important role achieving equal protein expression levels. The best experimental design was developed and represents the basis for the presented results.

Figure 21: (A) Principle of co-immunoprecipitation: HA Co-IP detecting Wnt protein via MuSK-HA trapped by anti HA antibody and magnetic A beads; **(B) Interaction of Wnt protein with HA-MuSK after HA-immunoprecipitation:** HEK cell lysates are shown together with the negative control without antibody and the total protein lysates for general protein expression pattern. Negative control incubated only with magnetic protein-A beads show almost no unspecifically bound protein. Immunoblotting of HA-IP samples using anti myc antibody illustrates detection of Wnt protein bound specifically to MuSK. It can be detected alone after separation from the protein complex with MuSK.



6.3.3 Wnt, MuSK, Lrp4 colocalization in Cos-7 cells

To further investigate Wnt-MuSK interaction, colocalization studies of Wnt, MuSK and Lrp4 in Cos-7 cells were performed (see section 5.8.4 for staining procedure). Therefore, cells were transfected with HA-MuSK, Wnt4/9a/11-myc and Lrp4-GFP. For staining of the cell surface, transfected Cos-7 cells were fixed in PFA, blocked, incubated in primary and secondary antibody and mounted. Total MuSK, Lrp4 or Wnt staining includes an additional permeabilization step with triton between fixation and blocking. MuSK was detected via its HA tag, Wnt via its myc tag and Lrp4 was GFP coupled. Untransfected (UT) cells treated with different antibody combinations were used as a control to exclude staining artefacts. Cells were fixed, permeabilized for total protein staining, stained and imaged using confocal microscopy with a 63x oil objective (for procedure see section 5.8.4).

The staining results are demonstrated in Figures 22 and 23. Colocalization of Wnt and MuSK in Figure 22 is shown in yellow and enlarged in cut-out sections. Total protein stainings of permeabilized Cos-7 cells reveal clear accumulation of Wnt and MuSK in perinuclear compartments (i.e ER or Golgi) in cells co-transfected with MuSK and Wnt4, 9a and 11. Surface staining shows co-localization in small puncta form in Wnt9a and Wnt4 co-transfected cells. Wnt11-MuSK transfections display co-localization in a continuous area along the cell surface. Cells additionally transfected with Lrp4 are shown in Figure 23. Cos-7 cells were transfected with MuSK, Lrp4 and Wnt4, 9a and 11, respectively and colocalization is observed in white. Surface staining shows colocalization in a continuous form along the surface in cells transfected with MuSK, Lrp4 and Wnt4 or 9a, respectively. Colocalization in MuSK, Lrp4 and Wnt11 transfected cells can be seen in small puncta form on the cell surface. In Figure 23, cells co-transfected with Wnt4 and 11 show higher colocalization signal than cells co-transfected with Wnt9a. Co-localization in total protein staining appears, as in Figure 22, in perinuclear regions. Unfortunately, Lrp4-GFP was detected in high amount in the nucleus. It appeared to be rather accumulating in the cell,

than being expressed on the cell surface. This could explain the low colocalization signal of the three proteins.

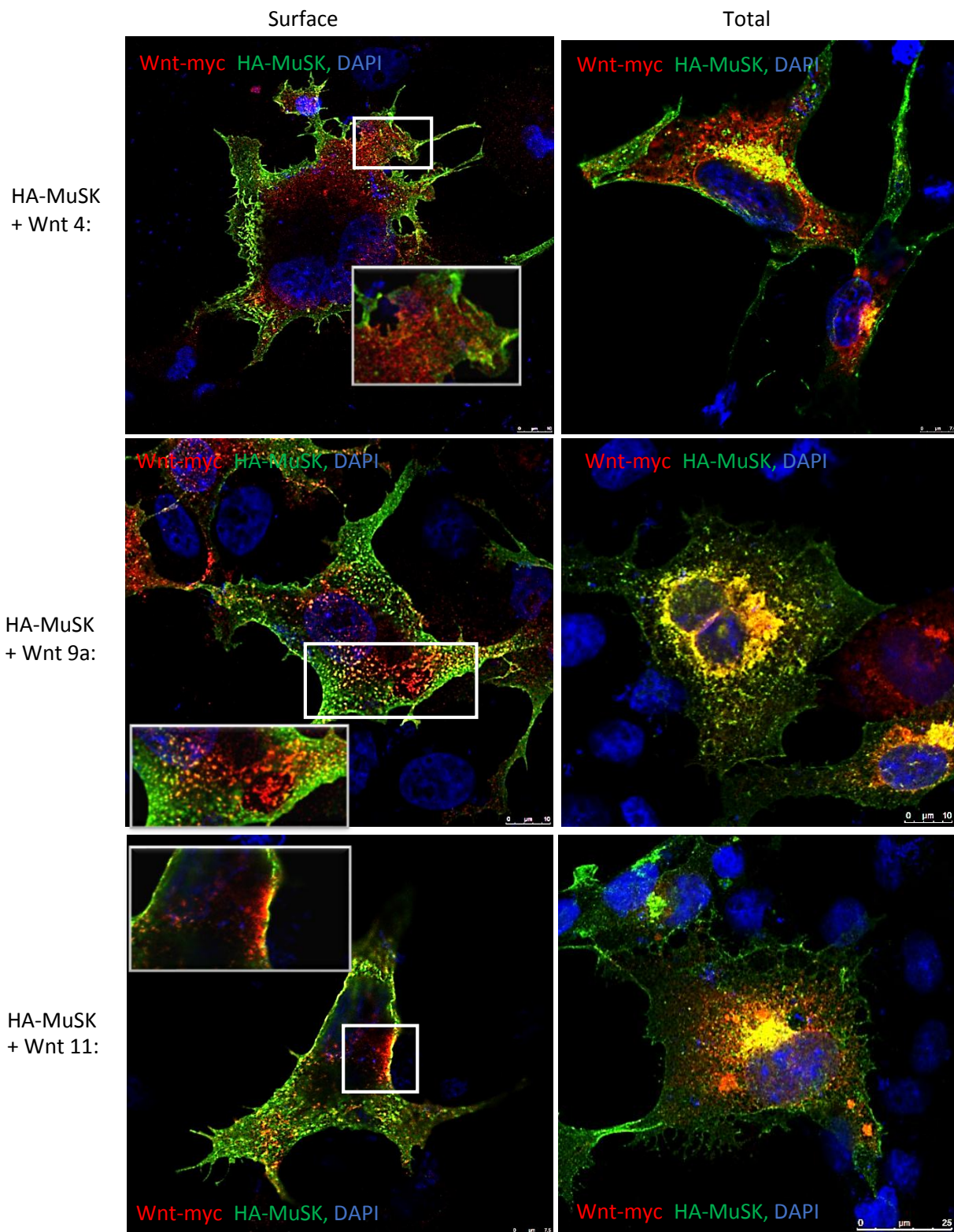


Figure 22: Wnt and MuSK co-localization in Cos-7 cells. Myc-his tagged Wnt4, 9a and 11 were co-transfected with HA-MuSK. It was distinguished between surface and total protein stainings. Wnts were detected via their myc-tag, MuSK via its HA-tag. DAPI was used additionally to stain nucleic acid. Clear colocalization in perinuclear compartments can be seen in yellow in total stainings. Co-localization in surface protein staining appears as small puncta or continuous form in certain areas (cut out areas enlarged).

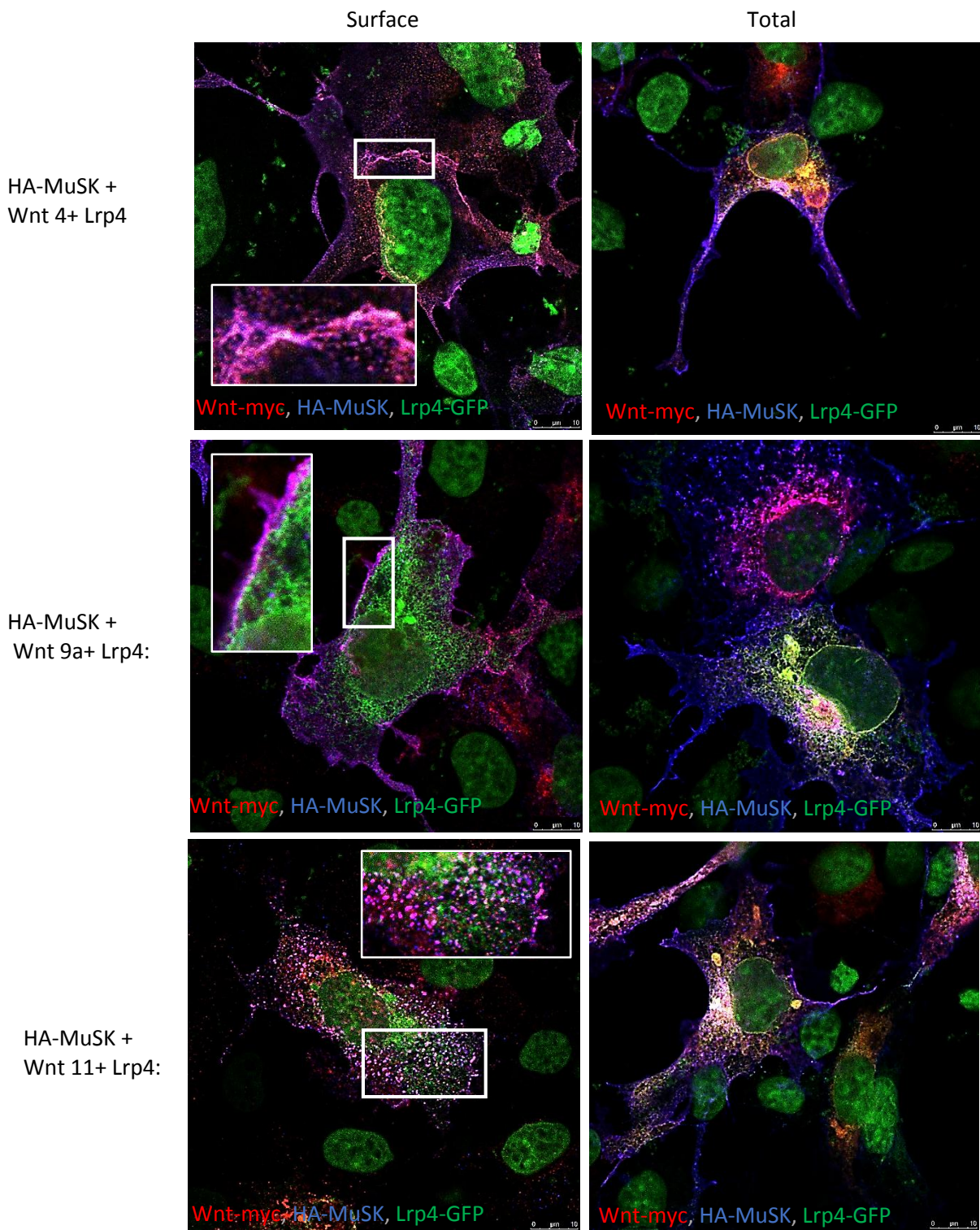


Figure 23: Colocalization of Wnt, MuSK and Lrp4 in Cos-7 cells. Myc-his tagged Wnt4, 9a and 11 were co-transfected via turbofect with HA-MuSK and Lrp4-GFP. It was distinguished between surface and total protein stainings. Wnt were detected via their myc-tag, MuSK via its HA-tag, Lrp4 was already GFP coupled. Colocalization of all three proteins is indicated in white.

7 Discussion and Outlook

7.1 Downregulation of candidate proteins in C2 cells

This Master's Thesis is divided into two parts. The goal of the first part was to establish C2 mouse muscle cell lines where specific MuSK downstream phospho-target proteins are downregulated in a doxycycline-dependent manner using RNAi. The expression system used for RNAi-mediated downregulation of candidate protein is called TET-On-System, which is designed for a tight regulation of target genes or proteins in mammalian cells with a minimal dosage of doxycycline (Chao et al., 2012; Fellmann et al., 2013). The Tet-On system uses a two-component conditional expression system that requires a reverse tetracycline transactivator (rtTA) and a tetracycline-responsive element (TRE) promoter driving shRNA expression (Gossen et al., 1995; Zuber et al., 2011) and leading to target gene downregulation. Since GFP is co-expressed upon Dox stimulation, it serves as a control for the efficiency of tet-induced shRNA expression.

I aimed to investigate the effect of protein downregulation on AChR clustering. Therefore, C2C12 Tet muscle cells were infected with retroviral vectors targeting proteins Dyn2 (dyn2.838 and dyn2.1316), FAK (ptk.352 and ptk.2316), Lrp4 (lrp4.1058, lrp4.1346 and lrp4.1489) and EB3 (mapre.423 and mapre.1355). After infection, the C2 muscle cell lines were tested on their proper proliferation, differentiation into multinucleated myotubes and GFP expression in doxycycline treated samples. Expression of shRNAs and their function in downregulation of target proteins were controlled using biochemistry methods and assaying the effect on AChR clustering.

The chosen target proteins used in downregulation experiments play a potential role in MuSK internalization and downstream signaling:

- EB3 is a microtubule plus-end protein, expressed in myotubes and accumulating at sites where microtubules attach to AChR clusters

(Schmidt et al., 2012). The delivery of AChRs to the adult NMJ via microtubules is not yet fully understood but Basu et al. in 2015 (Basu et al., 2015) reported that microtubule plus-end proteins like CLASP2 and its interaction partner LL5 β as well as GSK3 β participate in the regulation of AChR cluster density in agrin-induced clusters. The knockout of LL5 β , CLASP2 or the treatment with microtubule- and actin-depolymerizing drugs inhibits microtubule capturing and focal vesicle delivery to agrin-induced clusters. Therefore, it can be suggested that EB3 downregulation has a negative effect in AChR cluster formation.

- The GTPase Dynamin-2 is a known master regulator in endocytosis, endocytotic internalization and therefore regulates several signaling pathways. The key-process is clathrin-mediated endocytosis (CME) which is responsible for the internalization of portions of the plasma membrane and extracellular matrix proteins (McMahon & Boucrot, 2011). Dynamin-2 is encircling the neck of the budding vesicle and performs vesicle scission (Chappie et al., 2011; Ferguson & De Camilli, 2012; Hinshaw & Schmid, 1995). Dynamin-2 is pre-and postsynaptically expressed, participating in synaptic vesicle recycling and signaling receptor internalization e.g. MuSK endocytosis after agrin stimulation (Okamoto, Gamby, Wells, Fallon, & Vallee, 2001; Tanifuji, Funakoshi-Tago, Ueda, Kasahara, & Mochida, 2013; Zhu et al., 2008). Mutations in Dynamin-2 can lead to a dysfunction in endocytosis, signal trafficking pathways and AChR clustering resulting in myopathies like myasthenia gravis (MG), Charcot-Marie-Tooth (CMT) disease or centronuclear myopathy (CNM) (Gonzalez-Jamett et al., 2014; Koutsopoulos et al., 2011; Tinelli, Pereira, & Suter, 2013). CMT-linked mutations are localized in the lipid-binding N-terminal region of the PH domain of Dynamin-2 whereas CNM-linked mutations can be found in the C-terminal helix of the PH domain (Bohm et al., 2012).
- Focal adhesion kinase (FAK) interacts with Src and is involved in focal adhesion assembly, cytoskeletal rearrangements and

stabilization of AChR clusters (Tsai et al., 2012). Interestingly, AChR cluster maturation is associated with proteins like LL5 β , Paxillin, Vinculin or Talin (Durnberger et al., 2014; T. J. P. J. R. Sanes, 2013) and tyrosine phosphorylation of Paxillin seems to be FAK- and Src-dependent (Durnberger et al., 2014). So far, very little is known about the effect of FAK downregulation on AChR clustering but due to its known function, we suggested that FAK downregulation might impair MuSK endocytosis and therefore lead to decreased AChR clustering.

Hence, a downregulation of one the chosen target proteins is supposed to impair MuSK internalization and AChR clustering. For the proteins Dyn2, EB3 and FAK successful downregulation of approx. 50% was demonstrated by immunoblot analysis of endogenous protein. FAK downregulated cell lines were additionally tested on the ability of AChR clustering, however, the results varied in different shRNA-targeted cell lines and do not seem to affect AChR clustering. Possible reasons could be unspecific effects of RNAi, insufficient downregulation or even inhomogeneous data analysis. However, AChR cluster assays were only performed once and due to missing evidence, FAK downregulation and the effect on AChR clustering remain elusive and have to be further investigated.

7.1.1 Downregulation of Lrp4

Lrp4 is an important keyplayer in AChR clustering and NMJ formation in motoneurons. Lrp4 binds agrin, interacts with MuSK (Kim & Burden, 2008; W. Zhang et al., 2011), and participates in the initiation of AChR clustering, thus, making it a useful tool studying AChR clustering and NMJ formation. Mice lacking LRP4 die at birth and do not form NMJs, indicating a critical role in NMJ formation (Weatherbee et al., 2006).

Expression of shRNAs targeting Lrp4 led to a significant downregulation of protein expression and impaired AChR clustering. This was demonstrated assaying AChR cluster formation where myotubes did

not show any AChR clusters. These downregulation approaches can therefore be used for further experiments examining MuSK internalization, its activation and AChR clustering.

7.2 Isolation of Wnt proteins and their interaction with MuSK

The topic of the second part of this thesis are Wnt proteins and their interaction with MuSK. Recently, several studies have reported a function for Wnts in MuSK activation and NMJ formation (Barik, Zhang, et al., 2014; Messeant et al., 2015; Takamori, 2012). In 2012, Strohlic et al. (Strohlic et al., 2012) reported the interaction and activation of MuSK by Wnt4 performing co-immunoprecipitations. Wnt9a and Wn11 were shown to interact with MuSK and stimulate AChR clustering using recombinant Wnt proteins (B. Zhang et al., 2012). In this Master's Thesis I tried to establish a common method, testing the interaction between Wnt4, 9a and 11 proteins and MuSK. In addition, the purification of recombinant Wnt proteins was attempted.

7.2.1 Purification of Wnt11 protein

Numerous articles about Wnt proteins and their possible interaction with MuSK and further effect on NMJ formation are published (Barik, Zhang, et al., 2014; Strohlic et al., 2012; B. Zhang et al., 2012). The aim was to establish stably Wnt expressing cell lines, the purification of secreted Wnt protein from the medium and the investigation of possible changes in AChR clustering or MuSK phosphorylation upon Wnt stimulation. Wnt4, 9a and 11 were chosen to be the targets because of the fact that all three bind MuSK. In addition, Wnt4 and Wnt11 are able to activate MuSK (Strohlic et al., 2012; B. Zhang et al., 2012). Wnt subcloning and stable transfection into CHO cells was successful. However, protein expression of Wnt4 and 9a was low, so I continued with purification experiments using only Wnt 11. Isolation via gravity purification column

was carried out similar to other publications (Willert et al, 2003) and I was able to detect his-tagged Wnt proteins performing immunoblotting of purified fractions. However, the amount of the obtained protein was not sufficient. Further subcloning was done in order to achieve a higher Wnt expression and secretion rate. A doubletag and a different promoter were introduced into the pcDNA3.1 vector and the established stable cell line was again tested biochemically and with immunocytochemistry methods. Despite these experimental adjustments, Wnt protein secretion remained low. As Willert et al. already depicted 2003 (K. Willert et al., 2003), and 2008 (K. H. Willert, 2008), Wnt isolation in its active and soluble form in cell culture is difficult. In large part because of its hydrophobic nature, which is due to one or more posttranslational lipid modifications. Numerous studies explain different attempts to produce secreted Wnt, but overexpression of the proteins in cultured cells mostly results in accumulation of misfolded protein in the ER (Kitajewski, Mason, & Varmus, 1992). Consistent with these reports, total cell lysates always showed high Wnt protein expression, corresponding supernatants, however, showed little protein detection. This supports the theory of accumulated Wnt protein in the cell.

7.2.2 Determination of the interaction between Wnt4 and MuSK by co-immunoprecipitation

As Strohlic et al. already reported in 2012 (Strohlic et al., 2012) using co-immunoprecipitation, Wnt4 interacts with MuSK CRD and induces MuSK phosphorylation but not MuSK Δ CRD (MuSK lacking the CRD) phosphorylation. Equally in zebrafish, Jing et al. (Jing et al., 2009) showed that Wnt11r binds to the CRD of *unplugged*/MuSK ectodomain performing immunoprecipitation. Additionally, Zhang et al. (B. Zhang et al., 2012) provided evidence that Wnt9a and Wnt11 interact with MuSK using recombinant Wnt proteins. With co-immunoprecipitation, I wanted to proof that Wnt4, together with Wnt9a and Wnt11 interact with MuSK. Due to a time consuming troubleshooting phase, I concentrated on Wnt4.

To verify that Wnt4 is specifically interacting with MuSK, co-immunoprecipitations of Wnt protein and MuSK were performed. Therefore, HEK cells were transiently transfected with HA-tagged MuSK and myc-tagged Wnt4. After HA-coimmunoprecipitation and immunoblotting using anti-HA and anti-myc antibody, Wnt protein could be detected alone. Wnt protein was not detected in Wnt4-myc single transfected HEK cells. This indicates that Wnt protein interacts with MuSK, dissociates after SDS-PAGE and is detectable after immunoblotting. Taken together, Wnt4 is found to specifically bind to MuSK, as Strohlic et al. already depicted in 2012 (Strohlic et al., 2012). About its ability to phosphorylate and activate MuSK nothing can be presumed with this finding. Therefore, separate MuSK phosphorylation assays have to be performed. Wnt9a and Wnt11 still remain to be tested.

To achieve these results, all experimental settings were extensively tested (Data not shown). Occurring unequal protein expression levels were minimized checking DNA quality, adapting DNA ratio between Wnt and MuSK and by using the less expressed construct (MuSK-HA; HA-MuSK is higher expressed) in overexpressing HEK cells. The next challenge was to reduce unspecific protein binding of beads and to achieve a higher stringency changing the immunoprecipitation washing conditions. ProteinA magnetic beads pre-coupled to HA-antibody incubated overnight with pre-cleared protein lysates (using pre-clearing beads) and increased NaCl concentration of washing buffer were the key to obtain clear immunoblotting signals. Furthermore, I found out that HA-immunoprecipitation is more effective than MuSK- or myc-immunoprecipitation.

7.2.3 Co-localization studies of Wnt protein, MuSK and Lrp4 using immunostaining and confocal microscopy

Studies were performed in assumption that the interacting proteins Wnt, MuSK and Lrp4 might show co-localization on the cell surface after

immunostaining of the candidate proteins. Gordon and Granato (Gordon et al., 2012) used dome-staged zebrafish embryos and showed MuSK internalization upon Wnt11r stimulation using immunostainings of MuSK and Wnt11r. Strochlic et al. (Strochlic et al., 2012) used mouse embryos to investigate the interaction between Wnt4 and MuSK. The interaction of Lrp4 with MuSK and Wnt proteins with MuSK was already shown in numerous studies in different model organisms. So far, no findings about the combined co-localization of the three proteins Wnt, MuSK and Lrp4 was reported. In my thesis I assumed that the interacting proteins Wnt, Lrp4 and MuSK can be tracked on the cell surface using immunostainings and confocal microscopy.

Co-localization of Wnt, MuSK and Lrp4 was investigated performing immunostaining of Cos7-cells fixed and stained on coverslips. Surface protein staining was compared with total protein staining to detect differences in distribution of the three proteins in the cell and on its surface. Therefore, total protein staining procedure contains an additional permeabilization step with triton. On the cell surface, co-localization with MuSK is visualized differently, either in puncta or continuous form, in all three tested Wnt (Figure 23) and with Lrp4 (Figure 24). In total cell stainings, the co-localization of the three Wnt proteins with MuSK and Lrp4 can be seen in perinuclear compartments. As already mentioned, this can refer to accumulated Wnt protein in the ER or Golgi upon overexpression, misfolding and wrong posttranslational lipid modifications. Production of secreted and active Wnt protein depends very much on its post-translational modification in the ER (Kurayoshi, Yamamoto, Izumi, & Kikuchi, 2007), which causes their high degree of insolubility and hydrophobicity. Wnts are palmitoylated, glycosylated and depend on cofactors to maintain their stability in their secreted form (Takada et al., 2006). While lipid modification is important triggering the activation of the intracellular Wnt signaling cascade, glycosylation is important for secretion of Wnt but not for their action (Kurayoshi et al., 2007). Heparan sulfate proteoglycans (HSPGs) such as glypican and syndecan are able to maintain Wnt solubility by

preventing their aggregation in the extracellular environment and stabilizing their signaling activity (Fuerer et al., 2010). Already one missing step in this Wnt production and modification procedure can lead to aggregated, misfolded and inactive protein. Hence, the correct expression of Wnt is important and might be affected by overexpression in immortalized cell lines.

8 Appendix

8.1 Reference List

- Barik, A., Lu, Y., Sathyamurthy, A., Bowman, A., Shen, C., Li, L., . . . Mei, L. (2014). LRP4 is critical for neuromuscular junction maintenance. *J Neurosci*, *34*(42), 13892-13905. doi: 10.1523/jneurosci.1733-14.2014
- Barik, A., Zhang, B., Sohal, G. S., Xiong, W. C., & Mei, L. (2014). Crosstalk between Agrin and Wnt signaling pathways in development of vertebrate neuromuscular junction. *Dev Neurobiol*, *74*(8), 828-838. doi: 10.1002/dneu.22190
- Basu, S., Sladeczek, S., Martinez de la Pena y Valenzuela, I., Akaaboune, M., Smal, I., Martin, K., . . . Brenner, H. R. (2015). CLASP2-dependent microtubule capture at the neuromuscular junction membrane requires LL5beta and actin for focal delivery of acetylcholine receptor vesicles. *Mol Biol Cell*, *26*(5), 938-951. doi: 10.1091/mbc.E14-06-1158
- Bergamin, E., Hallock, P. T., Burden, S. J., & Hubbard, S. R. (2010). The cytoplasmic adaptor protein Dok7 activates the receptor tyrosine kinase MuSK via dimerization. *Mol Cell*, *39*(1), 100-109. doi: 10.1016/j.molcel.2010.06.007
- Berwick, D. C., & Harvey, K. (2013). LRRK2: an eminence grise of Wnt-mediated neurogenesis? *Front Cell Neurosci*, *7*, 82. doi: 10.3389/fncel.2013.00082
- Berwick, Daniel C., & Harvey, Kirsten. (2013). *LRRK2: an éminence grise of Wnt-mediated neurogenesis?*; *Front. Cell. Neurosci.*, 31 May 2013.
- Bohm, J., Biancalana, V., Dechene, E. T., Bitoun, M., Pierson, C. R., Schaefer, E., . . . Laporte, J. (2012). Mutation spectrum in the large GTPase dynamin 2, and genotype-phenotype correlation in autosomal dominant centronuclear myopathy. *Hum Mutat*, *33*(6), 949-959. doi: 10.1002/humu.22067
- Bolliger, M. F., Zurlinden, A., Luscher, D., Butikofer, L., Shakhova, O., Francolini, M., . . . Sonderegger, P. (2010). Specific proteolytic cleavage of agrin regulates maturation of the neuromuscular junction. *J Cell Sci*, *123*(Pt 22), 3944-3955. doi: 10.1242/jcs.072090
- Borges, L. S., & Ferns, M. (2001). Agrin-induced phosphorylation of the acetylcholine receptor regulates cytoskeletal anchoring and clustering. *J Cell Biol*, *153*(1), 1-12.
- Borges, L. S., Yechikhov, S., Lee, Y. I., Rudell, J. B., Friese, M. B., Burden, S. J., & Ferns, M. J. (2008). Identification of a motif in the acetylcholine receptor β subunit whose phosphorylation regulates rapsyn association and postsynaptic receptor localization. *J Neurosci*, *28*(45), 11468-11476.
- Brinas, L., Vassilopoulos, S., Bonne, G., Guicheney, P., & Bitoun, M. (2013). Role of dynamin 2 in the disassembly of focal adhesions. *J Mol Med (Berl)*, *91*(7), 803-809. doi: 10.1007/s00109-013-1040-2
- Burden, S. J. (2011). SnapShot: Neuromuscular Junction. *Cell*, *144*(5), 826-826 e821. doi: 10.1016/j.cell.2011.02.037
- Burden, S. J., Yumoto, N., & Zhang, W. (2013). The role of MuSK in synapse formation and neuromuscular disease. *Cold Spring Harb Perspect Biol*, *5*(5), a009167. doi: 10.1101/cshperspect.a009167
- Cartaud, A., Stetzkowski-Marden, F., Maoui, A., & Cartaud, J. (2011). Agrin triggers the clustering of raft-associated acetylcholine receptors through actin cytoskeleton reorganization. *Biol Cell*, *103*(6), 287-301. doi: 10.1042/bc20110018

- Chao, J. S., Chao, C. C., Chang, C. L., Chiu, Y. R., & Yuan, C. J. (2012). Development of single-vector Tet-on inducible systems with high sensitivity to doxycycline. *Mol Biotechnol*, *51*(3), 240-246. doi: 10.1007/s12033-011-9461-z
- Chappie, J. S., Mears, J. A., Fang, S., Leonard, M., Schmid, S. L., Milligan, R. A., . . . Dyda, F. (2011). A pseudoatomic model of the dynamin polymer identifies a hydrolysis-dependent powerstroke. *Cell*, *147*(1), 209-222. doi: 10.1016/j.cell.2011.09.003
- Chevessier, F., Faraut, B., Ravel-Chapuis, A., Richard, P., Gaudon, K., Bauche, S., . . . Hantai, D. (2004). MUSK, a new target for mutations causing congenital myasthenic syndrome. *Hum Mol Genet*, *13*(24), 3229-3240. doi: 10.1093/hmg/ddh333
- Chin, Y. H., Lee, A., Kan, H. W., Laiman, J., Chuang, M. C., Hsieh, S. T., & Liu, Y. W. (2015). Dynamin-2 mutations associated with centronuclear myopathy are hypermorphic and lead to T-tubule fragmentation. *Hum Mol Genet*, *24*(19), 5542-5554. doi: 10.1093/hmg/ddv285
- Choi, J., & Holtzer, H. (1990). *MyoD converts primary dermal fibroblasts, chondroblasts, smooth muscle, and retinal pigmented epithelial cells into striated mononucleated myoblasts and multinucleated myotubes; Proc Natl Acad Sci U S A. 1990 Oct;87(20):7988-92.*
- Dobbins, G. C., Luo, S., Yang, Z., Xiong, W. C., & Mei, L. (2008). alpha-Actinin interacts with rapsyn in agrin-stimulated AChR clustering. *Mol Brain*, *1*, 18. doi: 10.1186/1756-6606-1-18
- Durnberger, G., Camurdanoglu, B. Z., Tomschik, M., Schutzbier, M., Roitinger, E., Hudecz, O., . . . Herbst, R. (2014). Global analysis of muscle-specific kinase signaling by quantitative phosphoproteomics. *Mol Cell Proteomics*, *13*(8), 1993-2003. doi: 10.1074/mcp.M113.036087
- Fellmann, C., Hoffmann, T., Sridhar, V., Hopfgartner, B., Muhar, M., Roth, M., . . . Zuber, J. (2013). An optimized microRNA backbone for effective single-copy RNAi. *Cell Rep*, *5*(6), 1704-1713. doi: 10.1016/j.celrep.2013.11.020
- Ferguson, S. M., & De Camilli, P. (2012). Dynamin, a membrane-remodelling GTPase. *Nat Rev Mol Cell Biol*, *13*(2), 75-88. doi: 10.1038/nrm3266
- Fuerer, C., Habib, S. J., & Nusse, R. (2010). A study on the interactions between heparan sulfate proteoglycans and Wnt proteins. *Dev Dyn*, *239*(1), 184-190. doi: 10.1002/dvdy.22067
- Glass, D. J., Bowen, D. C., Stitt, T. N., Radziejewski, C., Bruno, J., Ryan, T. E., . . . Yancopoulos, G. D. (1996). Agrin acts via a MuSK receptor complex. *Cell*, *85*(4), 513-523.
- Gomez, A. M., & Burden, S. J. (2011). The extracellular region of Lrp4 is sufficient to mediate neuromuscular synapse formation. *Dev Dyn*, *240*(12), 2626-2633. doi: 10.1002/dvdy.22772
- Gonzalez-Jamett, A. M., Haro-Acuna, V., Momboisse, F., Caviedes, P., Bevilacqua, J. A., & Cardenas, A. M. (2014). Dynamin-2 in nervous system disorders. *J Neurochem*, *128*(2), 210-223. doi: 10.1111/jnc.12455
- Gordon, L. R., Gribble, K. D., Syrett, C. M., & Granato, M. (2012). Initiation of synapse formation by Wnt-induced MuSK endocytosis. *Development*, *139*(5), 1023-1033. doi: 10.1242/dev.071555
- Gossen, M., Freundlieb, S., Bender, G., Muller, G., Hillen, W., & Bujard, H. (1995). Transcriptional activation by tetracyclines in mammalian cells. *Science*, *268*(5218), 1766-1769.
- Hallock, P. T., Xu, C. F., Park, T. J., Neubert, T. A., Curran, T., & Burden, S. J. (2010). Dok-7 regulates neuromuscular synapse formation by recruiting

- Crk and Crk-L. *Genes Dev*, 24(21), 2451-2461. doi: 10.1101/gad.1977710
- Hankey, P. A. (2009). Regulation of hematopoietic cell development and function by Stat3. *Front Biosci (Landmark Ed)*, 14, 5273-5290.
- Hannoush, R. N. (2008). Kinetics of Wnt-driven beta-catenin stabilization revealed by quantitative and temporal imaging. *PLoS One*, 3(10), e3498. doi: 10.1371/journal.pone.0003498
- He, X., Semenov, M., Tamai, K., & Zeng, X. (2004). LDL receptor-related proteins 5 and 6 in Wnt/beta-catenin signaling: arrows point the way. *Development*, 131(8), 1663-1677. doi: 10.1242/dev.01117
- Henriquez, J. P., Webb, A., Bence, M., Bildsoe, H., Sahores, M., Hughes, S. M., & Salinas, P. C. (2008). Wnt signaling promotes AChR aggregation at the neuromuscular synapse in collaboration with agrin. *Proc Natl Acad Sci U S A*, 105(48), 18812-18817. doi: 10.1073/pnas.0806300105
- Herbst, R., & Burden, S. J. (2000). The juxtamembrane region of MuSK has a critical role in agrin-mediated signaling. *EMBO J*, 19(1), 67-77. doi: 10.1093/emboj/19.1.67
- Hinshaw, J. E., & Schmid, S. L. (1995). Dynamin self-assembles into rings suggesting a mechanism for coated vesicle budding. *Nature*, 374(6518), 190-192. doi: 10.1038/374190a0
- Hubbard, S. R., & Gnanasambandan, K. (2013). Structure and activation of MuSK, a receptor tyrosine kinase central to neuromuscular junction formation. *Biochim Biophys Acta*, 1834(10), 2166-2169. doi: 10.1016/j.bbapap.2013.02.034
- Jang, Y.N., & Baik, E.J. (2013). *JAK-STAT pathway and myogenic differentiation; JAKSTAT.2013 Apr1; 2(2): e23282.*
- Jing, L., Lefebvre, J. L., Gordon, L. R., & Granato, M. (2009). Wnt signals organize synaptic prepattern and axon guidance through the zebrafish unplugged/MuSK receptor. *Neuron*, 61(5), 721-733. doi: 10.1016/j.neuron.2008.12.025
- Kim, N., & Burden, S. J. (2008). MuSK controls where motor axons grow and form synapses. *Nat Neurosci*, 11(1), 19-27. doi: 10.1038/nn2026
- Kisseleva, T., Bhattacharya, S., Braunstein, J., & Schindler, C. W. (2002). Signaling through the JAK/STAT pathway, recent advances and future challenges. *Gene*, 285(1-2), 1-24.
- Kitajewski, J., Mason, J. O., & Varmus, H. E. (1992). Interaction of Wnt-1 proteins with the binding protein BiP. *Mol Cell Biol*, 12(2), 784-790.
- Koneczny, I., Cossins, J., Waters, P., Beeson, D., & Vincent, A. (2013). MuSK myasthenia gravis IgG4 disrupts the interaction of LRP4 with MuSK but both IgG4 and IgG1-3 can disperse preformed agrin-independent AChR clusters. *PLoS One*, 8(11), e80695. doi: 10.1371/journal.pone.0080695
- Koutsopoulos, O. S., Koch, C., Tosch, V., Bohm, J., North, K. N., & Laporte, J. (2011). Mild functional differences of dynamin 2 mutations associated to centronuclear myopathy and Charcot-Marie Tooth peripheral neuropathy. *PLoS One*, 6(11), e27498. doi: 10.1371/journal.pone.0027498
- Kurayoshi, M., Yamamoto, H., Izumi, S., & Kikuchi, A. (2007). Post-translational palmitoylation and glycosylation of Wnt-5a are necessary for its signalling. *Biochem J*, 402(3), 515-523. doi: 10.1042/bj20061476
- Li, Y., Jiang, B., Ensign, W. Y., Vogt, P. K., & Han, J. (2000). Myogenic differentiation requires signalling through both phosphatidylinositol 3-kinase and p38 MAP kinase. *Cell Signal*, 12(11-12), 751-757.
- Liu, Y. W., Lukiyanchuk, V., & Schmid, S. L. (2011). Common membrane trafficking defects of disease-associated dynamin 2 mutations. *Traffic*, 12(11), 1620-1633. doi: 10.1111/j.1600-0854.2011.01250.x

- LuisKandl, S., Woller, B., Schlauf, M., Schmid, J. A., & Herbst, R. (2013). Endosomal trafficking of the receptor tyrosine kinase MuSK proceeds via clathrin-dependent pathways, Arf6 and actin. *FEBS J*, *280*(14), 3281-3297. doi: 10.1111/febs.12309
- Luo, Z. G., Wang, Q., Zhou, J. Z., Wang, J., Luo, Z., Liu, M., . . . Mei, L. (2002). Regulation of AChR clustering by Dishevelled interacting with MuSK and PAK1. *Neuron*, *35*(3), 489-505.
- Maselli, R. A., Arredondo, J., Cagney, O., Ng, J. J., Anderson, J. A., Williams, C., . . . Wollmann, R. L. (2010). Mutations in MUSK causing congenital myasthenic syndrome impair MuSK-Dok-7 interaction. *Hum Mol Genet*, *19*(12), 2370-2379. doi: 10.1093/hmg/ddq110
- Matsumoto-Miyai, K., Sokolowska, E., Zurlinden, A., Gee, C. E., Luscher, D., Hettwer, S., . . . Sonderegger, P. (2009). Coincident pre- and postsynaptic activation induces dendritic filopodia via neurotrypsin-dependent agrin cleavage. *Cell*, *136*(6), 1161-1171. doi: 10.1016/j.cell.2009.02.034
- McMahon, H. T., & Boucrot, E. (2011). Molecular mechanism and physiological functions of clathrin-mediated endocytosis. *Nat Rev Mol Cell Biol*, *12*(8), 517-533. doi: 10.1038/nrm3151
- Messeant, J., Dobbertin, A., Girard, E., Delers, P., Manuel, M., Mangione, F., . . . Strohlic, L. (2015). MuSK frizzled-like domain is critical for mammalian neuromuscular junction formation and maintenance. *J Neurosci*, *35*(12), 4926-4941. doi: 10.1523/jneurosci.3381-14.2015
- Ochoa, G. C., Slepnev, V. I., Neff, L., Ringstad, N., Takei, K., Daniell, L., . . . De Camilli, P. (2000). A functional link between dynamin and the actin cytoskeleton at podosomes. *J Cell Biol*, *150*(2), 377-389.
- Okamoto, P. M., Gamby, C., Wells, D., Fallon, J., & Vallee, R. B. (2001). Dynamin isoform-specific interaction with the shank/ProSAP scaffolding proteins of the postsynaptic density and actin cytoskeleton. *J Biol Chem*, *276*(51), 48458-48465. doi: 10.1074/jbc.M104927200
- Pato, C., Stetzkowski-Marden, F., Gaus, K., Recouvreur, M., Cartaud, A., & Cartaud, J. (2008). Role of lipid rafts in agrin-elicited acetylcholine receptor clustering. *Chem Biol Interact*, *175*(1-3), 64-67. doi: 10.1016/j.cbi.2008.03.020
- Perez-Garcia, M. J., & Burden, S. J. (2012). Increasing MuSK activity delays denervation and improves motor function in ALS mice. *Cell Rep*, *2*(3), 497-502. doi: 10.1016/j.celrep.2012.08.004
- Sabourin, L. A., & Rudnicki, M. A. (2000). The molecular regulation of myogenesis. *Clin Genet*, *57*(1), 16-25.
- Samuel, M. A., Valdez, G., Tapia, J. C., Lichtman, J. W., & Sanes, J. R. (2012). Agrin and Synaptic Laminin Are Required to Maintain Adult Neuromuscular Junctions. *PLoS One*, *7*(10).
- Sanes, J. R., & Lichtman, J. W. (2001). Induction, assembly, maturation and maintenance of a postsynaptic apparatus. *Nat Rev Neurosci*, *2*(11), 791-805. doi: 10.1038/35097557
- Sanes, T.J. Proszynski; J.R. (2013). Amotl2 interacts with LL5beta, localizes to podosomes and regulates postsynaptic differentiation in muscle. *J. Cell Sci.* *126*, 2225-2235.
- Schmidt, N., Basu, S., Sladeczek, S., Gatti, S., van Haren, J., Treves, S., . . . Brenner, H. R. (2012). Agrin regulates CLASP2-mediated capture of microtubules at the neuromuscular junction synaptic membrane. *J Cell Biol*, *198*(3), 421-437. doi: 10.1083/jcb.201111130
- Serna, I.L. de la, & Imbalzano, A.N. (2005). *MyoD targets chromatin remodeling complexes to the myogenin locus prior to forming a stable DNA-bound complex; Mol Cell Biol.* 2005 May;25(10):3997-4009.

- Shi, L., Fu, A. K., & Ip, N. Y. (2012). Molecular mechanisms underlying maturation and maintenance of the vertebrate neuromuscular junction. *Trends Neurosci*, *35*(7), 441-453. doi: 10.1016/j.tins.2012.04.005
- Sidiropoulos, P. N., Miehe, M., Bock, T., Tinelli, E., Oertli, C. I., Kuner, R., . . . Suter, U. (2012). Dynamin 2 mutations in Charcot-Marie-Tooth neuropathy highlight the importance of clathrin-mediated endocytosis in myelination. *Brain*, *135*(Pt 5), 1395-1411. doi: 10.1093/brain/aws061
- Stetzkowski-Marden, F., Gaus, K., Recouvreur, M., Cartaud, A., & Cartaud, J. (2006). Agrin elicits membrane lipid condensation at sites of acetylcholine receptor clusters in C2C12 myotubes. *J Lipid Res*, *47*(10), 2121-2133. doi: 10.1194/jlr.M600182-JLR200
- Strochlic, L., Falk, J., Goillot, E., Sigoillot, S., Bourgeois, F., Delers, P., . . . Legay, C. (2012). Wnt4 participates in the formation of vertebrate neuromuscular junction. *PLoS One*, *7*(1), e29976. doi: 10.1371/journal.pone.0029976
- Takada, R., Satomi, Y., Kurata, T., Ueno, N., Norioka, S., Kondoh, H., . . . Takada, S. (2006). Monounsaturated fatty acid modification of Wnt protein: its role in Wnt secretion. *Dev Cell*, *11*(6), 791-801. doi: 10.1016/j.devcel.2006.10.003
- Takamori, M. (2012). Structure of the neuromuscular junction: function and cooperative mechanisms in the synapse. *Ann N Y Acad Sci*, *1274*, 14-23. doi: 10.1111/j.1749-6632.2012.06784.x
- Tanifuji, S., Funakoshi-Tago, M., Ueda, F., Kasahara, T., & Mochida, S. (2013). Dynamin isoforms decode action potential firing for synaptic vesicle recycling. *J Biol Chem*, *288*(26), 19050-19059. doi: 10.1074/jbc.M112.445874
- Till, J. H., Becerra, M., Watty, A., Lu, Y., Ma, Y., Neubert, T. A., . . . Hubbard, S. R. (2002). Crystal structure of the MuSK tyrosine kinase: insights into receptor autoregulation. *Structure*, *10*(9), 1187-1196.
- Tinelli, E., Pereira, J. A., & Suter, U. (2013). Muscle-specific function of the centronuclear myopathy and Charcot-Marie-Tooth neuropathy-associated dynamin 2 is required for proper lipid metabolism, mitochondria, muscle fibers, neuromuscular junctions and peripheral nerves. *Hum Mol Genet*, *22*(21), 4417-4429. doi: 10.1093/hmg/ddt292
- Tsai, P. I., Wang, M., Kao, H. H., Cheng, Y. J., Lin, Y. J., Chen, R. H., & Chien, C. T. (2012). Activity-dependent retrograde laminin A signaling regulates synapse growth at Drosophila neuromuscular junctions. *Proc Natl Acad Sci U S A*, *109*(43), 17699-17704. doi: 10.1073/pnas.1206416109
- Valenzuela, D. M., Stitt, T. N., DiStefano, P. S., Rojas, E., Mattsson, K., Compton, D. L., . . . et al. (1995). Receptor tyrosine kinase specific for the skeletal muscle lineage: expression in embryonic muscle, at the neuromuscular junction, and after injury. *Neuron*, *15*(3), 573-584.
- Vincent, Angela. (2002). *Unravelling the pathogenesis of myasthenia gravis; Nature Reviews Immunology 2, 797-804 (October 2002)*.
- Viola, A., & Gupta, N. (2007). Tether and trap: regulation of membrane-raft dynamics by actin-binding proteins. *Nat Rev Immunol*, *7*(11), 889-896. doi: 10.1038/nri2193
- Wang, J., Jing, Z., Zhang, L., Zhou, G., Braun, J., Yao, Y., & Wang, Z. Z. (2003). Regulation of acetylcholine receptor clustering by the tumor suppressor APC. *Nat Neurosci*, *6*(10), 1017-1018. doi: 10.1038/nn1128
- Wang, J., Ruan, N. J., Qian, L., Lei, W. L., Chen, F., & Luo, Z. G. (2008). Wnt/beta-catenin signaling suppresses Rapsyn expression and inhibits acetylcholine receptor clustering at the neuromuscular junction. *J Biol Chem*, *283*(31), 21668-21675. doi: 10.1074/jbc.M709939200

- Wang, Y., Cao, H., Chen, J., & McNiven, M. A. (2011). A direct interaction between the large GTPase dynamin-2 and FAK regulates focal adhesion dynamics in response to active Src. *Mol Biol Cell*, 22(9), 1529-1538. doi: 10.1091/mbc.E10-09-0785
- Watty, A., Neubauer, G., Dreger, M., Zimmer, M., Wilm, M., & Burden, S. J. (2000). The in vitro and in vivo phosphotyrosine map of activated MuSK. *Proc Natl Acad Sci U S A*, 97(9), 4585-4590. doi: 10.1073/pnas.080061997
- Weatherbee, S. D., Anderson, K. V., & Niswander, L. A. (2006). LDL-receptor-related protein 4 is crucial for formation of the neuromuscular junction. *Development*, 133(24), 4993-5000. doi: 10.1242/dev.02696
- Weiss, W., Weiland, F., & Gorg, A. (2009). Protein detection and quantitation technologies for gel-based proteome analysis. *Methods Mol Biol*, 564, 59-82. doi: 10.1007/978-1-60761-157-8_4
- Willert, K., Brown, J. D., Danenberg, E., Duncan, A. W., Weissman, I. L., Reya, T., . . . Nusse, R. (2003). Wnt proteins are lipid-modified and can act as stem cell growth factors. *Nature*, 423(6938), 448-452. doi: 10.1038/nature01611
- Willert, K. H. (2008). Isolation and application of bioactive Wnt proteins. *Methods Mol Biol*, 468, 17-29. doi: 10.1007/978-1-59745-249-6_2
- Yumoto, N., Kim, N., & Burden, S. J. (2012). Lrp4 is a retrograde signal for presynaptic differentiation at neuromuscular synapses. *Nature*, 489(7416), 438-442. doi: 10.1038/nature11348
- Zhang, B., Liang, C., Bates, R., Yin, Y., Xiong, W. C., & Mei, L. (2012). Wnt proteins regulate acetylcholine receptor clustering in muscle cells. *Mol Brain*, 5, 7. doi: 10.1186/1756-6606-5-7
- Zhang, B., Luo, S., Wang, Q., Suzuki, T., Xiong, W. C., & Mei, L. (2008). LRP4 serves as a coreceptor of agrin. *Neuron*, 60(2), 285-297. doi: 10.1016/j.neuron.2008.10.006
- Zhang, W., Coldefy, A. S., Hubbard, S. R., & Burden, S. J. (2011). Agrin binds to the N-terminal region of Lrp4 protein and stimulates association between Lrp4 and the first immunoglobulin-like domain in muscle-specific kinase (MuSK). *J Biol Chem*, 286(47), 40624-40630. doi: 10.1074/jbc.M111.279307
- Zhu, D., Yang, Z., Luo, Z., Luo, S., Xiong, W. C., & Mei, L. (2008). Muscle-specific receptor tyrosine kinase endocytosis in acetylcholine receptor clustering in response to agrin. *J Neurosci*, 28(7), 1688-1696. doi: 10.1523/JNEUROSCI.4130-07.2008
- Zuber, J., McJunkin, K., Fellmann, C., Dow, L. E., Taylor, M. J., Hannon, G. J., & Lowe, S. W. (2011). Toolkit for evaluating genes required for proliferation and survival using tetracycline-regulated RNAi. *Nat Biotechnol*, 29(1), 79-83. doi: 10.1038/nbt.1720

8.2 List of Figures

Figure 1: <i>Development of the synapse; its invagination process and basal lamina proteins</i>	11
Figure 2: <i>Motor axons release Agrin and ACh</i>	12
Figure 3: <i>Postsynaptic maturation</i>	13
Figure 4: <i>Neuromuscular diseases</i>	14
Figure 5: <i>Agrin-Lrp4-Musk complex</i>	16
Figure 6: <i>MuSK architecture and structure</i>	18
Figure 7: <i>Structure of Lrp4 and its interaction with agrin</i>	18
Figure 8: <i>The acetylcholine receptor (AChR)</i>	25
Figure 9 <i>Structure of the pentameric, adult muscle AChR</i>	26
Figure 10 <i>The steps of myogenic differentiation</i>	27
Figure 11: <i>Overview of Wnt signaling pathways</i>	30
Figure 12: <i>Analyzing cluster assays</i>	59
Figure 13: <i>EB3-GFP downregulation in mapre.423 and mapre.1355 expressing cell lines.</i>	62
Figure 14: <i>RNAi-mediated depletion of Lrp4 in C2 cell lines</i>	64
Figure 15: <i>Dyn2 downregulation in stable Dnm2.838 and Dnm2.1316 expressing cell lines.</i>	66
Figure 16: <i>RNAi-mediated depletion of Dynamin at three different differentiation states (I-III)</i>	67
Figure 17: <i>Efficient RNAi-mediated downregulation of FAK in Ptk2.352 and Ptk2.2316 stable expressing C2 cell lines</i>	68
Figure 18: <i>RNAi-mediated depletion of Lrp4 impairs AChR clustering.</i>	69
Figure 19: <i>The effect of shRNA-mediated depletion of FAK on AChR clustering.</i>	71
Figure 20: <i>Silver staining and immunoblot analysis of purified his-Wnt11 fractions.</i>	73
Figure 21: <i>Principle of co-immunoprecipitation.</i>	75
Figure 22: <i>Wnt and MuSK colocalization stainings in Cos-7 cells.</i>	78
Figure 23: <i>Colocalization of Wnt, MuSK and Lrp4 in Cos-7 cells.</i>	79

8.3 Statutory Declaration

I declare that I have developed and written this Master's Thesis independently by myself, that I have not used other than the declared sources and that I have explicitly marked all material, which has been quoted either literally or by content from the used sources. Beyond this I assure that the work has not been used, neither completely nor in parts, to pass any previous examination or is being published elsewhere.

St.Pölten, February 2016

8.4 Curriculum Vitae



Personal Data

Name: Sandra Parzer
Address: Russengasse 12/5/19
3100 St.Pölten
Austria
Date of birth: 2.10.1988
Email: sandra.parzer@gmail.com

Education & Training

WS12-SS16 Master Molecular Biology with a focus on Neurobiology at the University of Vienna
2014-2015 Master's Thesis at the Center for Brain Research, Medical University of Vienna, Department of Synapse Formation, Group: Dr. Ruth Herbst
2013 'Erasmus prácticas' at University INEF La Coruña, Galicia, Spain, Laboratory of Neurosciences, Group: Prof. Miguel Fernandez del Olmo
WS07-SS12 Bachelor Microbiology and Genetics at the University of Vienna
2011 1 month internship and 2 months Bachelor's thesis at the Cancer Research Institute of the Medical University of Vienna, Supervisor: Prof. Ferdinand Steinböck
1999- 2007 Primary and secondary school Bundesreal- /und Bundesoberstufenrealgymnasium Schulring 16, St.Pölten; Focus on education in music and instruments

St.Pölten, February 2016

8.5 Lebenslauf



Persönliche Daten

Name: Sandra Parzer
 Adresse: Russengasse 12/5/19
 3100 St.Pölten
 Austria
 Geburtsdatum: 2.10.1988
 Email: sandra.parzer@gmail.com

Ausbildung

WS12-SS16 Master Molekulare Biologie mit Schwerpunkt Neurobiologie an der Universität Wien

2014-2015 Masterarbeit am Zentrum für Hirnforschung, Medizinische Universität Wien, Sektion für Synapsenbildung unter der Leitung von Dr. Ruth Herbst

2013 'Erasmus prácticas' an der Universität INEF La Coruña, Galizien, Spanien, Labor für Neurobiologie, Gruppe: Prof. Miguel Fernandez del Olmo

WS07-SS12 Bachelor in Mikrobiologie und Genetik an der Universität Wien

2011 1-monatiges Praktikum und 2-monatige Bachelorarbeit am Zentrum für Krebsforschung der Medizinischen Universität Wien, Supervisor: Prof. Ferdinand Steinböck

1999- 2007 Bundesreal- /und Bundesoberstufenrealgymnasium Schulring 16, St.Pölten

St.Pölten, Februar 2016